FU JEN STUDIES

NATURAL SCIENCES

NO. 21 1987

目 次 CONTENTS

續 (Continue)

FU JEN CATHOLIC UNIVERSITY

TAIPEI, TAIWAN, REPUBLIC OF CHINA

目　次（續）　CONTENTS (continued)

乳糖酶之研究

1. 乳糖問題、酵素性質、來源及應用

食品營養系暨研究所

鄭淑文* 蔡英傑** 丘志威

摘要

本篇係綜合近十幾年來有關乳糖酶的學術報告，就乳糖不耐症，乳糖在食品上的問題，乳糖酶的分佈、特性及應用作系統的整理。此外，並介紹國內乳糖酶的研究近況。

前言

隨人種，民族的不同，大多數東方人，尤其是成年人在喝牛乳後數小時即有腹痛、脹氣、甚至腹瀉等不適的症狀出現[1]。直到最近十幾年，科學家們才了解乳糖不耐症（lactose intolerance）與乳糖酶（β-galactosidase）間的相關性。在食品加工方面，乳糖雖具有改良食物風味，質地或參與褐變反應（browning reaction）的功用，但是濃縮或冷凍乳製品的乳糖結晶問題却一直困擾着食品工業界，爲此，有關乳糖酶的性質、來源、及應用等的研究更形重要。

乳糖不耐症

乳糖是乳汁中所特有的醣類，佔牛乳中醣類總重量的99.8%以上，堪稱爲乳汁中唯一的醣類[2]。乳糖以雙醣的形態被攝食，但並非以此形式被吸收進入血液中，而是必須先經分解爲葡萄糖及半乳糖方可由小腸吸收。存在於小腸黏膜中的乳糖酶即擔任分解乳糖爲單醣的功能（圖1）。人體腸道內缺乏乳糖酶或其活性相當低時，未經吸收之乳糖進入小腸後部或大腸內，吸收大量水份並爲腸中的微生物利用，代謝，產生乳酸及二氧化碳，引起腹痛、脹氣、腹瀉的現象，在臨床醫學上則稱之爲乳糖不耐症[1,3]。

乳糖不耐症分爲先天性及後天性兩種。世界上大部份的人口都有乳糖不耐症的現象[4]，而且多屬於後天性[1]。Kretschmer[5]的研究報告指出，乳糖的耐受程度是一種具有可遺傳的特性，因此具有種族特異性。早期的報告亦發現高加索人，黑人及亞洲人患乳糖不耐症的比例較白人爲高[3,6]。有關不同人種之成年人缺乏乳糖酶的情形亦詳列於表1。

* 嘉南藥學專科學校食品衛生科
**陽明醫學院生化科

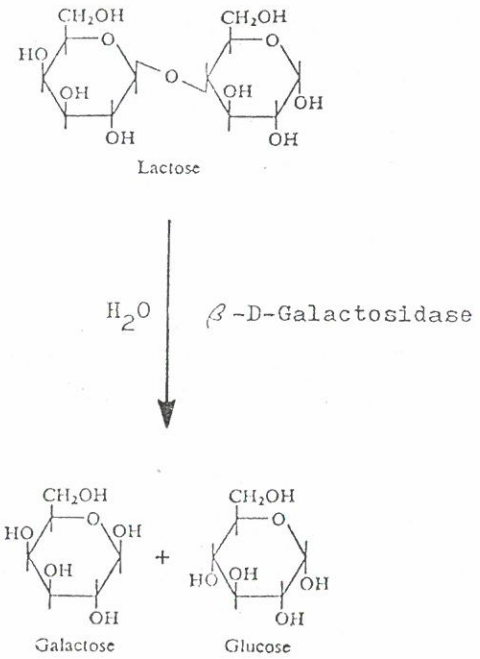

Fig. 1. Reaction catalyzed by β-galactosidase.
圖1. 乳糖酶參與之化學反應

表1. 不同人種之成年人缺乏乳糖酶的情形

Table 1. Percentages of adult β-galactosidase deficiency in some different populations

Race	Percentage (%)
Sweden	3
Denmark	3
Finland	16
Switzerland	17
England	20-30
U. S. S. R. (Moscow)	25
U. S. A. whites	6
U. S. A. blacks	73
Africa hamites	10
Africa negroids	~ 100
Japan and probably the whole Far East	~ 100

Source: Dahlqvist, 1984[1]

乳糖酶在人體妊娠後期始出現，出生後迅速上升至最高活性，但在一歲半至三歲時又下降至低點[7]。乳糖酶缺乏的結果，使得乳糖中的能量雖經攝食却不能爲身體所利用。乳糖之熱量佔牛乳總熱量的 30～60 %，對於熱量不足的病人而言，分解乳糖可用來提供能量，同時促進牛乳蛋白質的利用。 Dahlqvist[1] 及 Rosensweig[8] 曾就乳糖不耐症作詳細的文獻回顧，並指出低乳糖牛乳製品之發展是解決乳糖不耐症的有效方法。

乳糖在食品加工上的問題

乳糖之甜味度極低，如表 2 所示，其相對甜度只有蔗糖的15%，與其他常用單糖之甜度亦相差甚遠。乳糖的溶解度亦不高，在 25°C 時只有22%，僅約蔗糖的 3 分之 1 ，葡萄糖或半乳糖的 2.7分之 1 [9]。在 0°C 時溶解度更低，只有12%。因此冷凍或冷藏之乳製品，例如煉乳，冰淇淋及濃縮乳清等即因乳糖的形成而有砂質（sandiness）口感，進而影響乳品品質及增加加工上的困難。

歐美國家乳酪工業的持續發展却產生了乳清所造成的公害問題。乳清的主要固形物除了灰分外就是乳糖及乳清蛋白(whey protein)。據估計，100 kg 乳清含 3.5 kg 的生物需氧量 (Biological oxygen demand, B.O.D.) 和 6.8 kg 的化學需氧量 (chemical oxygen demand, C.O.D.)[10]。乳清曾被利用爲肥料及飼料，但是效果不理想[11]。近來，歐美國家利用超濾技術 (ultrafiltration) 由乳清回收濃縮蛋白 (whey protein concentrate) 及含高量乳糖之乳清濾液 (whey permeate)，前者已經廣泛地被應用於許多食品配方中[11-13]。由於乳糖的市場有限，乳清濾液却未能被充份的利用。因此，如何有效的解決乳糖所帶來的問題一直是學術界及工業界努力的目標。

表 2. 與10%蔗糖溶液比較其他單醣的相對甜度

Table 2. Relative sweetness of various sugars (equivalent to 10% aqueous sucrose solution)

Sugar	Sweetness value
Sucrose	100
Galactose	70
Glucose	70-75
Fructose	140-175
Lactose	15

Sources: Shukla, 1975[7] and Dicker, 1982[9].

乳 糖 酶

乳糖酶反應機制

乳糖酶（EC 3, 2, 1, 23）俗稱 lactase，學術名稱爲 β-galactosidase 或 β-D-galactoside galactohydrolase，能够斷裂 β-1→4 glycoside 鍵結，分解乳糖成爲葡萄糖及半乳糖。乳糖酶之活化中心乃是由一個 sulfhydryl 與一個

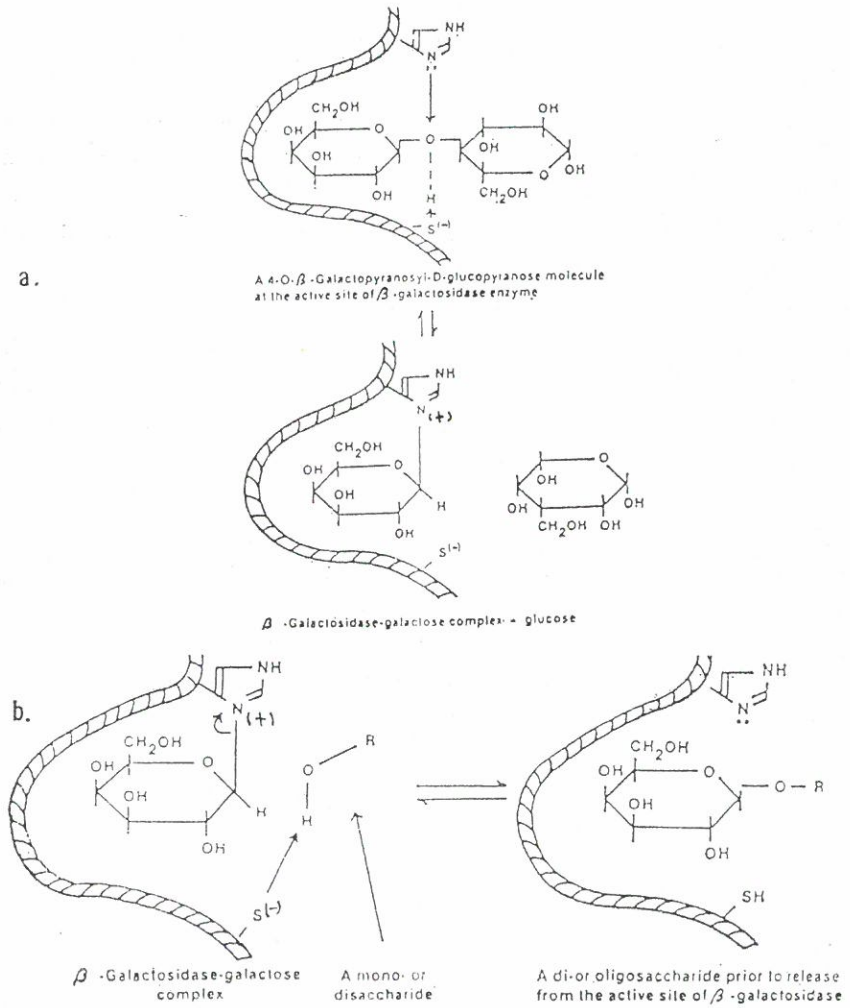

Source: Richmond and Gray, 1981[15]

Fig. 2. Proposed mechanism of lactose hydrolysis by β-galactosidase.

圖2. 乳糖酶水解乳糖之可能機制

imidazole group 所組成[14,15]。Wallenfels 及 Weil[16] 和 Shukla[7] 曾提出乳糖酶之反應機制，如圖 2a 所示，乳糖酶與乳糖作用首先斷裂 β-1→4 鍵結，產生乳糖酶與半乳糖之複合物及一分子葡萄糖。而乳糖酶同時可以催化一些寡糖之生合成反應。如圖 2b 所示，在乳糖酶與半乳糖之複合物中，酵素活化中心之 S-group 可由一單醣或雙醣之一級醇碳處摘取一個 H^+，使得此單醣或雙醣與半乳糖之 C-1 結合，令酵素活化中心之 imidazole group 與半乳糖間之 C-N 鍵斷裂，而有雙醣，寡醣或水分子之生成[17]。Gest 和 Mandelstam[18] 研究大腸桿菌 (*E. coli* ML 308) 之乳糖酶發現，每個分子之活化中心數目受溫度之高低而改變，隨溫度上升而增加，例如在 4～6°C 時平均活化中心數爲1.0，但在 20～22°C 之間則平均活化中心數爲 4.7。因此可能在低溫時，並非所有的活化中心都能發揮功用。而 subunit 之數目亦因爲酵素來源不同而有別[19]，如 *E. coli* 乳糖酶共有 4 個 subunits[20]；而由 *Streptococcus lactis* 獲得之乳糖

表 3. 乳糖酶的可能來源

Table 3. Possible sourses of β-galactosidase

Plants	Animal organs
Peach	Intestine
Apricot	Brain and skin tissue
Almond	
Kefir grains	
Tips of wild roses	
Alfalfa seed	Fungi
Coffee	*Neurospora craussa*
Yeast	*Aspergillus foetidus*
Sacharomyces lactis	*Aspergillus niger*
Saccharomyces fragilis	*Aspergillus flavus*
Candida pseudotropicalis	*Aspergillus oryzae*
Bacteria	*Aspergillus phoenicis*
Escherichia coli	*Mucor pupucillus*
Bacillus megaterium	*Mucor meihei*
Thermus equaticus	
Streptococcus lactis	
Streptococcus thermophilus	
Lactobacillus bulgaricus	
Lactobacillus helareticus	

Source: Shukla, 1975[7].

酶則無明顯之 subunit，但有 2 個 iso-form。這些性質在 Shukla[7] 與 Wallenfels 及 Weil[16] 報告中均有詳細敍述。

乳糖酶對於 β-galactosidic 鍵結具有特異性，且酵素活性由於基質之 aglycone moiety 之不同而有差別。O-Nitrophenyl-beta-D-galactopyranoside (ONPG) 乃是一種經常被使用來測定乳糖酶活性的基質。與乳糖相比，ONPG 則有較低的 Km 及較高的最大反應速率。

乳糖酶之分佈與特性

乳糖酶之分佈極爲廣泛，植物、動物或微生物細胞中均有該酵素的存在（表 3）。一般而言，微生物爲乳糖酶之最佳來源，有關這方面的資料在 Shukla[7] 的報告中有詳細的記載。酵素之結構大小、性質、最佳反應條件如最適反應 pH 值、反應溫度、抑制物質、輔助因子、熱安定性及對反應基質之特異性等，隨酵素來源不同而有異（表 4）[21-24]。依 Wierzbicki 及 Kosikowski[25] 調查報告，一般而言，由黴菌分離之乳糖酶的最適 pH 值在 3 至 5 之間；由細菌及酵母菌所得之酵素則最適反應 pH 爲 5 至 7。在反應最適溫度方面，黴菌乳糖酶一般

表 4. 不同菌源的乳糖酶之性質比較

Table 4. Characteristics of β-galactosidase from various organisms

	K. fragilis[a]	*A. oryzae*[b]	*P. citrinum*[c]	*Bacillus.* L-12[d]
MW	203,000	105,000	110,000	
Opt. pH	6.8	4.5 (ONPG) 4.8 (lactose)	4.5	6.0
Opt. Temp.	40°C	46°C	50°C	55°C-60°C
pI	4.4	4.2	6.4	
Km	4.0 mM (ONPG) 21.0 mM (lactose)	0.72 mM (ONPG) 18.0 mM (lactose)	1.7 mM (ONPG) 25.0 mM (lactose)	
Inhibitor	Ag^+, Hg^{++}	Ag^+, Hg^{++}, Cu^{++}	Cu^{++}, Hg^{++}	Zn^{++}, Cu^{++}, Hg^{++}, Fe^{++}
Activator	K^+, Mn^{++}, Co^{++}, Mg^{++}			K^+, Mn^{++}, Mg^{++}

Sources: (a) Uwajima *et al.*, 1972[21]; (b) Tanaka *et al.*, 1975[22]; (c) Watanabe *et al.*, 1979[23]; (d) 廖朝暐, 1984[24]

在 50°C 左右；酵母菌乳糖酶則約爲 40°C。若由耐高溫菌體分離得到的酵素則最適反應溫度偏高，例如表4所列 *Bacillus* L12 的乳糖酶高達 55-60°C。

儘管這些酵素在化學及物理結構上有差異，但其將乳糖水解的功能並無不同，而且這些不同的特性更能適合食品工業不同的需求。

乳糖酶的應用

乳糖酶在歐美早已大量工業化生產，專利申請亦相當可觀[26-28]。由酵母菌 *Kluyveromyces lactis*、*K. fragilis* 及黴菌 *Aspergillus niger*、*A. oryzae* 獲得之乳糖酶最適用於食品或乳品工業。目前以前三者所生產之乳糖酶用途最廣[29,30]。

因爲可溶性酵素使用後不可回收及增加成本的缺點，許多研究均朝向發展能够將酵素重複或連續使用的技術。這些包括以超濾法（ultrafiltration）再使用酵素[26]，將酵素置於超濾膜中[31]或將酵素固定於擔體[32,33]。雖然 *A. niger* 乳糖酶可以固定化形式利用，但是 *K. lactis* 乳糖酶經固定化後却呈現不穩定的性質[34,35]。然而隨着固定化方法的改進，義大利米蘭之 Centrale del Latte 公司使用 Snamprogetti 技術成功地利用纖維嵌入法固定 *K. lactis* 乳糖酶並已工業化生產低乳糖牛乳[36]。

過去十幾年間，利用乳糖酶發展了許多低乳糖牛乳及低乳糖乳製品，包括全脂乳、脫脂乳、煉乳、buttermilk、冰淇淋、cottage cheese、chedder cheese 及由乳清製造糖漿[25,34,38-45]。這些低乳糖產品除了克服乳糖不耐症外，更能因爲乳糖的水解而增加甜味，改善結晶性，降低冰點，及改變黏稠度等[37,46-48]。

最近 Giec 及 Kosikowski[49] 利用 *K. lactis* 乳糖酶在低溫下進行濃縮乳清乳糖水解的速率比較。Chiu 及 Kosikowski[50] 更利用超濾技術從濃縮乳清中回收乳糖並分別經乳糖酶及葡萄糖轉化酶（glucose isomerase）處理後製造高果糖糖漿。

國內現況

國外調查報告早已指出東方人的乳糖不耐症極爲普遍，但國內一直沒有這方面的臨床調查報告。直到197?年，臺灣大學醫學院宋瑞樓教授等[51]調查發現國人中有 91.7%缺乏乳糖酶，其中88%有乳糖不耐症的現象。近來，榮民總醫院與臺大醫院腸胃科醫師之臨床病例研究發現，國人乳糖不耐症患者比例確實相當高，成年人佔92%，青少年佔84%，學童佔70%。目前臺灣由於經濟形態改變，牛乳及其製品的消費量逐年增加，如何解決乳糖不耐症已是刻不容緩。但國內市售的乳糖酶及臨床上爲解決嬰兒先天乳糖酶缺乏所使用的酵素均由國外進口，耗費大量的外滙。

目前，清華大學、陽明醫學院、中興大學、輔仁大學及嘉義農專等學術單位已有乳糖酶動力學、菌種篩選和酵素的分離純化、固定化、及應用等研究。雖然於民國七十五年六月，國內兩家主要食品公司推出低乳糖鮮乳，但是有關發展低乳糖鮮乳及其他乳製品的學術研究仍不多見。

參考文獻

(1) A. Dahlqvist, *Nutr. Abstr. and Rev. in Clinical Nutr.* 54, 649 (1984).
(2) 林慶文, 乳品製造學, 華香園出版社, 臺北市, (1982).
(3) 黃伯超, 食品營養與講座, 健康世界雜誌社, 臺北市, (1984).
(4) R. L. Pike and M. L. Brown, *Nutrition: An Integrated Approach*, 2nd ed., p. 218, John Wiley and Sons, Inc., NY, (1975).
(5) N. Kretschmer, *Gastroenterolology* 61, 805 (1971).
(6) M. A. Nandi and E. S. Parham, *J. Amer. Diet. Assoc.* 61, 258 (1972).
(7) T. P. Shukla, *CRC Crit. Rev. in Food Technol.* 5, 325 (1975).
(8) N. S. Rosensweig, *J. Dairy Sci.* 52, 585 (1969).
(9) R. Dicker, *Dairy Industries International* 47, 19 (1982).
(10) *Milk Industry Foundation, Manual for Milk Plant Operators*, 3rd ed., (Milk Industry Foundation, Washington, D. C.) (1967).
(11) A. Hill, *Modern Dairy* 61, 12 (1982).
(12) S. Crocco, *Food Enz.* 47, 59 (1975).
(13) S. Elias, *Food Enz.* 51, 81 (1979).
(14) A. V. Fowler and I. Zabin, *J. Biol. Chem.* 253, 5521 (1978).
(15) M. L. Richmond and J. I. Gray, *J. Dairy Sci.* 64, 1759 (1981).
(16) K. Wallenfel and R. Weil, *The Enzymes*, **Vol. 5,** 3rd ed., p. 616, Academic Press, NY, NY, (1972).
(17) M. Aroson, *Arch. Biochem. Biophys.* 39, 370 (1952).
(18) H. Gest and J. Mandelstam, *Nature* 211, 72 (1966).
(19) M. E. Goldberg and S. J. Edelstein, *J. Mol. Biol.* 46, 431 (1969).
(20) R. Wallenfels, *Method in Enzymology*, **Vol. 5,** p. 212, Academic Press, NY, NY, (1972).
(21) T. Uwajima, H. Yagi and O. Terada, *Agr. Biol. Chem.* 36, 570 (1972).
(22) Y. Tanaka, A. Kangamiishi, A. Kiuchi and T. Horiuchi, *J. Biochem.* 77, 241 (1975).
(23) L. E. Wierzbicki and F. V. Kosikowski, *J. Dairy Sci.* 56, 26 (1973).
(24) 廖朝暐, 大同學報, 14, 161 (1984).
(25) Y. Watanabe, Y. Kibesaki, S. Sakai and Y. Tsujisaks, *Agr. Biol. Chem.* 43, 943 (1979).
(26) R. A. Edwards, P. M. Cantrell and J. J. Miller, *Aust. Patent* 470, 927 (1973).
(27) M. W. Griffiths, D. D. Muir and J. D. Philips, *U. S. Patent* 4,332,895 (1982).
(28) H. Young and R. P. Healey, *U. S. Patent* 2,776,928 (1957).
(29) H. H. Nijpels and P. M. Rheinlander, *Food Engineering Int'l.* 7, 55 (1982).
(30) B. Sprössler and H. Plainer, *Food Technol.* 37, 93 (1983).

(31) L. Roger, J.L. Thapon, J.L. Maubios and G. Brule, *Le Lait* **56**, 56 (1976).
(32) W.H. Pitcher, Jr., *Proceeding Whey Products Conference*, Chicago, IL, (1974).
(33) R. Hansen, *Nordeuropaeisk Mejeri-Tidsskrift* 43, 310 (1977).
(34) G.J. Woodward and F.V. Kosikowski, *J. Dairy Sci.* **58**, 792 (1975).
(35) E.H. Reimerdes and N. Scholz, *Milchwissenschaft* **36**, 608 (1981).
(36) W. Marconi and F. Morisi, In *Applied Biochemistry and Bioengineering*, **Vol. 2,** L.B. Wingard, E Katchalski-Katzir and L. Goldstein (Eds), p. 219, (Academic Press, NY, 1979).
(37) W.L. Wendorff, G.H. Amundson and N.F. Olson, *J. Milk Food Technol.* **33**, 451 (1970).
(38) C.P. Chiu and F.V. Kosikowski, *J. Dairy Sci.* **68**, 16 (1985).
(39) F.V. Kosikowski and L.E. Wierzbicki, *J. Dairy Sci.* **56**, 146 (1973).
(40) F.V. Kosikowski and L.E. Wierzbicki, *J. Dairy Sci.* **54**, 764 (1971).
(41) W.G. Engel, *Cult. Dairy Products J.* 8, 6 (1973).
(42) W.L. Wendorff and C.H. Amundson, *J. Milk Food Technol.* **34**, 300 (1971).
(43) D.M. Gyuricsek and M.P. Thompson, *Cult. Dairy Products J.* **11**, 12 (1976).
(45) C.K. Young, J.W. Stull, R.R. Taylor, R.C. Augus and T.C. Daniel, *J. Food Sci.* **45**, 805 (1980).
(46) A.G. Rand and P.M. Linklater, *Aust. J. Dairy Technol.* **26**, 63 (1973).
(47) T.A. Nickerson, *Proceedings Whey Products Conference*, (Chicago, IL, 1974).
(48) E.J. Guy and L.F. Edmondson, *J. Dairy Sci.* **61**, 543 (1978).
(49) A. Giec and F.V. Kosikowski, *J. Dairy Sci.* **66**, 396 (1983).
(50) C.P. Chiu and F.V. Kowsikowski, *J. Dairy Sci.* **69**, 959 (1986).
(51) J.L. Sung and P.L. Shih, *Asian J. of Med.* 8, 149 (1972).

β-Galactosidase

1. Review of Recent Research Releated to Food and Nutritional Concerns, Properties, Sources and Application

S. W. CHENG, Y. C. TSAI and C. P. CHIU

Graduate Institute of Nutrition and Food Science

ABSTRACT

Based on the literatures published in the past ten to fifteen years, several aspects of β-galactosidase are reviewed, including lactose intolerance, lactose problems in foods, β-galactosidase properties, sources, and applications. Current research and development of β-galactosidase in Taiwan is described also.

ON THE CONSTRUCTION OF KRYLOV SUBSPACE METHODS FOR SOLVING LARGE LINEAR SYSTEMS

LUHAN CHUANG and KANG C. JEA

Department of Mathematics

ABSTRACT

We discuss the use of Krylov subspace methods for solving large linear systems $Ax = b$. The two important elements of a Krylov subspace method are the choice of auxiliary matrix, and the construction technique of direction vectors. Some difficulties may occur when using these methods. We divide the difficulties that may occur into three kinds: break-down, stagnancy, and shock. We show that break-down will not occur if the auxiliary matrix Z is chosen such that ZA is nonzero-real. Stagnancy will not appear if the direction technique used is not of type-R. Shock will not happen if the direction vectors are M-semiorthogonal with respect to a nonzero-real matrix M. Moreover, we introduce a new method called the Unitary Basis Method, which adapts the auxiliary matrix dynamically. The advantages of this method that are it is unnecessary to choose Z before processing and it saves operations at each iteration. Furthermore, we adapt the idea of using the auxiliary matrix dynamically to other existing Krylov subspace methods, and find the advantage of time saving still appears.

1. INTRODUCTION

In this research we disscuss the use of Krylov subspace methods for solving the linear system

$$Ax = b \tag{1.1}$$

where A is a large sparse real nonsingular matrix of order $N \times N$, and b is a given $N \times 1$ real column vector. Such problems always arise in solving the elliptic partial differential equations with boundary conditions by finite difference methods or by finite element methods.

We consider a basic iterative method which is completely consistent with (1.1) and of the form

$$\begin{cases} x^{(n+1)} = Gx^{(n)} + k, & \text{for } n = 0, 1, 2, \ldots \\ G = I - Q^{-1}A, \quad k = Q^{-1}b, \end{cases} \tag{1.2}$$

where $x^{(0)}$ is an arbitrary initial guess, I is the N×N identity matrix, and Q is an N×N real nonsingular matrix. We assume the exact solution of (1.1) is $\bar{x}$, and define the nth error vector as

$$e^{(n)} = x^{(n)} - \bar{x}. \tag{1.3}$$

We also define the residual vector and pseudo-residual vector as

$$\begin{cases} r^{(n)} = b - Ax^{(n)}, \\ \delta^{(n)} = x^{(n+1)} - x^{(n)} = k - (I - G)x^{(n)}, \end{cases} \tag{1.4}$$

respectively.

Our discussions are restricted to the RF method as given in Young[9], i.e. Q=I in (1.2). Since a basic iterative method (1.2) with some nonsingular matrix Q for solving (1.1) is equivalent to applying the RF method on the preconditioned linear system

$$Q^{-1}Ax = Q^{-1}b. \tag{1.5}$$

Therefore, it is adequate to discuss the RF method only. Then $G = I - A$ in (1.2) and (1.4) implies $\delta^{(n)} = r^{(n)}$. Moreover, if $r^{(0)}=0$ we will have $x^{(0)} = \bar{x}$, and the problem is solved. Thus, we always assume $r^{(0)} \neq 0$.

In Section 2, we introduce some properties of Krylov subspaces, auxiliary matrices, and the relations between them. In Section 3, we introduce the construction of Krylov subspace methods, we give three different principles for building direction vectors, and analyze the source of difficulties for applying these methods. We define a new method in Section 4, called the "Unitary Basis Method", which is a Krylov subspace method and which adapts auxiliary matrices dynamically. The advantage of using this method is efficiency, since it requires very few operations at each iteration. But, it takes more storage locations than some existing methods. The results of our numerical experiments are listed in Section 5.

2. KRYLOV SUBSPCES AND AUXILIARY MATRICES

In this section, we introduce some properties of the Krylov

subspaces of R^N and the use of auxiliary matrices. For a given $r^{(0)} \neq 0$, the nth Krylov subspace generated by $r^{(0)}$ with respect to A is the subspace spanned by the set of vectors $\{r^{(0)}, Ar^{(0)}, \ldots, A^{n-1}r^{(0)}\}$. We denote it by $K_n(r^{(0)}, A)$. Here, n is any positive integer, and $K_0(r^{(0)}, A)$ denotes the set $\{0\}$. Moreover, the largest integer d such that $r^{(0)}, Ar^{(0)}, \ldots, A^d r^{(0)}$ are linearly independent is called the index of $r^{(0)}$ with respect to A. Thus, $d \leq N-1$. For a given matrix Z, we use $ZK_n(r^{(0)}, A)$ to denote the subspace generated by $\{Zr^{(0)}, ZAr^{(0)}, \ldots, ZA^{n-1}r^{(0)}\}$. A vector v on the hyperplane $x^{(0)} + S$ is said to satisfy the Galerkin condition with respect to the auxiliary matrix Z if its residual is orthogonal to the subspace ZS. That is

$$(b - Av, w) = 0, \quad \text{for all } w \in ZS. \tag{2.1}$$

Obviously, if d is the index of $r^{(0)}$ with respect to A, then the following two relations hold

$$K_n(r^{(0)}, A) \subsetneq K_{n+1}(r^{(0)}, A), \quad \text{for } n = 1, 2, \ldots, d,$$
$$K_n(r^{(0)}, A) = K_{d+1}(r^{(0)}, A), \quad \text{for } n > d.$$

Furthermore, the following property confirms the existence of the solution, $\bar{x}$, of (1.1) on the hyperplane $x^{(0)} + K_{d+1}(r^{(0)}, A)$.

Theorem 2.1 If d is the index of $r^{(0)}$ with respect to A, then $\bar{x} - x^{(0)} \in K_{d+1}(r^{(0)}, A)$, and $\bar{x} - x^{(0)} \notin K_n(r^{(0)}, A)$, for each $n = 0, 1, \ldots, d$.

The details of proof are given in Jea[5]. From the above theorem, there must exist a vector $y \in R^{d+1}$ satisfying

$$\bar{x} = x^{(0)} + (r^{(0)}, Ar^{(0)}, \ldots, A^d r^{(0)})\, y, \tag{2.2}$$

where $(r^{(0)}, Ar^{(0)}, \ldots, A^d r^{(0)})$ is an $N \times (d+1)$ matrix with columns $r^{(0)}, Ar^{(0)}, \ldots, A^d r^{(0)}$. Since $r^{(0)}, Ar^{(0)}, \ldots, A^d r^{(0)}$ are linearly independent, the vector y is unique. Therefore, by (2.2),

$$r^{(0)} = A(r^{(0)}, Ar^{(0)}, \ldots, A^d r^{(0)})\, y. \tag{2.3}$$

We note that the solution, y, of (2.3) will give us the exact solution $\bar{x}$ by (2.2). Thus, we try to solve (2.3) by choosing an auxiliary matrix Z which has the advantages of evaluating vector y

easily and ensuring the existence of a unique solution for the following linear system

$$(r^{(0)}, Ar^{(0)}, \ldots, A^d r^{(0)})^T ZA(r^{(0)}, Ar^{(0)}, \ldots, A^d r^{(0)})\, y = (r^{(0)}, Ar^{(0)}, \ldots, A^d r^{(0)})^T Zr^{(0)}. \tag{2.4}$$

Unfortunately, it is difficult to predict the index d beforehand, so (2.4) can not be constructed. We use an iterative technique to look for a vector $x^{(n)}$ gradually. Here $x^{(n)}$ lies on the hyperplane $x^{(0)} + K_n(r^{(0)}, A)$, and its residual is orthogonal to the subspace $ZK_n(r^{(0)}, A)$, i.e. $x^{(n)}$ satisfies the Galerkin condition (2.1). We need to know what type of auxiliary matrix Z may ensure a unique $x^{(n)}$ in $x^{(0)} + K_n(r^{(0)}, A)$, for $n = 1, 2, \ldots$, until $x^{(d+1)} = \bar{x}$ is reached. In other words, we must choose an auxiliary matrix Z which assures the existence of a unique solution for the following deduced linear system

$$(r^{(0)}, Ar^{(0)}, \ldots, A^{n-1} r^{(0)})^T ZA(r^{(0)}, Ar^{(0)}, \ldots, A^{n-1} r^{(0)})\, y = (r^{(0)}, Ar^{(0)}, \ldots, A^{n-1} r^{(0)})^T Zr^{(0)}, \tag{2.5}$$

for each $n = 1, 2, \ldots, d+1$. We also may construct another set of basis for $K_n(r^{(0)}, A)$, named $\{p^{(0)}, p^{(1)}, \ldots, p^{(n-1)}\}$, to replace the original set of basis $\{r^{(0)}, Ar^{(0)}, \ldots, A^{n-1} r^{(0)}\}$ in order to evaluate $x^{(n)}$ more efficiently. If n linearly independent vectors $p^{(0)}, p^{(1)}, \ldots, p^{(n-1)}$ have been constructed, (2.5) can be replaced by

$$(p^{(0)}, p^{(1)}, \ldots, p^{(n-1)})^T ZA(p^{(0)}, p^{(1)}, \ldots, p^{(n-1)})\, y = (p^{(0)}, p^{(1)}, \ldots, p^{(n-1)})^T Zr^{(0)}. \tag{2.6}$$

Next, we state two theorems on constructing the basis; the proofs of them are given in Chuang[12]. First of all, given two sets S and T where $S \subseteq T$, we say $x \in T - S$ if $x \in T$ but $x \notin S$.

Theorem 2.2 If d is the index of $r^{(0)}$ with respect to A and if $w \in K_n(r^{(0)}, A) - K_{n-1}(r^{(0)}, A)$, then $Aw \in K_{n+1}(r^{(0)}, A) - K_n(r^{(0)}, A)$, for any $1 \leq n \leq d$.

Theorem 2.3 If d is the index of $r^{(0)}$ with respect to A and if $w \in x^{(0)} + K_n(r^{(0)}, A) - K_{n-1}(r^{(0)}, A)$, then $b - Aw \in K_{n+1}(r^{(0)}, A) - K_n(r^{(0)}, A)$, for any $1 \leq n \leq d$.

The auxiliary matrix plays an important role in the Krylov subspace methods, so we want to discuss some of its properties. Let us begin with some definitions. Suppose that M is an N×N real matrix, and $p^{(0)}, p^{(1)}, \ldots, p^{(n-1)}$ are vectors in R^N, we say those vectors are pairwise M-semiorthogonal, if

$$(p^{(i)}, Mp^{(j)}) = 0, \quad \text{for all } j<i;\ i, j = 0, 1, \ldots, n-1. \tag{2.7}$$

Here, (.,.) denotes the inner product. Moreover, we say a matrix M is nonzero-real, if $(x, Mx) \neq 0$, for every real vector $x \neq 0$. Let us give the following theorems without proof, the details of proof are available in Chuang[12].

Theorem 2.4 Let S be an n dimensional subspace of R^N. If M is an N×N nonzero-real matrix, then zero vector is the only vector in S which is orthogonal to MS, and vice versa.

Theorem 2.5 Let S be an n dimensional subspace on R^N and let M be a nonzero-real matrix of order N×N. If $\{p^{(0)}, p^{(1)}, \ldots, p^{(n-1)}\}$ is a basis of S, then both matrices $(Mp^{(0)}, Mp^{(1)}, \ldots, Mp^{(n-1)})^T$ $(p^{(0)}, p^{(1)}, \ldots, p^{(n-1)}$ and $(p^{(0)}, p^{(1)}, \ldots, p^{(n-1)})^T (Mp^{(0)}, Mp^{(1)}, \ldots, Mp^{(n-1)})$ are nonsingular.

Theorem 2.6 Let S be an n dimensional subspace of R^N, and let A, Z be two real N×N matrices. Given $v \in R^N$, if A is nonsingular and ZA is nonzero-real, then there exists only one vector in the hyperplane V+AS that is orthogonal to the subspace Z^TS.

Therefore, if we choose an auxiliary matrix Z such that ZA is nonzero-real, then, by Theorem 2.4, the zero vector is the only vector in $ZAK_n(r^{(0)}, A)$ which is orthogonal to the subspace $K_n(r^{(0)}, A)$. Moreover, Theorem 2.6 ensures that if ZA is nonzero-real, then (2.6) has a unique solution. In other words, there exists only one vector, in the hyperplane $x^{(0)} + K_n(r^{(0)}, A)$, which satisfies the Galerkin condition with respect to Z. From Theorem 2.1 and Theorem 2.6, we find that this vector is the approximate solution $x^{(n)}$.

In general, we may relax the sufficient conditions in Theorems 2.4, 2.5, and 2.6. Let S be a subspace of R^M and let M be an N×N

real matrix. We say that M is nonzero-real with respect to S, if $(Mw, w) \neq 0$ for all $w \in S$. We can show that Theorem 2.4 and Theorem 2.5 are true if we replace 'M is nonzero-real' by 'M is nonzero-real with respect to S'. Similarly, in Theorem 2.6 we may replace 'ZA is nonzero-real' by 'ZA is nonzero-real with respect to S'.

3. KRYLOV SUBSPACE METHODS

In this section, we introduce an iterative method, named the Krylov subspace method, which is defined by choosing an auxiliary matrix, Z, and a construction technique of direction vectors, T. Here, the technique T indicates a certain way of selecting basis of $K_n(r^{(0)}, A)$. Let us denote such a method as KM(Z, T). Thus, at the nth iteration, we look for a vector $x^{(n)}$ from the hyperplane $x^{(0)} + K_n(r^{(0)}, A)$ which satisfies the Galerkin condition with respect to Z. The existence of a unique vector $x^{(n)}$ depends on the choice of Z. If such a $x^{(n)}$ does not exist, we say that a break-down has occured.

In fact, the Krylov subspace method is a generalization of the idealized generalized conjugate gradient method (IGCG method) considered by Young and Jea[10]. Moreover, we note that the choice of the direction technique T affects the requirement of computer storages and computation time.

Theorem 3.1 If the auxiliary matrix Z is chosen such that ZA is nonzero real with respect to $K_{d+1}(r^{(0)}, A)$, then any Krylov subspace method KM(Z, T) will not break down. Moreover, the following statements hold.

(1) $r^{(n)} \neq 0$ and $x^{(n)} \neq \bar{x}$, for $n = 0, 1, \ldots, d$,
(2) $r^{(d+1)} = 0$ and $x^{(d+1)} = \bar{x}$,
(3) $Zr^{(n)}$ is orthogonal to $K_n(r^{(0)}, A)$, for $n = 0, 1, \ldots, d+1$,
(4) $r^{(0)}, r^{(1)}, \ldots, r^{(d+1)}$ are mutually Z-semiorthogonal.

Another obstacle may occur in building the direction vectors. We say that the stagnancy of direction vectors has occured, if at some iteration $n < d+1$, the $n+1$st direction vector $p^{(n)}$ stays in

the same subspace $K_n(r^{(0)}, A)$. Such a construction technique will imply that $sp\{p^{(0)}, p^{(1)}, \ldots, p^{(n)}\} = K_n(r^{(0)}, A)$. Next, we introduce two criteria for constructing direction vectors which will not have stagnancy.

Theorem 3.2 Let $p^{(0)} = r^{(0)}$ and $1 \leq n \leq d$. If $p^{(m+1)} \in Ap^{(m)} + K_{m+1}(r^{(0)}, A)$, for each $m = 0, 1, \ldots, n-1$, then $sp\{p^{(0)}, p^{(1)}, \ldots, p^{(n)}\} = K_{n+1}(r^{(0)}, A)$.

Theorem 3.3 Let $p^{(0)} = r^{(0)}$ and $1 \leq n \leq d$. If $p^{(m+1)} \in A^{m+1} r^{(0)} + K_{m+1}(r^{(0)}, A)$, for each $m = 0, 1, \ldots, n-1$, then $sp\{p^{(0)}, p^{(1)}, \ldots, p^{(n)}\} = K_{n+1}(r^{(0)}, A)$.

We called the direction techniques in Theorem 3.2 and Theorem 3.3 type-AP and type-AR, respectively. Another direction technique which has been used by Hestenes & Stiefel[4], Vinsome[8], Elman[3], and Axelsson[1] will be called type-R here since it defines $p^{(0)} = r^{(0)}$ and constructs $p^{(n)}$ by choosing a vector from $r^{(0)} + K_n(r^{(0)}, A)$. Now, let us give an example to show that stagnancy may occur for the type-R case.

Example 3.4 Solve a linear system $Ax = b$, where

$$A = \begin{pmatrix} 0 & 0 & 0 & 0 & 0 & 1 \\ 0 & 0 & 0 & 0 & 1 & 0 \\ 0 & 0 & 0 & 1 & 0 & 0 \\ 0 & 0 & 1 & 0 & 0 & 0 \\ 0 & 1 & 0 & 0 & 0 & 0 \\ 1 & 0 & 0 & 0 & 0 & 0 \end{pmatrix}, \quad b = \begin{pmatrix} 3 \\ 3 \\ 3 \\ 1 \\ 1 \\ 1 \end{pmatrix}.$$

Let us start with $x^{(0)} = (1, 1, 1, 2, 2, 2)^T$, and choose $Z = A$ as the auxiliary matrix. Then $ZA = I$, a nonzero-real matrix. If we choose the type-R direction technique, then $p^{(0)} = r^{(0)} = (1, 1, 1, 0, 0, 0)^T$. The only vector in $x^{(0)} + K_1(r^{(0)}, A)$ which satisfies the Galerkin condition is $x^{(1)} = x^{(0)}$. Thus $r^{(1)} = r^{(0)}$ and type-R technique selects $p^{(1)}$ from $r^{(1)} + K_1(r^{(0)}, A)$ will give us a stagnant direction vector.

To specify the direction technique T in more detail, let us use the notation $T = [v, M - k]$ where v is the type of constructions, such as AP, AR, or R. Thus,

$$cp^{(n)} \in v^{(n-1)} + K_n(r^{(0)}, A),\ c \neq 0, \tag{3.1}$$

where $v^{(n-1)}=AP^{(n-1)}$, $v^{(n-1)}=Ar^{(n-1)}$ or $v^{(n-1)}=r^{(n-1)}$, for type-AP, type-AR, or type-R, respectively. Moreover, we assume the direction vectors are constructed as M-semiorthogonal to the previous k vectors, that is

$$(p^{(n)}, Mp^{(i)}) = 0, \quad \text{for } i = n-1, n-2, \ldots, n-k. \tag{3.2}$$

If it is M-semiorthogonal to all previous direction vectors, we write $M-\infty$.

We define $p^{(0)}=r^{(0)}$ and construct $p^{(n)}$ by (3,1) and (3.2). That is, $cp^{(n)} = v + a_{n-k}p^{(n-k)} + \ldots + a_{n-1}p^{(n-1)}$, and

$$(p^{(n-k)}, p^{(n-k+1)}, \ldots, p^{(n-1)})^T M(p^{(n-k)}, p^{(n-k+1)}, \ldots, p^{(n-1)})\, a = -v^T M((^{n-k)}, p^{(n-k+1)}, \ldots, p^{(n-1)}) \tag{3.3}$$

Obviously, $p^{(n)}$ will not be uniquely defined unless the matrix $(p^{(n-k)}, p^{(n-k+1)}, \ldots, p^{(n-1)})^T M(p^{(n-k)}, p^{(n-k+1)}, \ldots, p^{(n-1)})$ is nonsingular. A direction technique $[v, M-k]$ is said to be shocked at iteration n, if there does not exist a vector $p^{(n)}$, in $v+K_n(r^{(0)}, A)$, which satisfies (3.2). For the same Example 3.4, if we choose a a direction technique [AP, A − 1], it is easy to check that shock will occur.

Theorem 3.6 Let $[v, M-k]$ be a direction technique and $1 \leq n \leq d$. If M is nonzero-real with respect to $K_{d+1}(r^{(0)}, A)$, then shock will not happen.

From theorems of Section 2 and Section 3, we obtain the following theorem.

Theorem 3.7 Let Z and A be N×N matrices. If Z and ZA are nonzero-real then KM(Z,[AP, ZA−∞], KM(Z,[AP, ZA−*k*1]), KM(Z, [AR, ZA − ∞]), KM(Z,[AR, ZA − *k*2]), KM(Z,[R, ZA − ∞]), and KM(Z,[R, ZA − *k*3]) are equivalent, for positive integers *k*1, *k*2, and *k*3,

In Young & Jea[11] there are three equivalent forms of the IGCG method, these are ORTHODIR, ORTHOMIN, and ORTHORES. Here, by our notation, we express them as KM(Z,[AP, ZA − ∞]) for

ORTHODIR, KM(Z,[R, ZA − ∞]) for ORTHOMIN, and KM(Z, [R, ZA − ∞]) for ORTHORES. From Theorem 3.7, ORTHODIR, ORTHOMIN, and ORTHORES are equivalent, if Z and ZA are nonzero-real. Axelsson[1] considered the Axelsson's least squares method which can be expressed as KM(A^T,[AP, A^TA − 1]). From above, we know that break-down, stagnancy, and shock will not happen in this method, because both $ZA=A^TA$ and $M=A^TA$ are nonzero-real, and direction technique is of type-AP. Axelsson[7] also considered the Axelsson's Galerkin method which can be expressed as KM(I,[R, A − 1]). For this method break-down, stagnancy, and shock may happen, because both ZA=A, M=A, and the direction vectors are of type-R. Saad, Elman & Schultz[7] considered the GMRES method which can be expressed as KM(AT,[AP, I − ∞]). Break-down, stagnancy, and shock will not occur in this process because both $ZA=A^TA$ and M=I are nonzero-real, and the direction technique is of type-AP. Eisenstat, Elman & Schultz[2] considered the Generalized Conjugate Residual method which can be expressed as KM(A^T, [R, A^TA − ∞]), which will not have break-down and shock but stagnancy, because the direction technique is of type-R. Saad[6] considered the Full Orthogonalization Method (FOM) which can be expressed as KM(I,[AP, I − ∞]). This method will not have stagnancy and shock, but may break down, because ZA = A is not always nonzero-real.

4. THE UNITARY BASIS METHOD

A Krylov subspace method with the auxiliary matrix Z such that ZA is nonzero-real with respect to $K_{d+1}(r^{(0)}, A)$ will not break down. But, it is very difficult to select such a Z, except $Z = A^T$. Therefore, we adapt auxiliary matrices dynamically and then deduce a special kind of Krylov subspace method, which we called the Unitary Basis Method. It possesses a dynamical auxiliary matrix which contains a permutation matrix M, and an auxiliary matrix Z. For convenience, we denote this method by KM(ZM, T), where Z projects $p^{(i)}$ onto the unit vector e_{i+1}, for $i = 0, 1, \ldots, d$, and M is adapted to avoid break-down. Assume that break-down occurs at

iteration $n < d+1$, then we may interchange the nth row of M with the mth row, where $m > n$. For convenience, at the initial state of iteration n, we denote M by M_n. We claim this method can solve linear system (2.5). Moreover, we can evaluate $x^{(n)}$ with few operations, and $r^{(n)}$ has more zero components than $r^{(n-1)}$ has. Thus we will save on the computation time at each iteration.

The name of the unitary basis comes from the fact that the auxiliary matrix Z maps the basis $\{p^{(0)}, p^{(1)}, \ldots, p^{(n-1)}\}$ of $K_n(r^{(0)}, A)$ into the unitary basis $\{e_1, e_2, \ldots, e_n\}$ of R^N, since

$$ZP^{(i)} = e_{i+1}, \quad \text{for } i = 0, 1, 2, \ldots, d. \tag{4.1}$$

Therefore, we may evaluate the $n+1$st approximate solution $x^{(n+1)}$ from the hyperplane $x^{(0)} + K_{n+1}(r^{(0)}, A)$ by making its residual being orthogonal to the subspace $ZM_n K_{n+1}(r^{(0)}, A)$. In other words, its residual is orthogonal to the subspace $M_n{}^T \mathrm{sp}\{e_1, e_2, \ldots e_n\}$.

Now, we give two theorems on the unitary basis method, and the proofs are given in Chuang[12].

Theorem 4.1 If n vectors, $v^{(1)}, v^{(2)}, \ldots, v^{(n)}$, of R^N are linearly independent, then the following two properties hold:

(1) There exists an N×N elementary permutation matrix M such that each leading principal submatrix of $M(v^{(1)}, v^{(2)}, \ldots, v^{(n)})$ is nonsingular.

(2) There exists an N × N matrix Z such that $Z^T v^{(i)} = e_i$, for $i = 1, 2, \ldots, n$.

Theorem 4.2 If A is an N×N nonsingular matrix, and n vectors, $v^{(1)}, v^{(2)}, \ldots, v^{(n)}$ of R^N are linearly independent, then there exists an N×N permutation matrix M and an N×N matrix Z satisfying $Z^T v^{(i)} = e_i$, for $i = 1, 2, \ldots, n$, such that each leading principal submatrix of $(v^{(1)}, v^{(2)}, \ldots, v^{(n)})^T ZMA(v^{(1)}, v^{(2)}, \ldots, v^{(n)})$ is nonsingular.

We denote the n×N matrix $(e_1, e_2, \ldots, e_n)^T$ by $(I_n | 0_{N-n})$, and denote the elementary permutation matrix which interchanged the ith row with the jth row by $I_{i,j}$. We also use P_n to denote the matrix $(p^{(0)}, p^{(1)}, \ldots, p^{(n-1)})$. Now, the algorithm of the Unitary Basis Method KM(ZM, [R, I − 0]) is given as follows.

Algorithm KM(ZM,[R, I − 0]):

(1) Choose an inital vector $x^{(0)}$, and define $r^{(0)} = b - Ax^{(0)}$, $M_0 = I_N$ =the N×N identity matrix, and iteration number $n=0$.

(2) Evaluate AP_n.

(3) Find an elementary permutation $I_{n+1,m}$, $m > n+1$, such that the matrix $(I_{n+1} \mid O_{N-n-1})\, I_{n+1,m} M_n AP_{n+1}$ is nonsingular, and define $M_{n+1} = I_{n+1,m} M_n$.

(4) Solve the linear system
$(I_{n+1}|O_{N-n-1})\, M_{n+1} AP_{n+1} a^{(n)} = (I_{n+1}|O_{N-n-1})\, M_{n+1} r^{(n)}$.

(5) Evaluate $x^{(n+1)} = x^{(n)} + P_{n+1} a^{(n)}$ and $r^{(n+1)} = r^{(n)} - AP_{n+1} a^{(n)}$.

(6) Check convergence. If true, then stop, else set $n = n+1$, $p^{(n)} = r^{(n)}$ and go to step (2).

We may also adapt the idea of using a dynamical auxiliary matrix to the other Krylov subspace methods, such as KM(A^T, [AP, $A^TA - \infty$]), KM(A^T, R, $A^TA - \infty$]), KM(A^T,[AP, I − ∞]), KM(I,[AP, I − ∞]), and KM(I,[R, A − 1]), and obtain fairly good results which will be shown in the next section.

5. NUMERICAL RESULTS

In this section we choose two elliptic partial differential equations P1 and P2 with boundary value conditions as our test problems and discretisized by central differences. All the numerical results shown were calculated with the Cyber 180/830 at the Data Communication Institute.

$$(P1)\quad \begin{cases} U_{xx}+U_{yy}+aU_x = 2x(x-1)+y(y-1)[2-a(1-2x)] & \text{in } \Omega \\ U = xy(1-x)(1-y) & \text{on } \partial\Omega \end{cases}$$

where $\Omega = [0, 1] \times [0, 1]$ and we have the analytical solution $u = xy(1-x)(1-y)$.

$$(P2)\quad \begin{cases} U_{xx} + U_{yy} + aU_x = ay & \text{in } \Omega \\ U = 1 + xy & \text{on } \partial\Omega \end{cases}$$

where $\Omega = [0, 1] \times [0, 1]$. Here the analytical solution is $u = 1 + xy$.

The stopping criteria considered are

$$K_e^{(n)} = \| x^{(n)} - \bar{x} \|_2 / \| x^{(0)} - \bar{x} \|_2 < \varepsilon, \qquad (5.1)$$

Table 1. Solving P1 with $a=10$, $h=1/16$, by methods KM(A^T, [AP, A^TA-∞]), KM(A^T, [R, A^TA-∞]), and KM(A^T, [AP, I-∞])

Method / K_r / Iter. No.	KM(A^T, [AP, A^TA-∞])	KM(A^T, [R, A^TA-∞])	KM(A^T, [AP, I-∞])
1	.14401965469779 E +00	.14401965469779 E +00	.14401965469779 E +00
2	.13578160309106 E +00	.13578160309106 E +00	.13578160309106 E +00
3	.12842355828770 E +00	.12842355828770 E +00	.12842355828770 E +00
4	.12156678254031 E +00	.12156678254031 E +00	.12156678254031 E +00
5	.11508628069287 E +00	.11508628069287 E +00	.11508628069287 E +00
6	.10892972569158 E +00	.10892972569158 E +00	.10892972569157 E +00
7	.10316108979812 E +00	.10316108979812 E +00	.10316108979812 E +00
8	.98235119180877 E −01	.98235119180878 E −01	.98235119180878 E −01
9	.94048238900585 E −01	.94048238900588 E −01	.94048238900586 E −01
10	.89470377925622 E −01	.89470377925622 E −01	.89470377925622 E −01
11	.85396474556731 E −01	.85396474556732 E −01	.85396474556735 E −01
12	.81443536947276 E −01	.81443536947277 E −01	.81443536947279 E −01
13	.77507449544485 E −01	.77507449544489 E −01	.77507449544489 E −01
14	.73954142575958 E −01	.73954142575959 E −01	.73954142575962 E −01
15	.70321566592570 E −01	.70321566592573 E −01	.70321566592574 E −01
16	.67041468349850 E −01	.67041468349852 E −01	.67041468349853 E −01
17	.63768134239012 E −01	.63768134239015 E −01	.63768134239017 E −01
18	.60741855964659 E −01	.60741855964664 E −01	.60741855964665 E −01
19	.57813998811566 E −01	.57813998811569 E −01	.57813998811570 E −01
20	.55044313055814 E −01	.55044313055818 E −01	.55044313055821 E −01
21	.52412934176948 E −01	.52412934176952 E −01	.52412934176953 E −01
22	.49869191200804 E −01	.49869191200809 E −01	.49869191200810 E −01
23	.47440010163603 E −01	.47440010163607 E −01	.47440010163609 E −01
24	.45004769850654 E −01	.45004769850660 E −01	.45004769850661 E −01
25	.42563125040044 E −01	.42563125040050 E −01	.42563125040051 E −01
26	.39884964421934 E −01	.39884964421942 E −01	.39884964421943 E −01
27	.36799537106057 E −01	.36789537106068 E −01	.36799537106068 E −01
28	.32703769082562 E −01	.32703769082577 E −01	.32703769082578 E −01
29	.27003664957332 E −01	.27003664957356 E −01	.27003664957357 E −01
30	.19244345475308 E −01	.19244345475341 E −01	.19244345475342 E −01
31	.11314093483543 E −01	.11314093483573 E −01	.11314093483574 E −01
32	.55006693391664 E −02	.55006693391865 E −02	.55006693391867 E −02
33	.23566772186427 E −02	.23566772186529 E −02	.23566772186531 E −02
34	.93519608466425 E −03	.93519608466885 E −03	.93519608466918 E −03
35	.34515989732984 E −03	.34515989733174 E −03	.34515989733203 E −03
36	.12184354827877 E −03	.12184354827943 E −03	.12184354827985 E −03
37	.42003712455801 E −04	.42003712455927 E −04	.42003712456285 E −04
38	.15232604284075 E −04	.15232604284248 E −04	.15232604284032 E −04
39	.77258014041830 E −05	.77258014042044 E −05	.77258014038982 E −05
40	.57100858402287 E −05	.57100858403306 E −05	.57100858401908 E −05
41	.42147549734220 E −05	.42147549735197 E −05	.42147549735764 E −05
42	.22058061508508 E −05	.22058061508669 E −05	.22058061508482 E −05
43	.95698398318352 E −06	.95698398315146 E −06	.95698398299273 E −06

and,

$$K_r^{(n)} = \| b - Ax^{(n)} \|_2 = \| r^{(n)} \|_2 < \varepsilon , \tag{5.2}$$

with the tolerance, ε, being 10^{-6}.

First, we solve P1 with $a=10$, mesh size $h=1/16$, by KM(A^T, [AP, $A^TA-\infty$]), KM(A^T,[R, $A^TA-\infty$]), and KM(A^T,[AP, I$-\infty$]), and show that these three methods are equivalent, their K_r values are listed in Table 1. Next, we show the number of iterations taken to converge and the CPU time for solving P1 and P2 by six different Krylov subspace methods, including the Unitary Basis Method, in Table 2. It is easy to see that the Unitary Basis Method requires less CPU time than the other methods. In Fig. 1 and Fig. 2 we show the changes of K_r for Krylov subspace methods, these are KM(A^T,[AP, $A^TA-\infty$]), KM(A^T,[R, $A^TA-\infty$]), KM(A^T, [AP, I$-\infty$]), KM(I,[AP, I$-\infty$]), KM(I,[R, A$-$1]), and KM(ZM, [R, I$-$0]). Only three curves appear because KM(A^T, [AP, $A^TA-\infty$]), KM(A^T,[R, $A^TA-\infty$]), and KM(A^T,[AP, I$-\infty$]) are represented by the same curve 3, KM(I,[AP, I$-\infty$]) and KM(I,[R, A$-$1]) are represented by the same curve 2, and the

Table 2. Solving P1 and P2 by six Krylov subspace methods

Problem		P1	P1	P1	P2
Coefficient a		1	10	1	1
Order of linear system		225	225	441	441
KM(A^T, [AP, $A^TA-\infty$])	No. of iteration	32	30	42	62
	CPU seconds	5.516	4.916	16.262	29.097
KM(A^T, [R, $A^TA-\infty$])	No. of iteration	32	30	42	62
	CPU seconds	5.530	4.901	16.215	29.077
KM(A^T, [AP, I-∞])	No. of itesation	32	30	42	62
	CPU seconds	10.403	9.020	32.588	66.398
KM(I, [AP, I-∞])	No. of iteration	31	30	41	63
	CPU seconds	9.837	9.014	31.248	68.545
KM(I, [R, A-∞])	No. of iteration	31	30	41	63
	CPU seconds	8.574	7.874	27.024	58.556
KM(ZM, [R, I-0])	No. of iteration	40	35	56	86
	CPU seconds	6.780	5.375	22.707	48.207

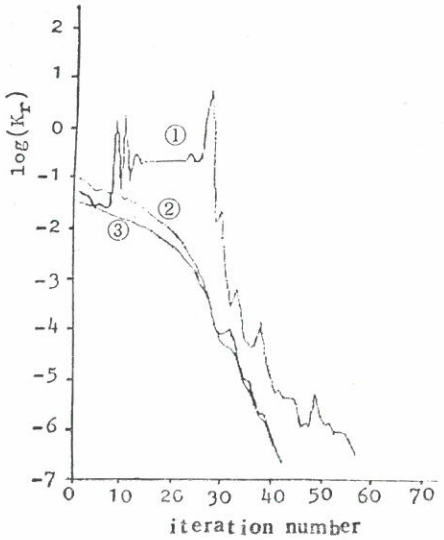

Fig. 1. Solving P1 with $a=1$ and $h=1/16$, by six Krylov subspace methods. 1: KM(ZM, [R, I-0]), 2: KM(I, [AP, I-∞]) and KM(I, [R, A-1]), and 3: KM(A^T, [AP, A^TA-∞]), KM(A^T, [R, A^TA-∞]), and KM(A^T, [AP, I-∞]).

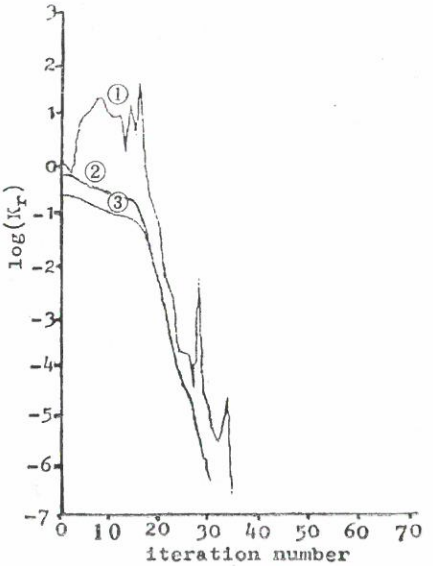

Fig. 2. Solving P1 with $a=10$ and $h=1/16$, by six Krylov subspace methods. 1: KM(ZM, [R, I-0]), 2: KM(I, [AP, I-∞]) and KM(I, [R, A-1]), and 3: KM(A^T, [AP, A^TA-∞]), KM(A^T, [R, A^TA-∞]), and KM(A^T, [AP, I-∞]).

Unitary Basis Method KM(ZM,[R, I − 0]) is expressed by curve 1.

Finally, in Table 3, we solve some problems by the five Krylov subspace methods KM(A^T,[AP, $A^TA - \infty$]), KM(A^T,[R, $A^TA - \infty$]), KM(A^T,[AP, I − ∞]), KM(I,[AP, I − ∞]), and KM(I,[R, A − 1]). For each one we compare the result of adapting a steady auxiliary matrix with that of adapting a dynamical auxiliary matrix. It is notable that in many cases by adapting a dynamical auxiliary matrix we have saved CPU time.

Table 3. Solving P1 and P2 by five Krylovsubspace methods. S denotes adapting steady auxilliary matrix, while D denotes adapting dynamical auxiliary matrix

Problem			P1	P2	P1	P1
Coefficient a			10	10	1	10
Order of linear system			49	49	225	225
KM(A^T, [AP, A^TA-∞])	S	No. of iteration	25	23	32	30
		CPU seconds	1.051	0.945	5.516	4.916
	D	No. of iteration	26	24	39	38
		CPU seconds	0.918	0.835	5.119	4.883
KM(A^T, [R, A^TA-∞])	S	No. of iteration	25	23	32	30
		CPU seconds	1.081	0.953	5.530	4.907
	D	No. of iteration	26	24	40	38
		CPU seconds	0.914	0.839	5.308	4.875
KM(A^T, [AP, I-∞])	S	No. of iteration	25	23	32	30
		CPU seconds	1.902	1.658	10.403	9.020
	D	No. of iteration	26	24	40	35
		CPU seconds	1.680	1.470	12.959	5.461
KM(I, [AP, I-∞])	S	No. of iteration	25	23	31	30
		CPU seconds	1.909	1.658	9.837	9.014
	D	No. of iteration	26	24	40	35
		CPU seconds	1.680	1.470	12.959	5.461
KM(I, [R, A-1])	S	No. of iteration	25	23	31	30
		CPU seconds	1.692	1.499	8.574	7.874
	D	No. of iteration	26	24	40	35
		CPU seconds	1.280	1.148	7.939	6.355

6. CONCLUSION

The Krylov subspace methods involve two main parts, one is the auxiliary matrix and the other is the direction technique. The auxiliary matrix determines the existence of an approximate solution at each iteration. One rule used to confirm the existence of a unique solution at each iteration is to choose an auxiliary matrix Z which satisfies the ZA is nonzero-real condition. On the other hand, the direction technique decides the construction of the direction vectors. In some cases the construction may fail because of stagnancy or shock. Stagnancy will not occur, if we use a type-AP or type-AR technique, but it may occur for type-R case. However, we can avoid this by choosing Z to be nonzero-real. Shock will not appear if the second auxiliary matrix M is nonzero-real.

Frankly speaking, it is not easy to check whether a matrix is nonzero-real. So we adapt the auxiliary matrix dynamically to the Krylov subspace method, and obtain a new method called the Unitary Basis Method. Moreover, the dynamical auxiliary matrix idea can be adapted to other Krylov subspace methods, which saves CPU time. We also remark that more memory storages are needed when adapting the auxiliary matrix dynamically.

ACKNOWLEDGEMENTS

We would like to express our thanks to Professor David M. Young at the Center for Numerical Analysis, The Univiversity of Texas at Austin, for his comments and his interest in this research. Financial support by the National Science Concil of the Republic of China under grant NSC-75-0201-M030D-01 is also gratefully acknowledged. Finally, we wish to thank the Data Communication Institute for providing time on the Cyber 180/830 computer.

REFERENCE

(1) O. Axelsson, *Lin. Alg. Appl.* 29, 1 (1980).
(2) S.C. Eisenstat, H.C. Elman, and M.H. Schulz, *SIAM J. Numer. Anal.* 20, 345 (1983).
(3) H.C. Elman, Iterative methods for large sparse nonsymmetric systems

of linear equations, Ph. D. Dissertation, alse Research Report 229, (Department of Computer science, Yale Univ., New Haven, CT., 1982).
(4) M.R. Hestenes, and E.L. Stiefel, *J. Res. Nat. Bur. Standards* 49, 409 (1952).
(5) Kang C. Jea, Generalized conjugate gradient acceleration of iterative methods, Ph. D. Dissertation (Report CNA-176, Center for Numerical Analysis, The University of Texas at Austin, 1982).
(6) Y. Saad, *Math. Com.* 37, 105 (1981).
(7) Y. Saad, and M.H. Schultz, GMRES: a generalized minimal residual algorithm for solving nonsymmetric linear systems, Research Report 254, (Department of Computer Science, Yale University, 1983).
(8) P.K.W. Vinsome, "ORTHOMIN, an iterative method for solving sparse sets of simultaneous linear equations," Paper SPE 5729, 4th Symposium of Numerical Simulation of Reservoir Performance of Soc. of Petr. Engrs. of AIME, Los Angeles, February 19-20 (1976).
(9) David M. Young, *Iterative Solution of Large Linear Systems*, (Academic Press, New York, 1971).
(10) David M. Young, and Kang C. Jea, *Lin. Alg. Appl.* 34, 159 (1980).
(11) David M. Young, and Kang C. Jea, *Generalized conjugate gradient acceleration of iterative methods, Part II: The nonsymmetrizable case*, Report CNA-163, Center for Numerical Analysis, (The University of Texas at Austin, 1981).
(12) 莊陸翰，用 Krylov 子空間法解非對稱線性系統，碩士論文，輔仁大學數學研究所 (1986).

Krylov 子空間法解大型線性系統之架構

數 學 系

莊 陸 翰 張 康

摘 要

我們探討用 Krylov 子空間法來解大型線性系統 $Ax=b$. Krylov 子空間法之兩個組成要素是輔助矩陣之選取與方向向量之建構規則。這些方法有時會發生障礙，無法繼續執行，我們歸納出三類障礙依其發生因由之不同而定名爲中斷 (break-down)，停滯 (stagnancy)，與休克 (shock)。我們指出如果輔助矩陣 Z 滿足 ZA 爲非零實的 (nonzero-real)，則中斷不會發生，如果方向向量不是 R-型架構，則停滯的現象不會出現，如果方向向量爲 M-半正交，且M爲非零實的，則休克亦不會產生。

NOTE ON MATRIX DIFFERENTIAL EQUATIONS

YI-CHING YEN

Department of Mathematics

ABSTRACT

Given a matrix differential equation $dX/dt = AX$ with ${}^tA = -A$, then the solution vectors of X are pairwise orthogonal. Applying this property, some other results can be deduced, such as when a column vector differential equation is solved, then the whole matrix differential equation can be solved uniquely under the given initial conditions.

1. INTRODUCTION

By the existance and uniqueness theorems of differential equations, it is known that given a matrix differential equation

$$\frac{dX}{dt} = A(t)\,X(t) + B(t),\quad X = \begin{bmatrix} x_{11} \cdots x_{1n} \\ \vdots \\ x_{m1} \cdots x_{mn} \end{bmatrix},$$

$$A = \begin{bmatrix} a_{11} \cdots a_{1m} \\ \vdots \\ a_{m1} \cdots a_{mm} \end{bmatrix} \quad \text{and} \quad B = \begin{bmatrix} b_{11} \cdots b_{1n} \\ \vdots \\ b_{m1} \cdots b_{mn} \end{bmatrix}, \qquad (1)$$

if the matrics A and B are continuous in $[a, b] \subseteq R$, then we have (a, b) as the maximum interval of existance of every solution of (1). In fact, given a constant matrix X_0 at $t_0 \in (a, b)$, then there exists a unique solution $X(t)$ satisfying $X(t_0) = X_0$[1].

It is also known that the general solution of (1) is a particular solution of (1) adding the general solution of the matrix defferential equation

$$\frac{dX}{dt} = A(t)\,X(t), \quad X = \begin{bmatrix} x_{11} \cdots x_{1n} \\ \vdots \\ x_{m1} \cdots x_{mn} \end{bmatrix}, \quad A = \begin{bmatrix} a_{11} \cdots a_{1m} \\ \cdots \\ a_{m1} \cdots a_{mm} \end{bmatrix},$$

$$A \in C^0[a, b]. \qquad (2)$$

Therefore, the solution of (2) is a major part of the solution of (1).

We will now determine some properties of the differential equation (2), restricting the number n of column vectors of $X(t)$ to be no more than the number m of row vectors, since every column vector of $X(t)$ belongs to m-dimensional vector space, in which n vectors satisfying $n>m$ are linearly dependent.

2. WE BEGIN OUR DISCUSSION WITH

Theorem 1. Given a matrix defferential equation

$$\frac{dX}{dt} = A(t)\,X(t), \quad X=\begin{bmatrix} x_{11} \cdots x_{1n} \\ \vdots \\ x_{m1} \cdots x_{mn} \end{bmatrix}, \quad A=\begin{bmatrix} a_{11} \cdots a_{1m} \\ \vdots \\ a_{m1} \cdots a_{mm} \end{bmatrix},$$
$$A\in C^0[a, b], \quad {}^tA = -A, \tag{3}$$

then for

$$X_j=\begin{bmatrix} x_{1j} \\ \vdots \\ x_{mj} \end{bmatrix}, \quad X_j \cdot X_k = \text{constant}, \quad 1\leq j, \quad k\leq n(\leq m). \tag{4}$$

Proof. By (4), we have

$$x_{ij}' = \sum_{k=1}^{m} a_{ik}\,x_{kj}, \quad \text{where} \quad x_{ij}' = \frac{d}{dt}x_{ij}. \tag{5}$$

Now

$$(X_j \cdot X_k)' = \left(\sum_{i=1}^{m} x_{ij}\,x_{ik}\right)'$$
$$= \sum_{i=1}^{m} (x_{ij}'\,x_{ik} + x_{ij}\,x_{ik}')$$
$$= \sum_{i=1}^{m}\left[\left(\sum_{l=1}^{m} a_{il}\,x_{lj}\right)x_{ik} + x_{ij}\left(\sum_{l=1}^{m} a_{il}\,x_{lk}\right)\right].$$

Interchanging i and l in the second term, we get

$$(X_j \cdot X_k)' = \sum_{1\leq i,\,l\leq n} (a_{il} + a_{li})\,x_{lj}\,x_{ik}$$
$$= 0, \tag{6}$$

since

$${}^tA = -A.$$

(6) implies that $X_j \cdot X_k = \text{constant}$, $1\leq j, k\leq n$.

Thus, for an initial condition $X_0 = I_n$, $t_0 \in (a, b)$, $n = m$, we get

$$X_j(t) \cdot X_k(t) = E_j \cdot E_k = \delta_{jk},$$

where

$$E_j = \begin{pmatrix} 0 \\ \vdots \\ 0 \\ 1 \\ 0 \\ \vdots \\ 0 \end{pmatrix} \Big\} j, \qquad j, k = 1, \ldots, n.$$

Hence we obtain:

Corollary. Let $X(t)$ be the solution of

$$X'(t) = A(t)\,X(t), \quad X(t_0) = I_n, \quad t_0 \in (a, b).$$

where

$$X = \begin{bmatrix} x_{11} \ldots x_{1n} \\ \vdots \\ x_{n1} \ldots x_{nn} \end{bmatrix}, \quad A = \begin{bmatrix} a_{11} \ldots a_{1n} \\ \vdots \\ a_{n1} \ldots a_{nn} \end{bmatrix}, \quad \in C^0[a, b],$$

$$^tA = -A, \tag{7}$$

then $X(t)$ is an orthogonal matrix $\forall t \in J \subseteq (a, b)$.

Theorem 2. Given a matrix differential equation

$$X'(t) = A(t)\,X(t), \quad X(t_0) = X_0, \quad t_0 \in (a, b),$$

where

$$X = \begin{bmatrix} x_{11} \ldots x_{1n} \\ \vdots \\ x_{n1} \ldots x_{nn} \end{bmatrix} \text{ and } A = \begin{bmatrix} a_{11} \ldots a_{1n} \\ \vdots \\ a_{n1} \ldots a_{nn} \end{bmatrix} \in C^0[a, b]. \tag{8}$$

If n linearly independent solutions of the matrix differential equation

$$\begin{bmatrix} \lambda_1 \\ \vdots \\ \lambda_n \end{bmatrix}' = -{}^tA(t) \begin{bmatrix} \lambda_1 \\ \vdots \\ \lambda_n \end{bmatrix}, \qquad t \in [a, b]. \tag{9}$$

are found within $t \in J \subseteq (a, b)$ and $t_0 \in J$, then (8) can be solved simultanously $\forall t \in J$.

Proof. Let $X^j = (x_j \ldots x_{jn})$,

$$X^j(t_0) = (x_{j1}(t_0) \ldots x_{jn}(t_0)), \qquad j = 1, \ldots, n. \tag{10}$$

Put

$$Y(t) = \sum_{j=1}^{n} \lambda_j(t)\, X^j(t), \tag{11}$$

then

$$\begin{aligned} Y' &= \sum_{j=1}^{n} (\lambda_j' X^j + \lambda_j X^{j\prime}) \\ &= \sum_{j=1}^{n} \left[\lambda_j' X^j + \lambda_j \left(\sum_{k=1}^{n} a_{jk} X^k \right) \right] \\ &= \sum_{j=1}^{n} \left(\lambda_j' + \sum_{k=1}^{n} a_{kj} \lambda_k \right) X^j \\ &= 0, \end{aligned} \tag{12}$$

since by (9),

$$\lambda_j' + \sum_{k=1}^{n} a_{kj} \lambda_k = 0. \tag{13}$$

Thus,

$$Y(t) = \text{constant}, \quad \forall t \in (a, b). \tag{14}$$

Let the n linearly independent particular solutions of λ_j be $\phi_j^1, \ldots, \phi_j^n$, $j = 1, \ldots, n$, then by (13),

$$\phi_j^{i\prime} + \sum_{k=1}^{n} a_{kj} \phi_k^i = 0, \quad i, j = 1, 2, \ldots, n. \tag{15}$$

Let

$$Y^i(t) = \sum_{j=1}^{n} \phi_j^i(t)\, X^j(t), \tag{16}$$

then as we have done in (14),

$$Y^i(t) = \text{constant}, \quad \forall t \in (a, b), \tag{17}$$

which implies that

$$\sum_{j=1}^{n} \phi_j^i(t)\, X^j(t) = \text{constant} = \sum_{j=1}^{n} \phi_j^i(t_0)\, X^j(t_0) = (c_1^i \ldots c_n^i), \tag{18}$$

say, $\forall t \in (a, b)$, $i = 1, \ldots, n$. Then

$$X(t) = (x_{jk}(t)), \quad 1 \leq j, \quad k \leq n,$$

can be found as

$$x_{jk}(t) = \frac{\begin{vmatrix} \phi_1^1(t) \dots c_k^1 \dots \dots \phi_n^1(t) \\ \vdots \\ \phi_1^n(t) \dots c_k^n \dots \dots \phi_n^n(t) \end{vmatrix}}{\begin{vmatrix} \phi_1^1(t) \dots \phi_j^1(t) \dots \phi_n^1(t) \\ \vdots \quad\quad \vdots \quad\quad \vdots \\ \phi_1^n(t) \dots \phi_j^n(t) \dots \phi_n^n(t) \end{vmatrix}}, \quad \forall t \in \mathrm{J} \subseteq (a, b). \tag{19}$$

$$\begin{vmatrix} \phi_1^1(t) \dots \phi_n^1(t) \\ \vdots \quad\quad \vdots \\ \phi_1^n(t) \dots \phi_n^n(t) \end{vmatrix} \neq 0, \quad \forall t \in \mathrm{J} \subseteq (a, b),$$

since it is the Wronskian determinant of n linearly independent particular solutions of λ_j, $j = 1, \dots, n$.

As its special case, we have the following:

Corollary. Given a matrix differential equation

$$\mathrm{X}'(t) = \mathrm{A}(t)\,\mathrm{X}(t), \qquad \mathrm{X} = \begin{bmatrix} x_{11} \dots x_{1n} \\ \vdots \quad\quad \vdots \\ x_{n1} \dots x_{nn} \end{bmatrix},$$

$$\mathrm{A} = \begin{bmatrix} a_{11} \dots a_{1n} \\ \vdots \quad\quad \vdots \\ a_{n1} \dots a_{nn} \end{bmatrix}, \tag{20}$$

A being continuous in $[a, b] \ni {}^t\mathrm{A} = -\mathrm{A}$, and the initial matrix $\mathrm{X}_0 = (x_{ij}^0)$ is given at $t_0 \in (a, b)$.

If n linearly independent particular solutions of any column vector of (20) are found, say,

$$\begin{bmatrix} x_{11} \\ \vdots \\ x_{n1} \end{bmatrix}' = \mathrm{A}(t) \begin{bmatrix} x_{11} \\ \vdots \\ x_{n1} \end{bmatrix} \tag{21}$$

is solved, then the unique matric solution $\mathrm{X}(t)$ of (20) satisfying $\mathrm{X}(t_0) = \mathrm{X}_0$ can be found immediately.

Proof. In the equation (21), we regard x_{j1} as λ_j, $j = 1, \dots, n$, and with ${}^t\mathrm{A} = -\mathrm{A}$, the equation (21) becomes the equation (9), which induces (20) to have the solution $\mathrm{X}(t)$ as given in (19).

REFERENCE

(1) L. Pontrayagin, *Ordinary Differential Equations*, (Addison Wesley, Reading Mass., 1962), p. 127.

矩陣微分方程式的幾個特性

數　學　系

顏　一　清

摘　要

給定矩陣微分方程式

$$\frac{dX}{dt} = AX, \quad {}^tA = -A \tag{1}$$

則其各行向量解相互正交。由此可推出若干性質，如：若(1)式中的一行向量得解，則(1)式整個對於給定的初具條件可得到唯一解。

SCINTILLATION ANALYSIS USING AN INDICATOR VARIABLE

JOHN R. KOSTER

Department of Physics

ABSTRACT

A method of analysing scintillation data is presented, suitable for cases where scintillation can be represented as an indicator (binary) variable. The method is applied to the problem of the dependence of scintillation at Lunping, Taiwan on magnetic activity, as expressed in the K_p indices. Successive refinements of the analysis are presented, and some new dependencies are found. The method is recommended for the analysis of other similar geophysical variables.

1. INTRODUCTION

In the analysis of scintillation data, the analyst is frequently faced with an annoying problem. The variable in the time series under consideration may have the value 0 for a large fraction of the observing time. In trying to do a statistical analysis of such data using linear regression, one is faced with the requirement that the variable be normally distributed. Since most of the data transformation methods available cannot cope with data of the kind mentioned, the requirement is frequently ignored. While the result may still have some meaning, the uncertainties limit the careful analyst to qualitative statements, while those who blithely ignore the requirements of the statistical method used may be led into error.

A great deal of scintillation data is available from widely scattered stations in the form of 15-minute values of the scintillation index, SI, expressed in decibels. In such problems as the design of communication systems, the amplitude of SI is of critical importance. This scintillation depth is not only a function of the particular location, but also of the look angle, since field-aligned irregularities are usually involved, and ray path direction relative to the magnetic

field is an important parameter. In many model studies, however, the presence or absence of scintillation is the important consideration. A possible method open to the analyst under these circumstances is the use of a regression model with an indicator response variable[1]. By 'indicator response variable' we mean one which has only two possible values, 0 or 1—a binary variable. We consider a model described by:

$$y_i = b_0 + b_1 x_i + e$$

where y_i is the response variable, x_i is the regression variable, and e is the error term. Since y_i can take only the values of 0 or 1, a reasonable probability model for the response is the Bernoulli distribution—i.e., a distribution in which the random variable y_i takes on the value 1 with a probability $P(y=1) = p_i$, and the value 0 with a probability $P(y=0) = 1 - p_i$. The mean of the Bernoulli distribution is:

$$E(y_i \mid x_i) = p_i$$

where $E(y_i|x_i)$ has the meaning: "the expectation of y_i when x takes the value x_i." We then write:

$$E(y_i \mid x_i) = b_0 + b_i x_i = p_i$$

and interpret the response as the probability that $y_i=1$ when the regression variable takes the value x_i.

The purpose of this paper is twofold. We intend to first explain how the indicator variable method may be used for the analysis of scintillation and other like variables. We next wish to illustrate its use by applying it to a simple case study—the dependence of scintillation at Lunping, Taiwan, on the planetary magnetic index K_p. We shall first look at the broad picture on a seasonal basis. We then consider some more precise limitations on time and on the amplitude of K_p.

2. THE DATABASE

Our regression variable will be the eight daily 3-hourly planetary K_p indices. Since our purpose in this first analysis is mainly

illustrative, we shall not introduce any complicating sophistications, but will use the daily sum of the K_p indices, with no compensation for the fact that Taiwan's local time leads UT by eight hours.

Our scintillation data will consist of values of the scintillation index (SI), expressed in *db* and determined at 15-minute intervals. We shall consider all values of SI, starting at sunset and extending over a period of 8 3/4 hours (35 15-minute time intervals). If more than N of these intervals have a value of SI equal to or greater than 3 *db*, y_i will have the value 1, otherwise y_i will have the value 0. We can experiment with different values of N—values of 1,2, or 3 will make little difference in the results of the analysis. In the results given in this paper, N has the value 3.

The SI data were taken at Lunping, Taiwan (longitude: 121° E, latitude: 25° N, dip: +31°), using the 136.112 Mhz signal radiated by ETS-2, in synchronous orbit at a nominal position of 130° E. longitude. Elevation and azimuth are approximately 60° and 160° respectively. The data were taken over the two year period 1 May, 1981 to 30 April, 1983 inclusive. Because the satellite beacon was switched off during periods of daily eclipsing, there is a gap of approximately 45 days et each equinox. A total of 526 days of valid data were obtained over the two-year interval.

For seasonal analysis we normally divide the year into 4 periods of approximately 91 days each, centered on the equinoxes and solstices. Because of the gap in the data at the equinoxes, however, the spring and autumn data are combined, and we shall determine results for three seasons: winter, equinox and summer.

To give an indication of the distribution of the two variables, the sum of the K_p indices, and the number of periods with SI equal to or greater than 3 *db*, we show boxplots of the raw data. The reader will recall that the boxplot displays a data set by means of a box whose center is the median of the distribution and whose ends (the 'hinges') are the lower and upper quartiles. The 'H-spread' is the distance between the upper and lower hinges, and a 'step' is equal to 1 1/2 H-spreads. The observation furthest from the median that still remains within 1 step from each hinge is shown with

a — sign. Individual points within the second step are marked by a O, those beyond the second step the symbol X. A number under the symbol indicates that multiple points fall at that location. The boxplot can thus show a great deal about the distribution of the variables at a glance.

It can be seen from Fig. 1 that the distribution of the sum of

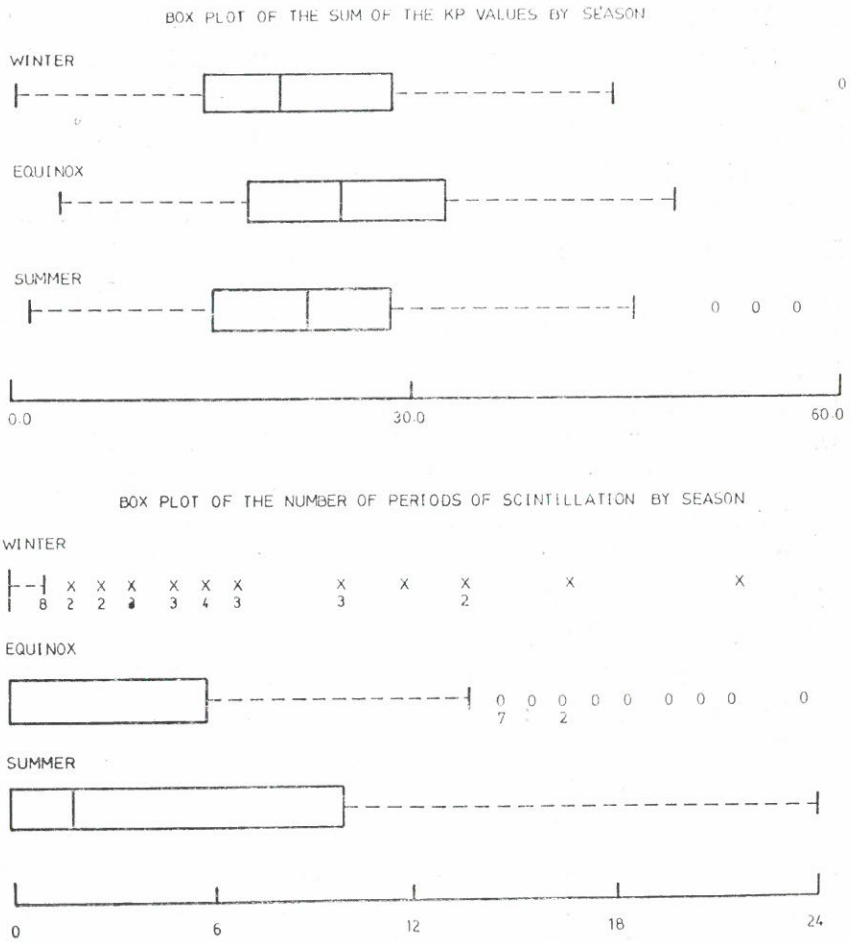

Fig. 1. Boxplots showing the distribution of the sum of K_p in winter, equinox, and summer (upper plot) and the number of 15-minute periods showing SI greater than 3 db for the corresponding seasons (lower plot).

K_p is at least approximately normal, and one whould not expect any serious problems in using it in a regression analysis. The SI variable, however, is quite another matter. For the winter season, the whole box has collapsed onto the origin, and all the non-zero values of SI are considered as 'outliers'. At the equinox the median is at the origin, while in the summer the lower quartile falls there. Although the upper portion of the last two distributions would appear to be more tractable, any attempt to transform these distributions into normal ones is clearly doomed to failure. Hence we have had recourse to an indicator variable.

3. ANALYSIS 1

In the analyses which follow, we shall follow quite closely the non-linear model given by Montgomery and Peck[1]. Our response is modelled using the so called 'logistic function':

$$E(y|x) = \exp(b_0 + b_1 x) / [1 + \exp(b_0 + b_1 x)]$$

This function has the characteristic S shape, with asymptotes at 0 and 1, ensuring that our estimated response function will lie between these limits. It also has the property of being easily linearized by the simple transformation:

$$p^* = \ln [E(y|x)) / (1 - E(y|x))] = \ln [p / (1 - p)]$$

and our linearized model becomes:

$$p^* = b_0 + b_1 x$$

To fit the logistic response, we must have repeat observations on y at each level of x. We shall do this by sorting our data, using x as key, and then dividing them into ten decile groups. For each group we then have:

$\bar{x}_i$ = the mean value of x in the group, and

$\bar{p}_i = c_i / n_i$

where $i=1,2,\ldots 10$, n_i is the number of observations in the group, and c_i is the number of 1's in the group. We now have $\bar{p}^* = \ln [\bar{p}_i / (1 - \bar{p}_i)]$ as our response variable.

One problem remains. The variance of the errors is not constant, which means a violation of the basic regression assumptions. The use of weighted least squares, with weights chosen so as to be inversely proportional to the variance of p_i* will overcome this problem. If n is large, the variance of p_i* is given by:

$$V(p_i^*) = 1/[n_i\, p_i(1-p_i)]$$

where p_i is the true probability that $y_i=1$ when $x=x_i$. If p_i is replaced by its estimated value from above, then:

$$V(\bar{p}_i^*) = 1/[n_i\, \bar{p}_i(1-\bar{p}_i)]$$

and our weights are given by:

$$w_i = n_i\, \bar{p}_i(1-\bar{p}_i), \quad i = 1,2,\ldots, m$$

Table 1 shows, by way of example, the variables and their values, as used for the analysis of our data for the winter season. The actual regression analysis is done using a standard linear regression subroutine which uses weighted least squares. The RLFOR routine from the IMSL (International Mathematics and Statistics Library) scientific subroutine library was used in this example. The adequacy of the model was carefully investigated for

Table 1. Sample of input data for analysis of SI versus the sum of K_p for winter

Group	$\bar{X}$	$\bar{P}$	P*	Weight
1	38.0556	0.3333	−0.6931	4.0000
2	30.8333	0.1111	−2.0794	1.7778
3	27.6111	0.1667	−1.6094	2.5000
4	24.5556	0.0556	−2.8332	0.9444
5	21.5000	0.0556	−2.8332	0.9444
6	19.3333	0.0556	−2.8332	0.9444
7	17.3889	0.1111	−2.0794	1.7778
8	14.8889	0.1111	−2.0794	1.7778
9	11.1667	0.1111	−2.0794	1.7778
10	6.4500	0.0500	−2.9444	0.9500

all three seasons using residual analysis, and the model seems to meet all the required criteria.

4. RESULTS OF ANALYSIS 1

The values of some basic parameters for all three seasons are summarized in Table 2. Variables shown are: the season; the number of days' data for that season (NOP); the value of F (from the statistical F-distribution); the probability that this value of F could arise purely by chance (Q); and the coefficient of determination (PCT), usually represented by R^2 and interpreted as the percent of the variation explained by the regressor, x. Also shown are the regression coefficients b_0 and b_1, and their standard errors.

The plots of the calculated probability of scintillation at Lunping as a function of the value of the sum of the K_p values are shown in Fig. 2, with a separate curve for each of our three seasons. Values of the coefficient of determination (R^2) for the three seasons are shown at the top of Fig. 3. R^2 is, of course, a positive quantity, but when the correlation coefficient is negative, we plot the corresponding R^2 in the negative direction, to emphasize the negative correlation involved.

5. DISCUSSION

These results are in broad agreement with many of those reported in the literature for equatorial stations[2,3] and also with those for Asian mid-latitudes[4]. Winter in Asia shows an extremely small probability of scintillation, but p does increase with magnetic activity. Summer (in Asia) shows a very large amount of scintillation, but it exhibits a very small dependence on magnetic activity. The equinoxes show the often reported negative dependence, with a slope whose absolute value is considerably larger than that for other seasons. Equinoctial days during magnetic disturbances exhibit an extremely small probability of scintillation, according to this result. We shall soon have to amend this statement somewhat, as later results will show.

Table 2. Results from the three analyses done in this paper
Symbols are described in the text

Season	NOP	F	Q	PCT	B(0)	S.E.	B(1)	S.E.
Regression of S.I. on SUMKP								
Win.	182	11.7450	0.0090	59.4843	−3.2598	0.4410	0.0577	0.0168
Equ.	166	11.4800	0.0095	58.9323	1.3152	0.5848	−0.0806	0.0238
Sum.	178	1.0772	0.3297	11.8669	−0.7062	0.4523	0.0188	0.0181
K_p=0 to K_p=9 inclusive								
Season	NOP	F	Q	PCT	B(0)	S.E.	B(1)	S.E.
Regression of S.I. on K_p(5)								
Win.	183	24.1128	0.0012	75.0878	−3.6203	0.3980	0.5468	0.1114
Equ.	175	0.0820	0.7819	1.0141	−0.9087	0.4619	−0.0381	0.1332
Sum.	180	1.0789	0.3293	11.8840	−1.5727	0.4610	0.1429	0.1375
Regression of S.I. on K_p(6)								
Win.	183	7.6008	0.0248	48.7205	−3.4181	0.5164	0.3740	0.1357
Equ.	175	4.1630	0.0756	34.2266	−0.1703	0.3474	−0.2153	0.1055
Sum.	180	15.9681	0.0040	66.6224	−1.3002	0.1603	0.1866	0.0467
Regression of S.I. on K_p(7)								
Win.	183	17.6403	0.0030	68.7991	−4.5791	0.4347	0.5245	0.1249
Equ.	175	9.7238	0.0143	54.8630	−0.9093	0.2192	−0.2233	0.0716
Sum.	180	3.9895	0.0808	33.2752	−1.6060	0.2679	0.1624	0.0813
K_p=0 to KP=4 inclusive								
Season	NOP	F	Q	PCT	B(0)	S.E.	B(1)	S.E.
Regression of S.I. on K_p(5)								
Win.	183	4.2901	0.0721	34.9068	−2.9971	0.4761	0.3206	0.1548
Equ.	175	18.4995	0.0026	69.8107	0.0421	0.2923	−0.4736	0.1101
Sum.	180	24.2416	0.0012	75.1874	−0.2182	0.2284	−0.4058	0.0824
Regression of S.I. on K_p(6)								
Win.	183	3.7136	0.0901	31.7034	−3.3396	0.5627	0.3364	0.1746
Equ.	175	43.0721	0.0002	84.3359	0.3145	0.1877	−0.4509	0.0687
Sum.	180	16.2312	0.0038	66.9847	−1.4482	0.1743	0.2546	0.0632
Regression of S.I. on K_p(7)								
Win.	183	12.4381	0.0078	60.8574	−4.5735	0.4709	0.5221	0.1480
Equ.	175	8.5919	0.0190	51.7838	−0.8699	9.2152	−0.2384	0.0813
Sum.	180	0.6852	0.4318	7.8895	−1.4398	0.2915	0.0852	0.1029
K_p=4 to K_p=9 inclusive								
Season	NOP	F	Q	PCT	B(0)	S.E.	B(1)	S.E.
Regression of S.I. on K_p(5)								
Win.	183	700.9600	0.0000	98.8716	−4.3382	0.1290	0.7228	0.0273
Equ.	175	19.9243	0.0021	71.3511	−4.8578	0.8460	0.7590	0.1700
Sum.	180	2737.4377	0.0000	99.7086	−6.3593	0.1044	1.0598	0.0203
Regression of S.I. on K_p(6)								
Win.	183	109.9331	0.0000	93.2165	−2.6530	0.1006	0.2372	0.0226
Equ.	175	0.5048	0.4976	5.9359	−1.8004	1.0916	0.1686	0.2372
Sum.	180	0.1677	0.6929	2.0534	−0.4315	0.2089	0.0177	0.0432
Regression of S.I. on K_p(7)								
Win.	183	42.4304	0.0002	84.1365	−3.3820	0.1880	0.2871	0.0441
Equ.	175	0.1163	0.7419	1.4325	−1.7528	0.6072	−0.0447	0.1312
Sum.	180	87.0066	0.0000	91.5795	−3.3268	0.2547	0.5190	0.0556

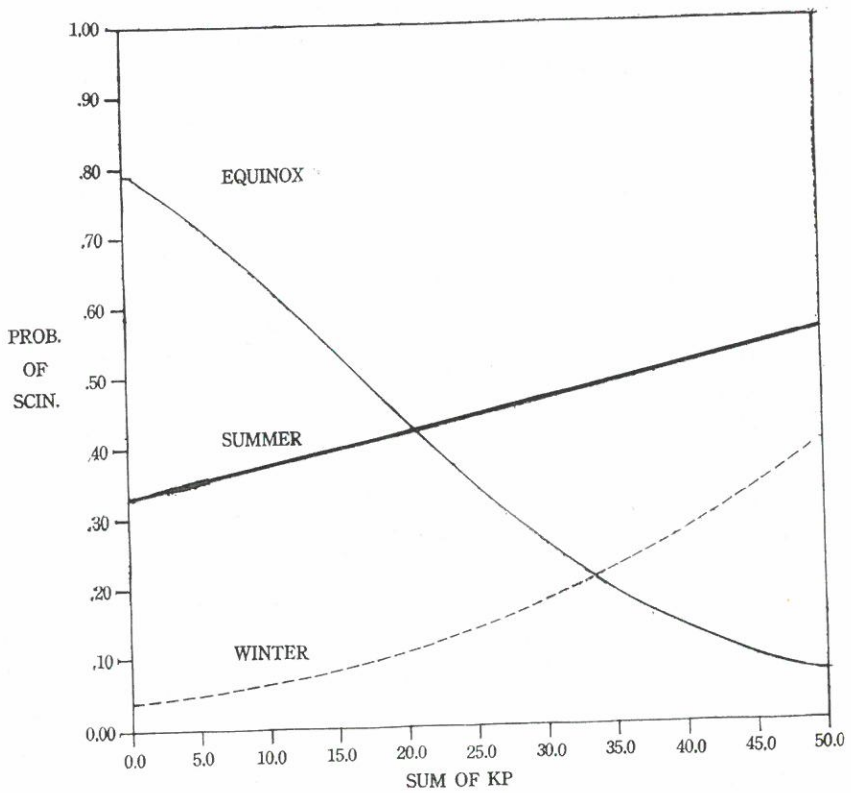

Fig. 2. The probability of scintillation as a function of the sum of K_p for winter, equinox and summer.

One practical problem can easily arise in the analysis described above. It can happen that, in the determination of $\bar{p}_i(=c_i/n_i)$, c_i may assume the values of 0 or n_i, and we have a $\bar{p}_i$ value of 0 or 1, either of which will cause problems, since we use the natural log of $\bar{p}_i$ and $1-\bar{p}_i$. Cox[5] discusses this problem at some length, and suggests various methods of dealing with it. In most cases, it can be easily met by altering c_i by $+1$ or -1 as required, without significantly altering the result of the analysis. Alternatively, $\bar{p}_i$ can be replaced by $\bar{p}_i + e$, where e is an arbitrarily small quantity. In this case, w_i becomes extremely small, and the point has virtually no effect on the regression. This has no effect on the final

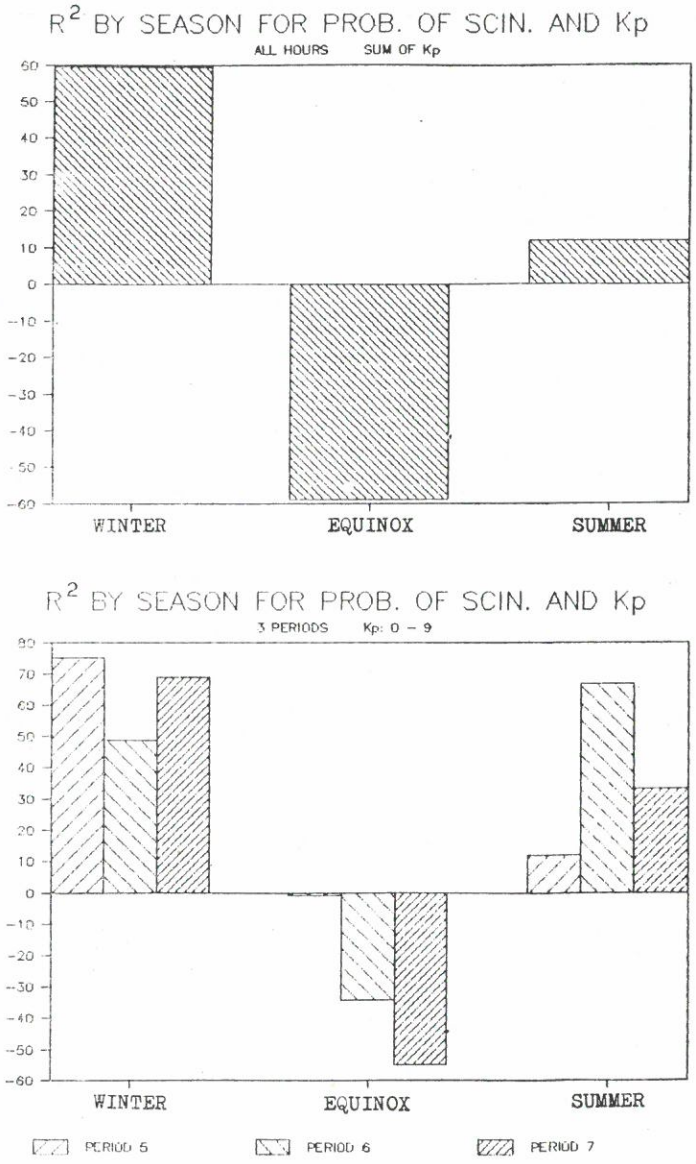

Fig. 3. Coefficient of determination (R^2) by season between (a) probability of scintillation and quantiles of the sum of K_p for the whole night, and (b) between the probability of scintillation and individual K_p values for three 3-hour periods.

probability curve, either, except possibly at the extreme ends, as Cox[5] notes.

6. A SECOND ANALYSIS—IMPROVING TIME RESOLUTION

The analysis performed thus far has proved to be exceptionally easy to use, and it has given us results in a form that is easy to interpret. But it has not not shown anything that could not have been discovered by the more conventional methods currently in use. It is always interesting to try to extend a new method beyond current usage, to see whether it will give useful new information.

With this in mind, we shall now attempt to improve our resolution in time, while using the same data base. We shall proceed by dividing the night into three intervals: post-sunset (20 to 23 H), midnight (23 to 02 H), and pre-dawn (02 to 05 H) local time. It will be noted that these intervals, after taking account of the fact that local time is 8 hours ahead of UT, correspond precisely with the periods covered by K_{p5}, K_{p6}, and K_{p7} of the eight planetary K figures. We shall then analyze each of the three-hour periods separately. For each we shall group our data into ten categories, based on the 10 possible values of K_p (0 to 9 inc.). The three seasons will be treated separately.

The method of analysis is essentially the same as before, but now our groups will be of unequal size, because of the distribution of the K_p values. We must be aware of two possible violations of the requirements of our method. In the first case, n_i, the number of data points in a given group, may not be large—as we have assumed in deriving the expression for the variance which we have used in the determination of our weights. This will almost certainly cause no serious problems, however, since the corresponding weights will be extremely small, and thus make a negligible contribution to our linear regression. Secondly, we may even have some null groups, especially at $K_p=0$ or $K_p=9$. These will be dealt with by assigning to them vanishingly small values of $\bar{p}$, and correspondingly small vales of w.

Parameters arising from this analysis are shown in the appropriate entries in Table 2. The reader will note that the resulting probabilities of scintillation are basically the same as they were before—winter and summer show positive slopes of p vs K_p, while the equinox slopes are negative.

If, however, we compare the results of the three discrete time intervals, some new information emerges. This can be most clearly seen in Fig. 3(b), where we again show values of R^2 by season, the three intervals being shown separately for each season. We call attention to two important new pieces of information:

(1) In winter the value of R^2 is relatively large in the post-sunset and pre-dawn intervals, considerably smaller around midnight. In summer, the reverse is true. This fact will be used later in support of a contention that the scintillation producing mechanisms at Lunping are different in winter and in summer.

(2) The probability of scintillation during the post-sunset period at equinox and summer appears to have no significant correlation with K_p. This is the time period in which the equatorial bubble-formation mechanism is known to maximize. This surprising and highly anomalous result will be explained when we have the results of analysis 3.

7. A THIRD ANALYSIS—A NON-LINEAR KP DEPENDENCE

We shall now attempt a further extension of the method by changing the assumption that p^* is a monotonic and linear function of K_p. This implies that the slope of our p^* versus K_p curve may change sign as K_p goes from 0 to 9. In a recent paper concerning scintillation in Japan, Kumagai[4] states that the dependence of p on K_p changes for large values of K_p. For $K_p > 4$, scintillation almost always occurs and the slope of the p versus K_p curve is positive. To determine whether this is also true for Lunping, we can proceed in either of two ways. We can, still using our logistic function, fit a higher degree polynomial rather than a straight line to our values of p^* and K_p. Or we can try using two straight lines in succession—fitting one to the values of K_p from 0 to 4, and an

independent one to the values of K_p from 4 to 9. Both methods are extremely easy to implement, but since polynomial regression models are frequenty lacking in robustness, we shall opt for method 2, and stay with a linear model. The raw data need not be changed. We shall merely assign negligible weights to the unwanted part of the K_p distribution, and proceed exactly as before. Results are contained in Table 2, but we shall extract the relevant information and show it in simplified form in Fig. 4.

A study of Fig. 4 reveals several new items of information. Among these, the most important are:

(1) The surprising lack of correlation between the probability of scintillation and the K_p value in period 5 (post-sunset) of equinox and summer (see Fig. 3) is now explained. The correlation coefficient is large and negative when K_p is small, large and positive when K_p is large. Combining all K_p, as was done in analysis 2, masks the true relationship, suggesting no dependence of scintillation on K_p. The correlation is now seem to be strong, but non-linear.

(2) No season or time interval exhibits a significantly negative correlation when K_p is large. This is in full agreement with the finding of Kumagai for Japan. Our curve for the equinoctial season in Fig. 2 therefore needs amending, too. For larger values of the sum of K_p the slope should become positive. This positive slope appears for periods 5 and 6 in the data at the bottom of Table 2.

(3) The summer-time response of scintillation to K_p is puzzling. The reversal of correlation from negative to positive in period 5 is similar to the equinoctial behavior. Period 6 (midnight) has its correlation coefficient reduced from a high positive value to nearly zero, and period 7 is just the opposite. The reason for this is not obvious.

8. A WORKING HYPOTHESIS

This study of the relationship between VHF scintillation at Lunping and the degree of disturbance of the geomagnetic field as reflected in the value of the planetary index K_p was undertaken as

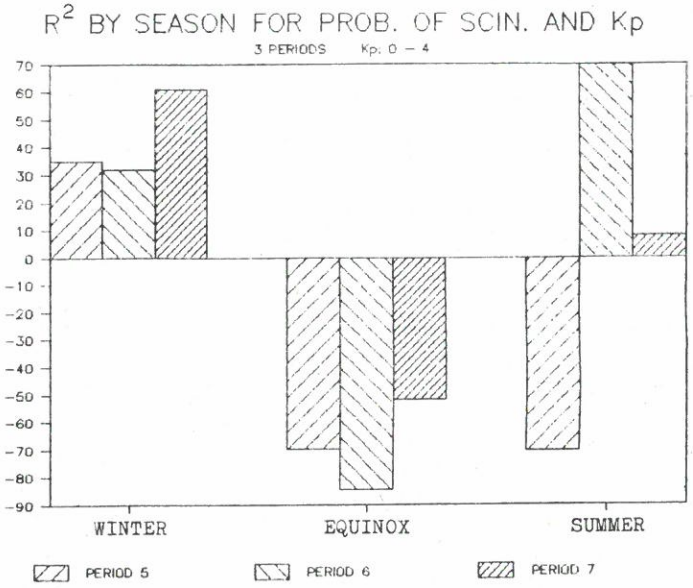

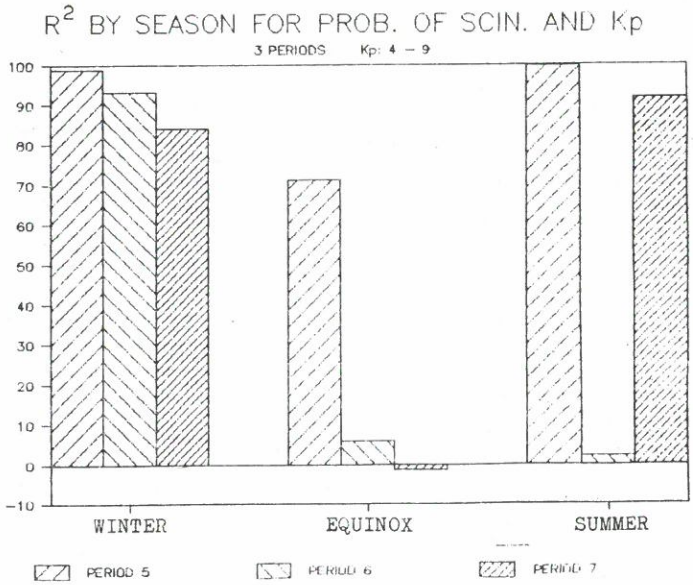

Fig. 4. Coefficient of determination (R^2) by season and period between probability of scintillation and K_p for (a) K_p values between 0 and 4, and (b) between 4 and 9.

a prelude to an attempt to establish the physical mechanisms responsible for Lunping scintillations. While these results are believed to be objectively correct, they are subject to a variety of interpretations—and possible interpretations are the subject of another paper. However, the results given above do suggest a working hypothesis concerning the origins of the scintillations. The elements of that hypothesis are:

a) Some scintillations of Lunping are attributable to the equatorial ionospheric bubble mechanism. It will be recalled that gigahertz scintillations show large equinoctial maxima and solstitial minima. Wernik *et al* have shown that this is case at Hong Kong and Guam in the Asian region[6]. It is generally agreed that the irregularities giving rise to these scintillations are produced by the equatorial bubble mechanism. It is also well known that this mechanism correlates negatively with K_p, especially in the pre-midnight hours. We therefore surmise that the equatorial bubble mechanism is a prime candidate for the explanation of much of our equinoctial scintillation. We shall call this mechanism 1.

b) Not all summer-time scintillations at Lunping can be attributed to irregularities formed by ionospheric bubbles at the equator. Gigahertz scintillation (and presumably equatorial bubbles) are relatively infrequent during the summer. Yet most of Lunping's scintillation occurs in the summer months, especially in June and July. An investigation of Manila TEC during these months shows that scintillation frequently occurs at Lunping when Manila TEC shows none of the usual signs of bubble formation[7]. Hence our working hypothesis would suggest that we must look for a second mechanism to explain the origin of much of the Lunping summer-time scintillation. We shall call this mechanism 2.

c) The origin of the scintillation during magnetic disturbances is problematical. It is almost certainly not due to mechanism 1, which shows a negative correlation with K_p. It may be identical with mechanism 2. Hence our hypothesis will include a mechanism 3—the irregularity production mechanism accompanying magnetic disturbances. It may or may not turn out to be distinct from mechanism 2.

9. CONCLUSION

In this paper we have presented a method that is easy to implement, robust, and potentially very useful in the analysis of scintillation, or of any other parameter met in geophysical research which lends itself to representation as an indicator variable. We have illustrated the method with a practical application, and not only verified for Lunping many characteristics of scintillation dependence on K_p that are already known for other equatorial and mid-latitude stations from more conventional methods of analysis, but also discovered a number of potentially new aspects of the dependence of SI on magnetic activity as reflected in K_p. The method itself seems to be quite widely used among statisticians, but has not yet been extensively applied to problems in ionospheric physics. It is felt that a more widespread use can contribute significantly to the solution of some outstanding problems that are less amenable to conventional methods.

ACKNOWLEDGEMENTS

Thanks are expressed to Dr. Yinn-Nien Huang for the provision of scintillation and TEC data from Lunping; to Dr. J. Klobuchar for TEC data from Manila.

This work has been sponsored by the National Science Council under Contract No. NSC 73-0204-M030-02.

REFERENCE

(1) D.C. Montgomery and A. Peck, *Introduction to linear regression analysis.* (John Wiley, 1982).
(2) J.R. Koster, *Planet. Spa. Sci.* 20, 1999 (1972).
(3) J.P. Mullen, *J. Atmos. Terr. Phys.* 35, 1187 (1973).
(4) H. Kumagai, *J. Geomag. Geoelectr.* 38, 267 (1986).
(5) D.R. Cox, *The Analysis of Binary Data.* (Methuen, London, 1970).
(6) A.W. Wernik, S. Franke, C.H. Liu, *Geophys. Res. Letters* 10, 2, 155 (1983).
(7) J.R. Koster, *Proceedings of The National Science Council of R.O.C.* 11, 1, 50 (1987).

以指示變數分析閃爍現象

物理系

高　士　達

摘　要

有一種分析閃爍數據的方法被提出，即以指示（二元）變數分析閃爍現象。此法可用於研究臺灣嵩坪上空閃爍現象與磁活動之關係，以 K_p 指數表示，成功的改善了分析方法，很多新的關係也被發現，此法亦適用於其他類似之地球物理變數的分析。

NARROW BAND PASS FILTERS

JEN-I CHEN and KUNG-TUNG WU

Department of Physics
Fu Jen Catholic University

ABSTRACT

The designs of all-dielectric optical narrow band pass filters of half-wave systems are carefully studied, and their properties are thoroughly investigated by the method of either the single stack calculation or the two effective interfaces analysis. Experimental fabrication and check are made with the use of MgF_2-CeO_2 interference multilayers. The results measured are found quite compatible with the designs.

INTRODUCTION

Multilayer filters have been designed with the equivalent layer systems[1,2], the single half-wave systems[3] and the double half-wave systems[4]. Filters of equivalent layer systems have been thoroughly studied in our previous works[2,5-7]. However, for the design of narrow band pass filters, it is much more efficient and economical to use single half-wave systems, on account of the number of layers used and the pass band shape desired. In this paper, we focus on the study and fabrication of narrow band pass filters of half-wave systems, that is multilayers consisting of different numbers of half-wave layers in between reflecting quarter-wave stacks. The best designs from theoretical calculations are chosen to be fabricated in the laboratory and their properties are measured.

Optical characteristics of half-wave multilayer systems can be evaluated by either the single stack calculation[8] or the two effective interfaces analysis[4]. The two effective interfaces analysis reveals more detailed information about the transmittance, the reflectance and the phase characteristics of two composing stacks, which are very helpful in the design.

Take the time factor of the light wave to be e^{-iwt}, the optical

properties of a homogeneous non-absorbing dielectric layer are completely represented by the following characteristic matrix

$$\mathrm{M} = \begin{pmatrix} \cos(k_0 nz\cos\theta) & -\frac{i}{p}\sin(k_0 nz\cos\theta) \\ -ip\sin(k_0 nz\cos\theta) & \cos(k_0 nz\cos\theta) \end{pmatrix} \tag{1}$$

where k_0 is the propagation vector of light in vacuum,

n is index of refraction,
z the thickness,
θ the incident angle,
$p = n\cos\theta$ for TE wave
$= \cos\theta/n$ for TM wave.

The characteristic matrix of a N-layer system is given by the consecutive product of individual matrices of each layer

$$\mathrm{M} = \prod_{j=1}^{N} \mathrm{M}_j \tag{2}$$

In the single stack calculation, one calculates the matrix of the multilayer as a whole. As light incidents from a medium of refractive index n_0, through a multilayer represented by

$$\mathrm{M} = \begin{pmatrix} m_{11} & -im_{12} \\ -im_{21} & m_{22} \end{pmatrix} \tag{3}$$

into another medium of index n_s, the reflection and transmission coefficients r and t are given by

$$\begin{aligned} r &= \frac{(m_{11}p_0 - m_{22}p_s) + i(m_{21} - m_{12}p_0p_s)}{(m_{11}p_0 + m_{22}p_s) - i(m_{21} + m_{12}p_0p_s)} \\ t &= \frac{2p_0}{(m_{11}p_0 + m_{22}p_s) - i(m_{21} + m_{12}p_0p_s)}. \end{aligned} \tag{4}$$

From these relations, one can easily derive the reflectance R and the transmittance T as

$$\begin{aligned} \mathrm{R} &= |r|^2 = \frac{(m_{11}p_0 - m_{22}p_s)^2 + (m_{21} - m_{12}p_0p_s)^2}{(m_{11}p_0 + m_{22}p_s)^2 + (m_{21} + m_{12}p_0p_s)^2} \\ \mathrm{T} &= \frac{p_s}{p_0}|t|^2 = \frac{4p_0p_s}{(m_{11}p_0 + m_{22}p_s)^2 + (m_{21} + m_{12}p_0p_s)^2} \end{aligned} \tag{5}$$

and the phase changes upon reflection and transmission as

$$\phi_R = \tan^{-1} \frac{2(m_{11} m_{21} p_0 - m_{22} m_{12} p_0 p_s^2)}{(m_{11} p_0)^2 - (m_{22} p_s)^2 - (m_{21})^2 + (m_{12} p_0 p_s)^2} \cdot \quad (6)$$

$$\phi_T = \tan^{-1} \frac{m_{21} + m_{12} p_0 p_s}{m_{11} p_0 + m_{22} p_s}$$

In case of a multilayer deposed on a substrate of index n_s, considering the reflection from the backside of the substrate, the transmittance measured in the surrounding medium p_0' is given by

$$T = \frac{4 p_0 p_0'}{(m_{11} p_0 + m_{22} p_s)^2 + (m_{21} + m_{12} p_0 p_s)^2} \cdot \left(\frac{2 p_s}{p_0' + p_s}\right)^2 \quad (7)$$

The two effective interface method splits a multilayer into two subsystems, along one of the half-wave layers, which act as two effective interfaces E_1, E_2 on both sides of the half-wave layer as shown in Fig. 1. Considering multiple reflections and transmissions at the two effective interfaces, one obtains the transmittance of the whole system as

$$T = \frac{T_1 T_2'}{(1-R)^2} \cdot \frac{1}{1 + \frac{4R}{(1-R)^2} \cdot \sin^2 \phi} \quad (8)$$

where

$$R = (R_1 R_2)^{1/2}, \quad \phi = \phi_{R1} + \phi_{R2} + \frac{2\pi nd}{\lambda}$$

R_1, R_2 and ϕ_{R1}, ϕ_{R2} are the reflectances and the phase changes on reflection from subsystem 1 and 2 respectively. T_1, T_2' are the transmittances of subsystem 1 and 2 respectively, $T_2 = T_2'$ if subsystem

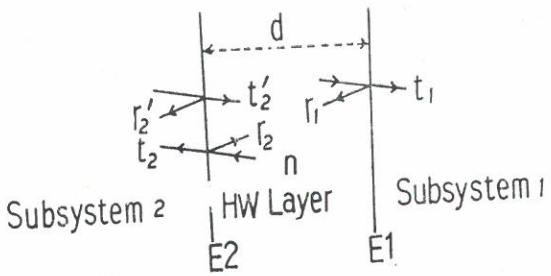

Fig. 1. Two effective interfaces representation of a multilayer.

2 has a semi-infinite extention of medium on the left hand side, as is the usual case.

Theoretical calculations have been done with an Apple II computer. An Applesoft program chained to the appleplot program has been written for both the single stack calculation and the two effective interfaces calculation. The results may be displayed numerically, or graphically.

DESIGN ANALYSIS

a. Single Half-Wave Systems

A single half-wave system consists of a single half-wave layer between two quarter-wave reflecting stacks, like a Fabry-Perot filter,

$$\left|\frac{\lambda_0}{4}\text{ stack}\right|\frac{\lambda_0}{2}\text{ spacer}\left|\frac{\lambda_0}{4}\text{ stack}\right|$$

The transmittance characteristics for a typical multilayer $n_0|(\mathrm{HL})^3|\mathrm{HH}|(\mathrm{LH})^3|n_0$, with refractive indices $n_0=1$, $n_H=2.1$ and $n_L=1.3$, is shown in Fig. 2. Here we use the convention : H, L for a quarter-wave layer of high, low index material respectively. λ_0 is the central wavelength of the pass band.

The transmission curve is symmetric with respect to $\lambda_0/\lambda=1$ and periodic with a period of 2. The pass band at $\lambda_0/\lambda=1$ becomes narrower and sharper as the number of layers in reflecting stacks of the ratio n_H/n_L increases. The stop bands on both sides of the central peak become wider as n_H/n_L increases. Interchange of H and L gives a worse transmission pattern, as displayed in Fig. 2(b).

The region including the fundamental pass band at $\lambda_0/\lambda=1$ and two side stop bands is just the stop band of the composing reflecting stacks of the system. Constructive interference of multiple reflections from two high reflecting stacks produces a central narrow pass band in the stop band of the reflecting stacks. Therefore the stop band width on either side of the pass band of the system can be estimated by calculating half the stop band of the composing reflecting stacks, and it is obtained as

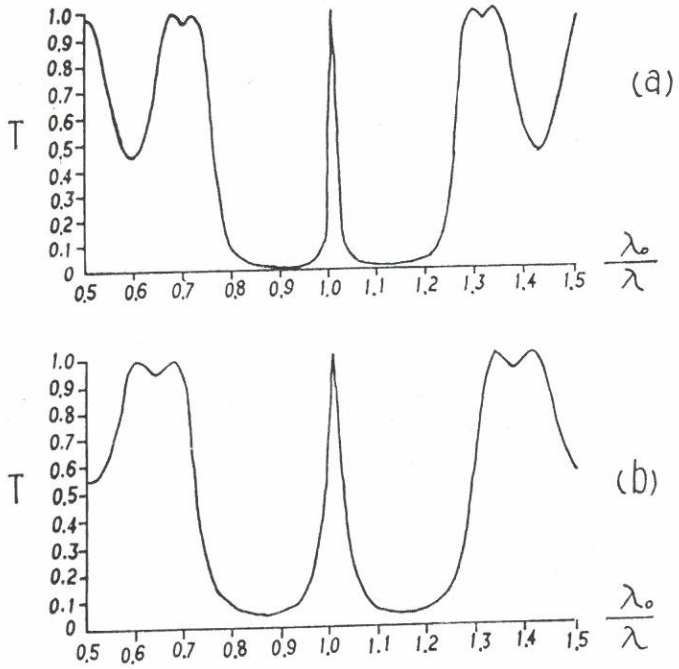

Fig. 2. Transmittances of SHW system with $n_H=2.1$, $n_L=1.3$.
(a) $(HL)^3|HH|(LH)^3$
(b) $(LH)^3|LL|(HL)^3$

$$\Delta(\lambda_0/\lambda) = 1 - \frac{2}{\pi}\sin^{-1}\frac{2}{\left(2+\frac{n_H}{n_L}+\frac{n_L}{n_H}\right)^{1/2}} \tag{9}$$

which is displayed graphically in Fig. 3. The stop band width is slightly different from the width of the stop band in equivalent layer systems, which is given by

$$\Delta(\lambda_0/\lambda) = \frac{2}{\pi}\sin^{-1}\left(\frac{n_H - n_L}{n_H + n_L}\right) \tag{10}$$

In the region of the central pass band, where R_1 and R_2 are essentially constant, the transmission of the system is well described by

$$T = \frac{T_0}{1 + F_0 \sin^2\phi} \tag{11}$$

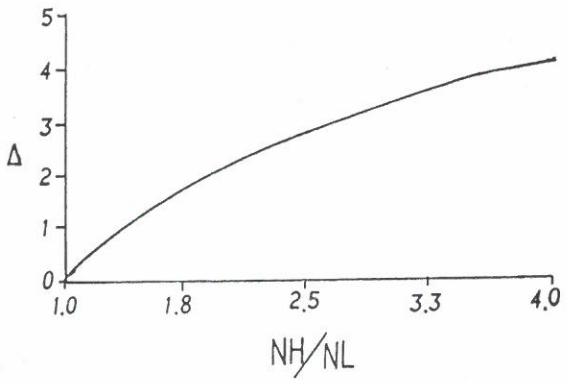

Fig. 3. The dependence of the stop band width of a quarter-wave stack on n_H/n_L.

with

$$T_0 = \frac{T_1 T_2'}{(1-R)^2}, \quad F_0 = \frac{4R}{(1-R)^2}$$

where T_0 and F_0 are almost frequency independent. And so the half-wave of the pass band is essentially determined by the Airy Sum, which is about 0.01 in the case of Fig. 2.

We are interested in the application of a single half-wave system to fabricate variable filters. If high reflecting stacks are employed, their reflectances and transmittances are nearly constant through their stop band, $1-\Delta < \lambda_0/\lambda < 1+\Delta$, and so Eq. (11) prevails. It is therefore possible to produce a variable filter by simply varying the thickness of the central half-wave layer of the system along a given path on the substrate. This variable filter is applicable in the range from $(1+\Delta)^{-1}$ to $(1-\Delta)^{-1}$.

The position of the central peak inside the stop band is determined by the phase relation as

$$\phi = \pi = \frac{1}{2}(\phi_{R1} + \phi_{R2} + \pi E \lambda_0/\lambda) \tag{12}$$

for a given thickness E of the half-wave layer,

$$nd = E \cdot \frac{\lambda_0}{4} \tag{13}$$

or,

$$E = (2 - \phi') / (\lambda_0/\lambda)$$
$$\phi' = (\phi_{R1} + \phi_{R2}) / \pi . \qquad (14)$$

Note that ϕ_{R1} and ϕ_{R2} are wave-number dependent. Computer calculation for the system $(HL)^3 \mid EH \mid (LH)^3$, with $n_H = 2.42$ and $n_L = 1.4$, gives the results of Fig. 4.

The figure shows that the variation of E is approximately linear in the region of interest $(1 - \Delta, 1 + \Delta)$. The half width of the central pass band increases as the peak shifts from the center to either side of the region of interest, from about 0.005 at $\lambda_0/\lambda = 1$ to 0.01 at $\lambda_0/\lambda = 1.25$ or 0.75. For $n_H = 2.42$ and $n_L = 1.4$, $\Delta = 0.1721$. The applicable range of the filter is $(0.853\,\lambda_0, 1.208\,\lambda_0)$.

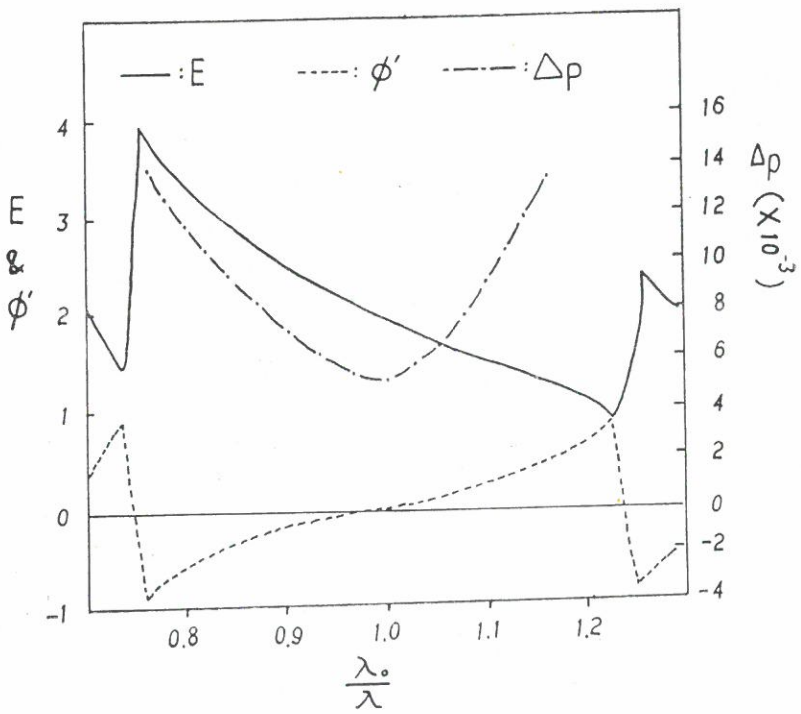

Fig. 4. Variations of peak position λ_0/λ and half width Δp of the pass band with thickness E for the system $(HL)^3|EH|(LH)^3$, $n_H = 2.42$, $n_L = 1.4$.

b. Double Half-Wave Systems

The shape of the pass band for SHW systems given by the Airy Sum is not ideal for a narrow band filter. A more desirable shape would be a flatter top with sharper edges. For this Smith[4] had investigated and recommended double half-wave systems (DHW) of the general type

$$\left|\frac{\lambda_0}{4}\text{ stack}\right|\frac{\lambda_0}{2}\text{ spacer}\left|\frac{\lambda_0}{4}\text{ stack}\right|\frac{\lambda_0}{2}\text{ spacer}\left|\frac{\lambda_0}{4}\text{ stack}\right|.$$

DHW systems show a pass band containing either two peaks with a central trough or just a single peak. The general shape in two-peak case is rectangular. DHW systems have applications to narrow band, wide band and low pass filters. Our main interest is in the application to narrow band filters.

DHW systems can be investigated and designed through the two effective interfaces analysis, using Eq. (8) with the help of Eqs. (5)-(6). Refer to the far left half-wave spacer, the remainder on its right and the quarter-wave on its left are regarded as subsystem 1 and subsystem 2 respectively.

As an example, the properties of the 19 layer DHW system $(HL)^2|HH|(LH)^2L(HL)^2|HH|(LH)^2$ with $n_H = 2.42$ and $n_L = 1.4$ are computer calculated and displayed in Fig. 5. In Fig. 5-(c), it shows that the DHW system has a flat pass band, with a pretty sharp edge, of half-width $\Delta p \simeq 0.025$, in contrast to $\Delta p \simeq 0.005$ for the 13 layer SHW system $(HL)^3|HH|(LH)^3$.

The influence of the number of layers in quarter-wave stacks on the pass band shape is also investigated. Consider the DHW system

$$(HL)^{N_2}|HH|(LH)^{N_2'}L(HL)^{N_1'}|HH|(LH)^{N_1}.$$

The study shows that with symmetric structure, $N_1=N_1'=N_2=N_2'$, it has the best shape. The pass band becomes narrower with steeper edges as the N's increase. For $N_1' + N_2' < N_1 + N_2$, a central trough exists between two peaks, which sinks deeper as $N_1'+N_2'$ decreases. The transmittance at the center rises as $N_1' + N_2'$ increases. As

$N_1' + N_2' > N_1 + N_2$, a central peak appears instead of two side peaks.

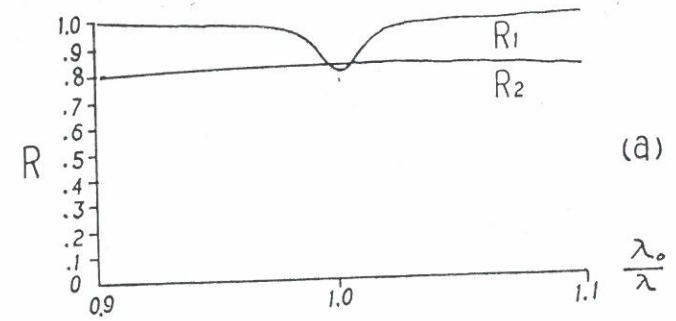

(a) Reflectances of subsystems.

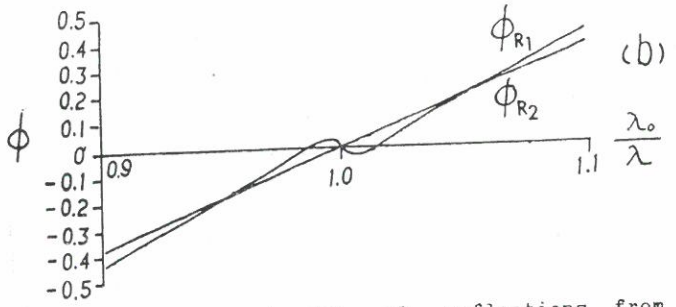

(b) Phase changes of reflections from subsystems.

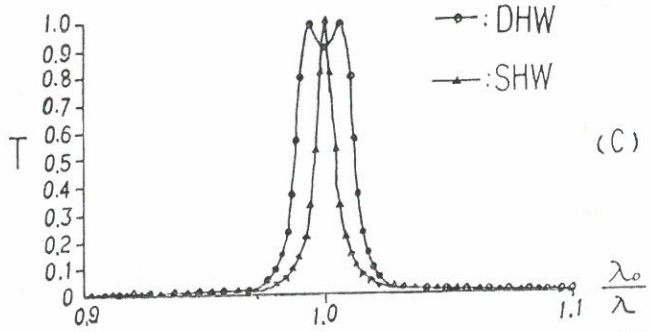

(c) Total transmittance in comparison with that of SHW system $(HL)^3|HH|(LH)^3$

Fig. 5. Two effective interfaces computation of DHW SYSTEM $(HL)^2|HH|(LH)^2\,L(HL)^2|HH|(LH)^2$, $n_H=2.42$, $n_L=1.4$.

For comparison, we have also investigated multilayer systems containing different numbers of half-wave layers, but with the same total number of layers. The results are shown in Fig. 6. The number of peaks appearing is equal to the number of equivalent half-wave

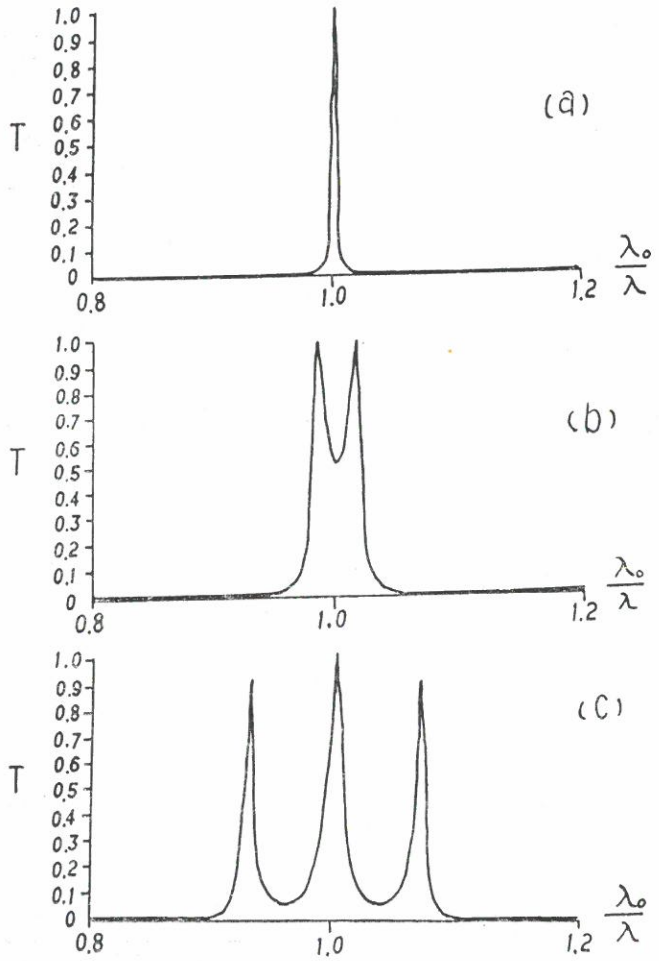

Fig. 6. Transmittances of various systems with same total number of layers. $n_H=2.42$, $n_L=1.4$.
(a) $(HL)^4|HH|(LH)^4$
(b) $(HL)^2|HH|LHLHLHL|HH|(LH)^2$
(c) $(HL)^2|HH|(LH)^2\,(HL)^2|HH|(LH)^2$

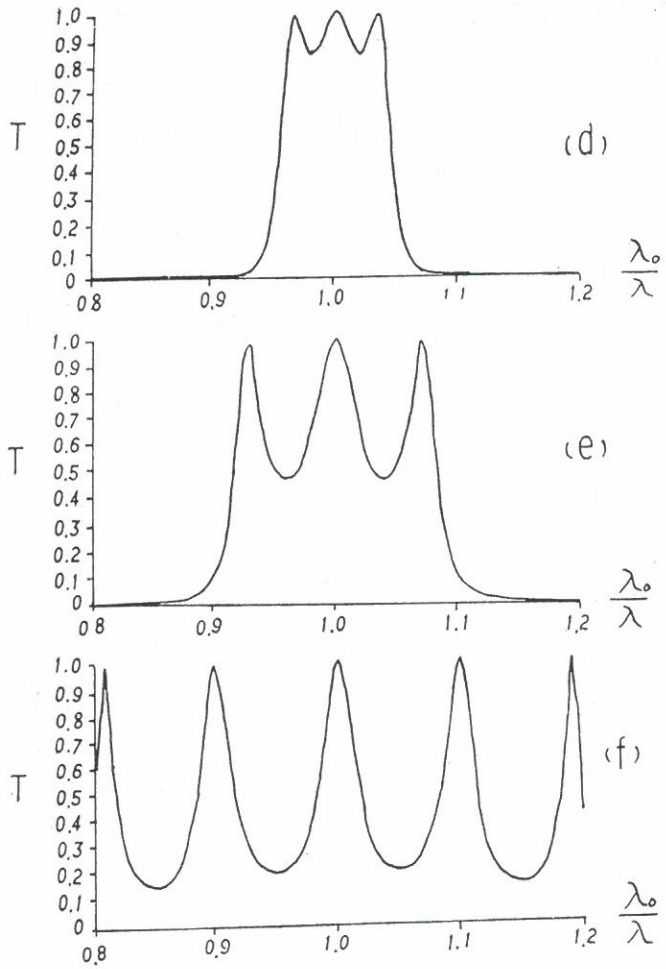

Fig. 6. (d) HL|HH|LHLHL|HH|LHLHL|HH|LH
(e) HL|HH|LHL|HH|LHL|HH|LH
(f) HL|HH|LHHL|HH|LHHL|HH|LH

layers of the system. Increasing the number of layers in the stacks will raise the transmission in the trough regions and pack the individual peaks closer.

Since a symmetric DHW system is equal to two equivalent SHW subsystems, separated by a single L layer, it may be plausible to narrow down the pass band width $\Delta\phi$ of the system by shifting

the peak of one of the SHW subsystems a distance $\Delta p/2$ by changing the thickness of its half-wave layer as shown in Fig. 4. However, the result turns out to be negative as shown in Fig. 7, for the transmission of the system $(HL)^2|HH|(LH)^2L(HL)^2|1.908H|(LH)^2$. The asymmetry of the pass band is due to the slight distortion of the band shape of the right SHW subsystem as its peak shifts. Therefore the only way to make a narrow pass band filter with a flat top and sharp edges is to use the DHW system with a high ratio n_H/n_L and a large number of layers in $\lambda/4$ stacks.

Variable filters of DHW systems can be designed in the same

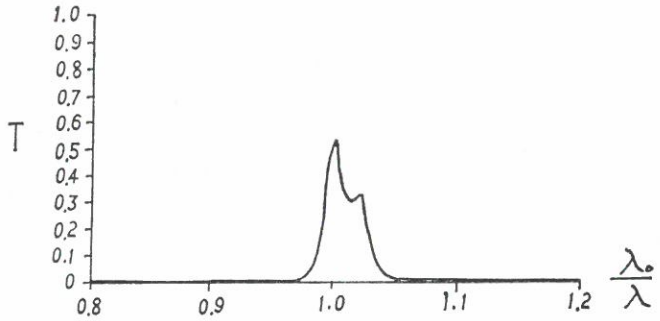

Fig. 7. Transmittance of $(HL)^2|HH|(LH)^2L(HL)^2|EH|(LH)^2$ with E=1.908.

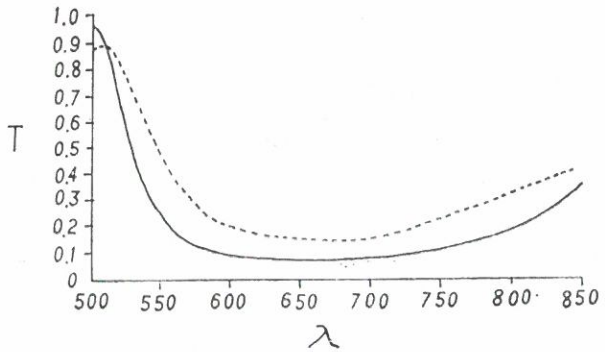

Fig. 8. Measured transmittance (dotted line) and calculated one (solid line) of $(LH)^4$.

way as these of SHW systems, simply by varying the thickness of both its half-wave layers simultaneously, according to the relation shown in Fig. 4.

EXPERIMENTAL FABRICATION AND TEST

In the actual fabrication of narrow band pass filters in experiments, MgF_2 and CeO_2 are used as the low and high index material respectively. The films are deposited at a deposition rate of about 5-10 Å/sec onto a substrate kept at 100°C. The refractive indices of the MgF_2 and CeO_2 films are carefully measured by transmittance measurements[2] and double checked by the Fizeau interference method[5]. The average refractive indices thus obtained are

$$n_H = 2.42, \quad n_L = 1.4 .$$

Microscope slides with index $n_s = 1.512$ are used for substrates.

A reflecting stack and two narrow band pass filters of both a single half-wave system and a double half-wave system were fabricated and tested. With λ_0 chosen to be 650 *nm*, the corresponding quarter-wave thicknesses are

$$H = 671 Å, \quad L = 1161 Å .$$

Transmittance curves experimentally measured (dotted lines) are displayed in comparison with the theoretical ones (solid lines) calculated from the actual deposited thickness. The results are fairly compatible with the designs in general. The broadening of the pass band width and the shifting of the peak of measured transmittances are mainly caused by errors in the refractive index determination and the deposition thickness control. In Fig. 9, for example, the peak shifts about $\Delta\lambda_0 \simeq 20$ *nm* and its edges shift from 660 *nm* and 680 *nm* to 635 *nm* and 710 *nm*.

The expanding of the band width can be regarded as outward shifting of its edges on both sides, which in turn can be estimated from the variation of the stop band edge of the reflecting stack with the refractive ratio n_H/n_L. For a given central wavelength $\lambda_c (\neq \lambda_0)$, the stop band edge wavelength λ_e is given by Eq. (9),

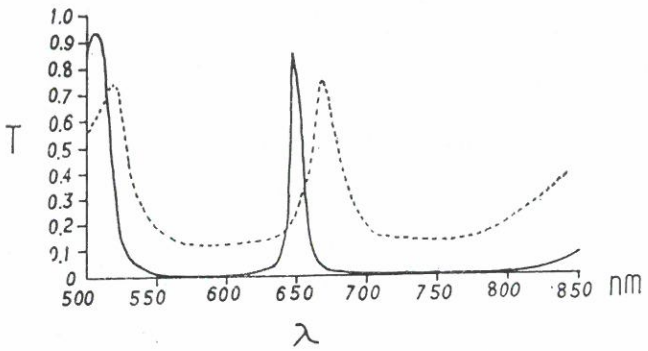

Fig. 9. Measured transmittance (dotted line) and calculated one (solid line) of $(HL)^3|HH|(LH)^3$.

$$\frac{\lambda_c}{\lambda_e} = 1 - \Delta = \frac{2}{\pi} \sin^{-1} \frac{2}{\left(2 + \frac{n_H}{n_L} + \frac{n_L}{n_H}\right)^{1/2}} \tag{15}$$

which is practically fixed by the value of n_H/n_L, as is the pass band width. For $n_H=2.42$ and $n_L=1.4$, $\lambda_c/\lambda_e \simeq 0.821$. As λ_e shifts from 660 *nm* to 635 *nm* $\lambda_c/\lambda_{e'} \simeq 0.853$. From Eq. (15), we find the corresponding value $n_H/n_L \simeq 1.592$. Note that n_L is less influential and the refractive index of MgF_2 is more accurately measured to be 1.38~1.4. The result implies that the actual refractive index of CeO_2 should be 2.21, 10% less than our previous measurements on thicker films over 4000 Å. This is interpreted mainly as a result of the inhomogeneity of the index of usual CeO_2 films[9], which leads to less than average index in thinner films such as the quarter-wave layers. In our experiments, a percentage error δ in thickness calibration will produce errors in measuring thickness t and refractive index n as

$$\frac{\Delta t}{t} = -\frac{\Delta n}{n} = \delta \quad \text{and} \quad \Delta(nt) = 0 .$$

The position of the central peak λ_0 is strictly determined by the optical thickness of the half-wave layers as $\lambda_0 = 2nt$. The shifting of the peak $\Delta\lambda_0 = 2\Delta(nt)$, can not be caused by the error in thickness calibration, but instead by the error in the thickness control on the

half-wave layer, produced by over growth after the shutter closed. As in Fig. 9, with $\Delta\lambda_0 \simeq 20\ nm$, the corresponding error, $\Delta t \simeq \Delta\lambda_0/2n$, is about 41Å or 3%.

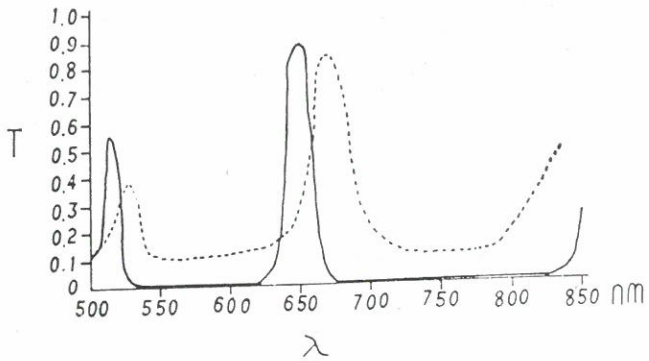

Fig. 10. Measured transmittance (dotted line) and calculated one (solid line) of $(HL)^2|HH|(LH)^2\,L(HL)^2|HH|(LH)^2$.

CONCLUSIONS

From a theoretical design analysis, we reach the following conclusions:

(1) All-dielectric narrow band filters have the advantage of high transmittance when compared with those of metal-dielectric combination, which have loss in reflections due to absorptions by the metal layers. However, they have the disadvantage of it being impractical to achieve a very narrow band width, say of a few nanometers.

(2) SHW systems have the narrowest band width, but DHW systems have the best band shape among all the half-wave systems. The band width is determined by the index ratio n_H/n_L and the number of layers in reflecting stacks.

(3) Variable filters can be designed by varying the optical thicknesses of the half-wave layers within the region of the stop band of the reflecting stacks.

In experiments, we find the following results:

(1) The measured results are quite compatible with the theoretical

designs. The peak shifts about 20 *nm* and the edges move about 20-30 *nm* on each side.

(2) Critical thickness control on the half-wave layers is essential to fix the peak position. In our case, a peak shift of 20 *nm* indicates a control error, caused by over growth of CeO_2 films, of about 42Å or 3%.

(3) The expanding of the band width is due to over estimation in measuring the refractive index of CeO_2. The band width indicates that $n_H \simeq 2.21$. This error is caused by the inhomogeneity of refractive index of the usual CeO_2 films.

ACKNOWLEDGEMENTS

This work was done under the support of the National Science Council of the Republic of China (contract number NSC75-0208-M030-01). Thanks are due Miss S.H. Lee for helping in computations and performing experiments and the National Science Council for continuing support.

REFERENCES

(1) A. Thelen, *Physics of thin films*, (Hass, G., M.E. Franeombe, and R.W. Hoffman ed.), **Vol.** 5, pp. 47-85, Academic Press, New York (1969).
(2) W.J. Lin, K.T. Wu and J. Chen, *Fu Jen Studies*, 17, 1 (1983).
(3) H.D. Polster, *J. Opt. Soc. Am.* 42, 21 (1952).
(4) S.D. Smith, *J. Opt. Soc. Am.* 48, 43 (1958).
(5) K.T. Wu and J. Chen, Multilayer interference films made of ZnS and MgF_2, NSC Research Report (1985).
(6) M.L. Hong, K.T. Wu and J. Chen, Multilayer interference films made of ZnS and cryolite, NSC Research Report (1986).
(7) C.L. Liu, K.T. Wu and J. Chen, Multilayer interference films made of CeO_2 and MgF_2, NSC Research Report (1986).
(8) M. Born and E. Wolf, *Principle of Optics* (2nd ed.), pp. 51-69, Pergamon Press, Oxford (1964).
(9) J.P. Borgogno, B. Lazarides and E. Pelletier, *Appl. Opt.* 21, 4020 (1982).

狹帶濾光器

輔仁大學物理研究所

陳振益 吳坤東

摘要

本文對於半波長系統之全介質狹帶濾光器之設計及其性質，利用整疊計算法及雙介面分析法，加以詳盡的研究分析。設計的結果，並以氟化鎂及二氧化鈰兩種薄膜之組合，製成成品加以測試。測試之結果與原設計相當符合。

METAL ION INTERACTIONS WITH BOVINE PROTHROMBIN FRAGMENT 1 STUDIED BY Ca(43) NMR

ELIZABETH H. MEI*

Department of Chemistry,
University of Minnesota

ABSTRACT

A calcium-43 NMR line width study on the interaction between Ca^{+2} and prothrombin fragment 1 clearly verified the postulate that that this protien pocesses two classes of binding sites.

INTRODUCTION

Biological metal ion NMR for ions such as the alkali and alkaline earth ions has developed slowly relative to ^{1}H, ^{2}H, ^{13}C, ^{19}F, and ^{31}P due to (1) the inherent NMR sensitivity and natural abundance of interesting isotopes are low, and (2) the majority of the elements of interest to us have magnetic nuclei spin $I>(1/2)$, i.e. they pocesses an electric quadrupole moment. An element with larger than 1/2 magnetic spin normally gives a broad NMR signal or splittings which makes the bandshape difficult to detect and hence seemingly devoid of interesting information. With the advent and quick development of computer technology and the application of fast Fourier transform (FFT) to data collection and analysis, metal ion NMR has provided a tremendous amount of information on various complexation reactions[1-5] during past decade.

Prothrombin is a Vitamin K dependent plasma protein. These proteins contain several multivalent cation binding sites. For prothrombin it has been estimated there exist from 6 to 15 sites[7]. From a fluorescence study, circular dichromism spectra indicate that ion binding induces at least two conformational changes in the protein[8].

* E. Mei, Ph. D. is an alumus of Fu Jen Catholic University.
Contact Address: P.O. Box 1231 Millbrae, Ca 94030.

The primary structure of bovine prothrominbin is completely known[9] and the binding sites are located in the so-called fragment 1 (F1) which posess residues from 1-156. Fragment 1 is a well-defined fragment of prothrombin and shows essentially the same binding properties towards Ca^{+2} and phospholipid as prothrombin itself[10]. In this paper I report the result of a Ca^{+2}-F1 binding study which is monitored by Ca(43) NMR.

EXPERIMENTAL

Protein preparation. Prothrombin fragment 1 was prepared as previously described[11]. Protein concentrations were determined by ultraviolet absorbance using $E_{280nm}=10.1$ for fragment 1[12]. Metal ion free samples of protein were prepared by dialyzing the protein for at least 12 hrs against 1000 ml volumes of 0.5 mM EDTA, PH 7.5. Subsequently the protein was dialyzed against three 2000 ml volume changes of distilled, deionized water. In all cases, the water was prepurified on a Barnstead reagent grade water purification system to give water with less than 1 ppm metal ion present. For NMR analysis, the protein solution was lyophilzed to dryness 2 times from D_2O containing 0.1 M NaCl. D_2O (100 ml) (Sigma) was extracted with 2 ml of 0.02% diphenothiocarbazone (Aldrich) in CCl_4 to remove contaiminating divalent cations. The D_2O was extracted with additional 5 ml aliquots of CCl_4 until colorless. The NaCl was passed through Chelex 100 (Bio-Rad) to remove divalent cations. All pH titration was measured on a Radiometer (Model 26) with a Radiometer GK2412 C electrode. Deuterated acid and base were used and reported pH values here are not corrected for deuterium isotope effects. The calcium binding with prothrombin fragment 1 activity was checked before and after NMR analysis by fluorescence change[13,14]. All protein samples for which spectra are presented were fully functional and showed 75% calcium dependent protein fluorence quenching at the end of NMR analysis.

REAGENTS

The $CaCl_2$ enriched isotope sample was converted from $CaCO_3$

(Oak Ridge, Tenn.) and concentration was determined by back titration with EDTA and $MgSO_4$.

NMR SPECTRA

The NMR spectrometer employed here was a Nicolet NT-300 operating with a 93 mm bore oxford magnet and the standard Nicolet multinuclear low frequency probe. The Calcium-43 NMR lineshape (I=7/2) is known to be nonlorentzian. Samples were contained in 12 mm Wilmad thin wall NMR tubes and measured at half maximum height of the absorption mode signal.

RESULTS

A previous Ca-Prothrombin fragment 1 (CaF1) study[15,16] by the Nelsestuen group indicated that at a neutral pH value, both prothrombin and its fragment 1 will involve self-association, when the concentration is greater then 50 micromolar, in the presence of Ca^{+2}. They postulated that prothrombin F1 contains six metal ion binding sites regardless of its state of aggregation. Two or three ions induce the conformational change and these sites generally are filled with higher affinity than the sites causing self-association. K.G. Mann[17] also proposed earlier that prothrombin fragment 1 has two classes of metal ion binding sites. One class, probably comprising two of the six sites, is fairly nonselective with respect to which metal ion is bound. The other sites are almost obligatory for Ca^{+2} and must be filled in order for dimerization, phospholipid binding and prothrombin activation to occur.

Here, I present the results of a Ca_nF1 Ca(43) NMR study ot pH=8.5. This pH value was chosen to eliminate the complication arising from the conformational change of prothrombin F1 itself. The high concentration of [F1]=2.27 mM assured that a visible S/N and that all the Ca^{+2}(43) added to the protein solution was bound. Since the interaction of Ca^{+2} with F1 is monitored by Ca(43) NMR, the self-association of F1 in the presence of Ca^{+2} can be easily distinguished.

$CaCl_2$ solution was gradually added to study the binding nature

of each Ca_nFl (n=1 to 6)by Ca(43) NMR. Its spectra are shown in Fig. 1. The dramatic difference in the spectra among CaFl, Ca_2Fl and Ca_6Fl at different temperatures indicate they experience different enviroments. From the linewidth change (Table 1) with temperature and stochiometry, we are convinced that there are two classes of binding. CaFl and Ca_2Fl are high affinity sites at Gla 15

Table 1. Linewidth (Hz) of Ca_nFl at various temperatures where [Fl]=2.27 mM and pH=8.44 in D_2O solution

°C	CaFl	Ca_2Fl	CaF_3Fl	CaF_4Fl	Ca_5Fl	Ca_6Fl
45	950	—*	879	708	462	380
27	950	771	623	525	401	227
12	—*	900	644	290	274	179

* Asymetric anisotropic lineshape. Half linewidth is difficult to express.

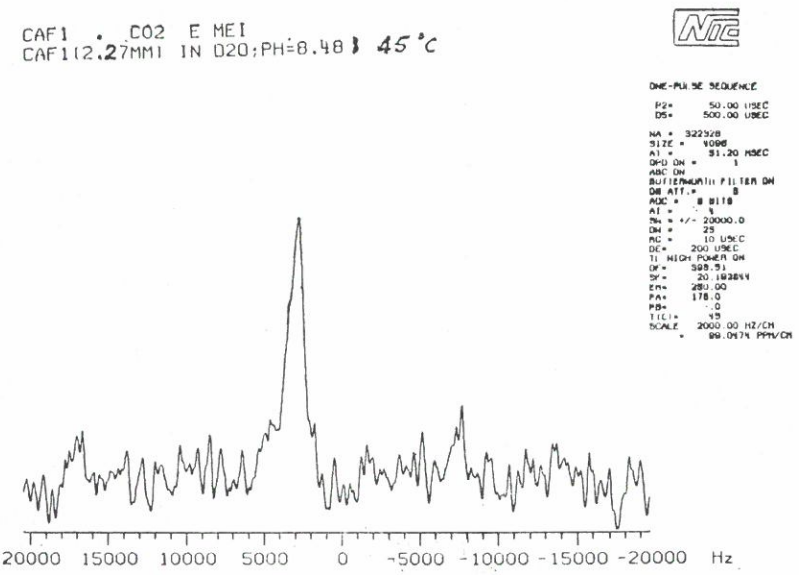

Fig. 1. Lineshape of Calcium prothrombin complexes (Ca_nFl) at 45°C, 27°C and 12°C. Where n=1, 2, and 6. The third spectrum of Ca_3Fl (bottom) is a display of full spectrum width in data collection.

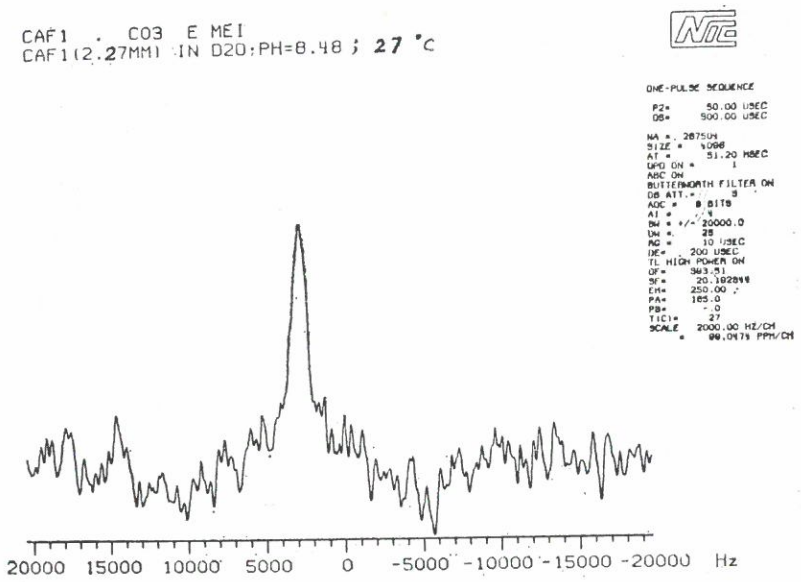

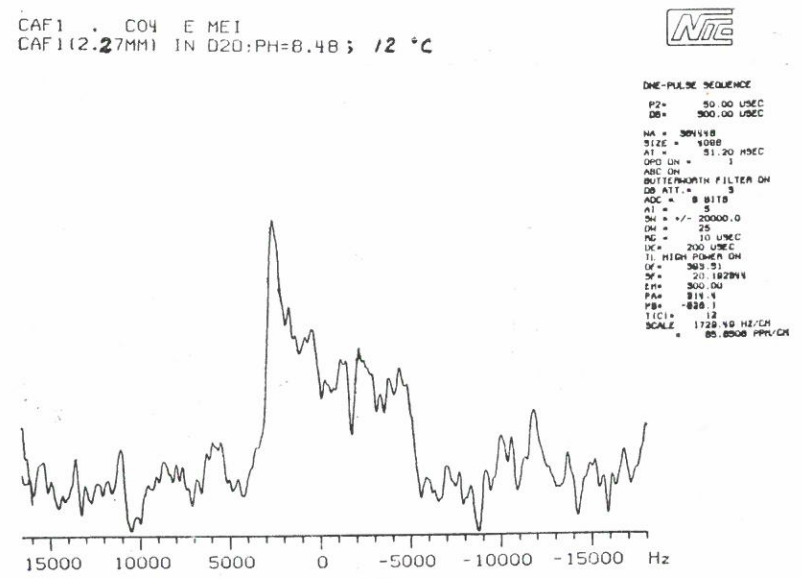

Fig. 1. Continued

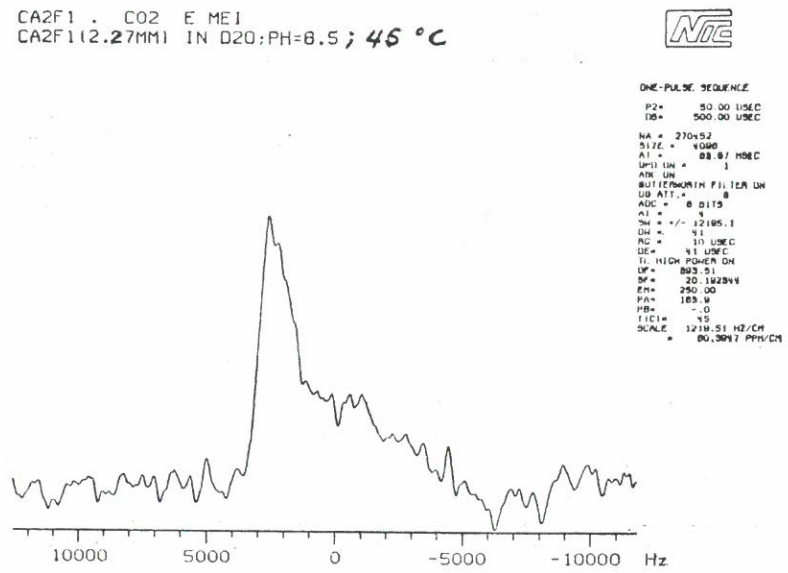

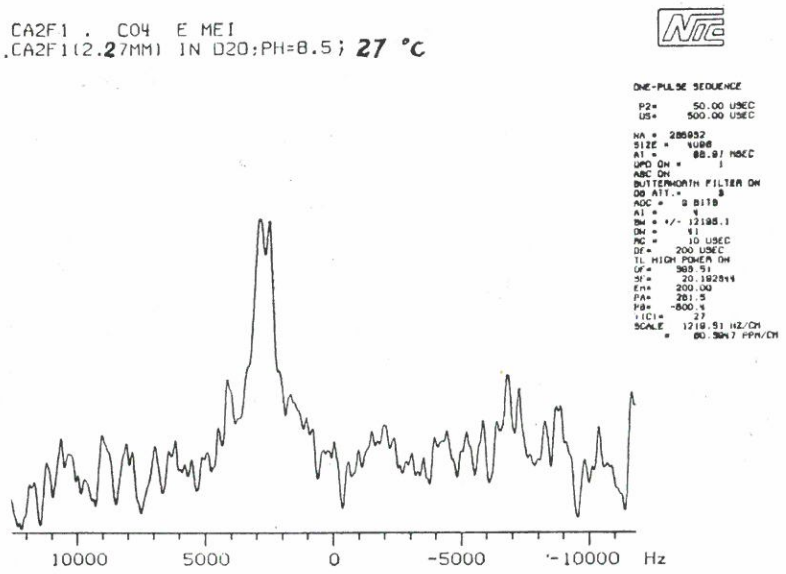

Fig. 1. Continued

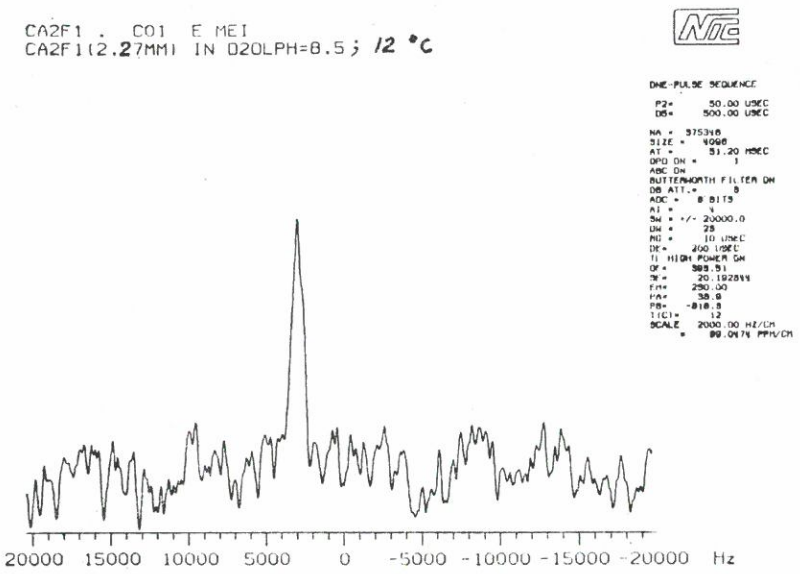

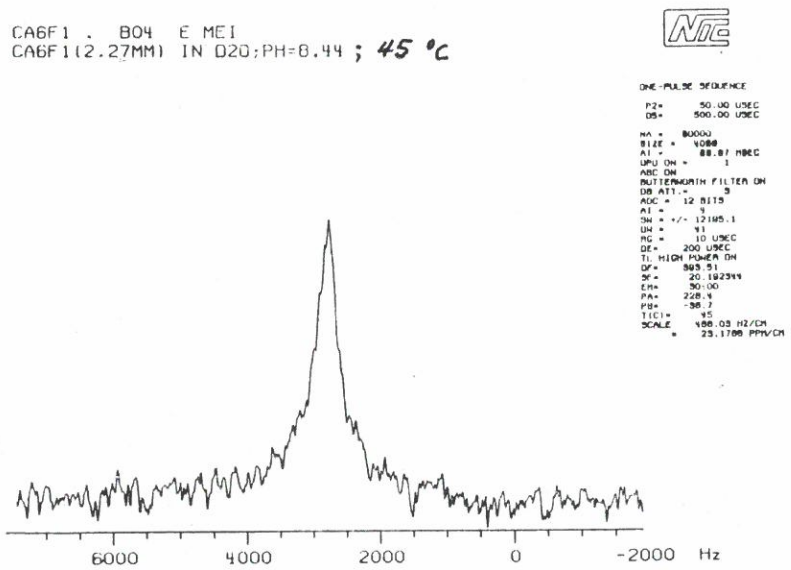

Fig. 1. Continued

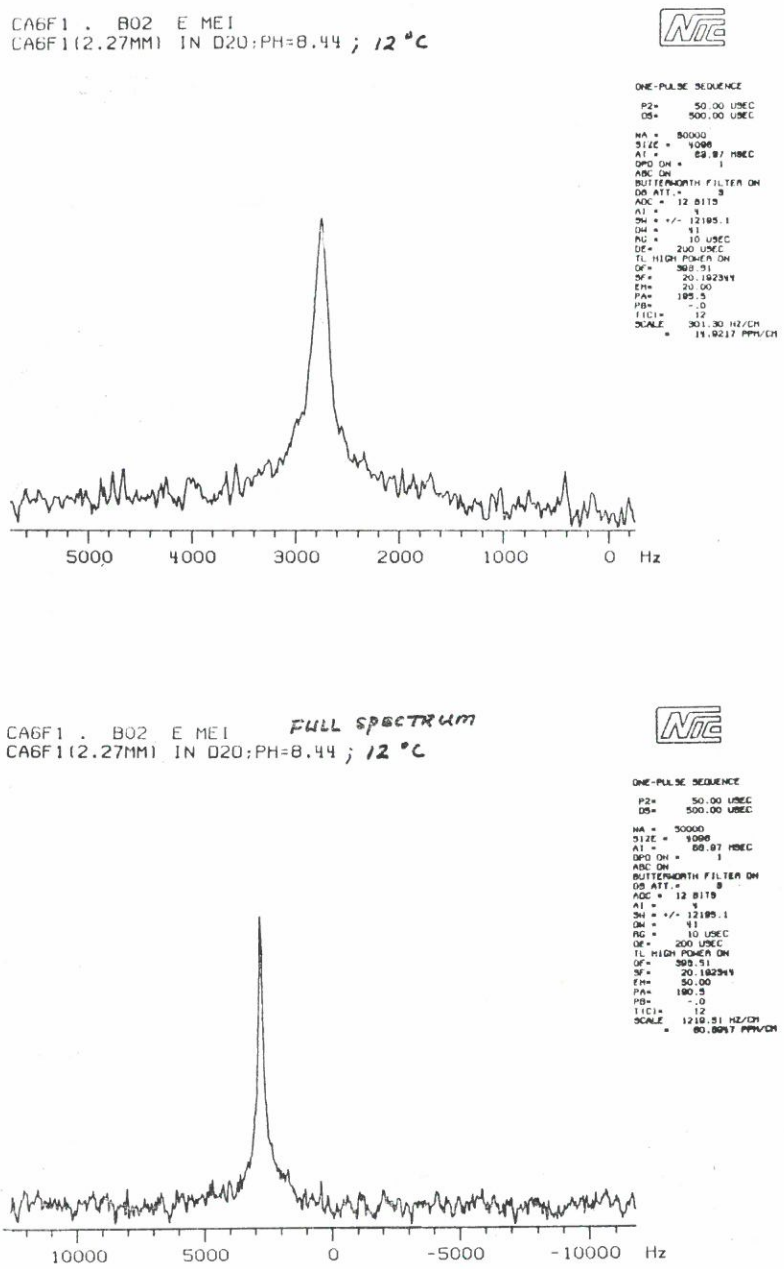

Fig. 1. Continued

and Gla 26[18]. For CaFl both 45°C and 27°C showed different lineshapes than the one at 12°C. The motion of the protien at this low temperature may have been slow enough to allow the NMR to observe an anisotropic Calcium signal. At −1°C, the linewidth was even broader and after 450 k scan only a weak signal was obtained. The S/N was too poor to define a significant lineshape. (The number of scan for CaFl at 12°C is NS=364 k). The enthalpy of complexation is known[19] and the ΔH is a small negative value. The averaged binding constant for calcium also has been reported[20] in the range of 10^4 M. Therefore a $K_a > 10^4$ for Ca_2Fl can be predicted and we may assume $[Ca]_{free}=0$. with confidence. Then the spectrum of Ca_2Fl most probably is a superposition of an isotropic lineshape and an anisotropic lineshape. When the temperature was low the anisotropic component gradually broadened and was burried under noise. The Ca_3Fl spectrum essentialy displayed a similar lineshape as Ca_6Fl. But a spectrum collected at 12°C after NS=177 k S/N was not as good as Ca_6Fl at 12°C (NS=50 k), even though the concentration of Ca^{+2} was only half of the Ca_6Fl.

When the mole ratio of Ca^{+2} vs Fl ≥ 3 the binding site is more or less located at the surface of the protein, these Ca^{+2} ions can easily form a bridge for dimerization. Being located between two Fl, the Ca^{+2} ion experienced an asymetric enviroment and hence a quardrupole pattern may appear. Due to the relative motion of Fl in the dimer, Ca^{+2} ion experiences several different mechanisms in the expression of its lineshape. (1) The rocking of two Fl introduces electric field gradient fluctuation around Ca^{+2} nuclei. (2) Some Ca^{+2} at the edge of bridging two Fl will experience an on-off exchange rate due to the rocking mechanism. Therefore, in addition to the forgoing two factors, the lineshape of Ca_nFl ($n=1$ to 6) at various temperatures is a combination of (1), (2), (3) quadrupolar relaxation and (4) anisotropy relaxation. A quantitative lineshape analysis computation is in process.

CONCLUSION

A calcium prothrombin fragment 1 NMR study illustrates the

special power of metal NMR which may provide information on complextion reactions at the immediate enviroment of an ion. In conjunction with PMR, CMR, ^{31}P NMR and sometimes the aid of shift reagent, the structure of metal-protein interaction, static and dynamic information can be mapped out thoroughly. For this work I have used Ca(43) NMR and have clearly verified the postulate of two binding classes in Ca-prothrombin complexation.

ACKNOWLEDGMENT

I would like to thank the University of Minnesota, Chemistry Department for the use of NMR facility and and support from National Institutes of Health, GM-2577. Great appreciation also to Prof. R.G. Bryant for the use of expensive Ca(43) isotope. Special thanks to Prof. G.L. Nelsestuen for the gift of Prothrombin fragment 1 and all the help provided in extracting and purifying this protein from blood.

REFERENCES

(1) Y.M. Cahen, J.L. Dye and A.I. Popov, *J. Phys. Chem.* 79, 1292 (1975).
(2) J.P. Kintzinger, J.M. Lehn, *JACS* 96, 3313 (1974).
(3) A. Delville, C. Detellier and P. Laszlo, *J. Magn. Reson.* 34, 301 (1979).
(4) E. Mei, A.I. Popov and J.L. Dye, *J. Phys.* Chem. 81, 1677 (1977).
(5) S. Forsén, T. Andersson, T. Drakenberg, E. Thulin and M·Swärd, *Fedn Proc. Fedn Am Socs. exp. Biol.* 41, 2981 (1982).
(6) R.G. Bryant, *JACS* 91, 1870 (1969) and *Biochem. Biophys. Res. Commun.* 40, 1162 (1970).
(7) G.L. Nelsestuen, M. Broderius, T.H. Zytkovicz and J.B. Howard, *Biochem. Biophys. Res. Commun.* 65, 233 (1975).
(8) G.L. Nelsestuen, *J. Biol. Chem.* 251, 5648 (1976) and G.L. Nelsestuen M. Broderius, G. Martin, *J. Biol. Chem.* 251, 6886 (1976).
(9) G. Olsson, L. Andersen, O. Lindqvist, L. Sjölin, S. Magnusson, T.E. Pertersen and L. Sottrup-Jensen, *FEBS Letters* 145, No. 2, 317 (1982).
(10) R.A. Henriksen and C.M. Jackson, *Arch. Biochem. Biophys.* 170, 149 (1975).
(11) C.H. Pletcher, R.M. Resnick, G.J. Wei, V.A. Bloomfield and G.L. Nelsestuen, *J. Biol. Chem.* 255, 7433 (1980).
(12) C.M. Heldebrant and K.G. Mann, *J. Biol. Chem.* 248, 3642 (1973).
(13) G.L. Nelsestuen, *J. Biol. Chem.* 251, 5648 (1976).
(14) G.L. Nelsestuen, R.M. Resnick, C.S. Kimm and C.H. Pletcher, *Vitamin K. Metabolism and Vitamin K-dependent Proteins* (J.W. Suttei Ed. University Park Press, Baltimore, 1980) p. 28-38.

(15) G. L. Nelsestuen, R. M. Resnick, G J. Wei, C.H. Pletcher and V. A. Bloomfield, *Biochem.* 20, 351 (1981).
(16) G. L. Nelsestuen and R. G. Bryant, private communication.
(17) F. G. Prendergast and K. G. Mann, *J. Biol. Chem.* 252, No. 3, 840 (1977).
(18) B. C. Furie, M. Blumenstein and B. Furie, *J. Biol. Chem.* 254, 12521 (1979).
(19) R. M. Resnick, G. L. Nelsestuen, *Biochem.* 19, 3028 (1980).
(20) B. Furie and B. C. Furie, *J. Biol. Chem.* 254, 9766 (1979).

用鈣(43)磁場共振法來觀察 Prothrombin Fragment 1 與鈣鹽結合的各種因素

梅 宏 綺

明尼蘇達大學化學系

摘 要

金屬元素的核磁場共振法來觀看離子與蛋白質的交互作用，此法常可得到靜態 (Static) 與 Dynamic 的資料，此篇報導 Ca-Prothrombin fragment 1 Ca(43) NMR 觀察結果，確實顯示了金屬核磁場共振法可以對 Biological systme 有所貢獻。

利用簡化之一般化標準加入法 (GSAM) 來消除液相層析法的空白值

化學系

陳 天 鐸　陳 壽 椿

摘　要

本文將一般化標準加入法 (Generalized Standard-Addition Method, GSAM) 運用在高效能液態層析儀 (HPLC) 的實驗中，並以電腦模擬高效能液態層析儀所產生之波峰 (Peak)，作爲一般化標準加入法的資料且用圖解法來簡化一般化標準加入法中複雜的數學運算，以測出分析物的濃度和解決空白值 (Background) 問題。

前　言

以前，標準加入法 (Standard-Addition Method) 被廣泛地應用在分析化學上，只要在不同體積且未知濃度的分析物 (Analyte) 中，加入一系列已知濃度的分析物，即可利用線性迴歸法 (Linear regression) 將分析物的濃度測出，此法雖可克服干擾物 (Interference) 的影響，却無法解決空白值 (Background) 的問題。近幾年來，Saxberg 和 Kowalski[1]提出了一般化標準加入法 (Generalized Standard-Addition Method, GSAM) 利用多重線性迴歸法和相當複雜的數學運算來測出分析物的濃度並解決背景問題[2-4]。

同樣的問題出現在原子吸收光譜分析中——空白值的校正往往是整個分析工作的關鍵步驟，對於十分不穩定的空白值問題，有許多方法被提出，其中一般化標準加入法是最普遍的方法之一[5]。

另外，在液相層析法中，由於管柱的衰退或溫度的變化，常使得底線 (Baseline) 漂移，影響到分析的結果。所以可將底線漂移問題當作空白值，再以一般化標準加入法來處理。

同時，在做液相層析峰的分離時，也常會遇到一些干擾的波峰存在，而要找出一理想的分離條件又是一件相當費事的步驟，往往會浪費許多的金錢和精力，大大地降低了分析的效率。因此，亦可將干擾峰當作空白值來處理。本文即是利用一般化標準加入法來解決液相層析峰的干擾問題。

理　論

根據皮爾定律 (Beer's Law)—$A=\varepsilon bc$ 可知吸收強度 (Response) 和分析

物的濃度成正比，故依此式可推導出一般化標準加入法的關係式，如式(1)。本法中用到二個自變數 (Independent Variables)—分析物的體積和加入的濃度，一個因變數 (Dependent Variable)—波峰的面積，且它們之間會有以下的關係：

$$A_i = B + Sa_i + SCv_i \qquad (1)$$

其中：$i = 1, 2, \ldots N$　有 N 個波峰

A_i　第 i 個波峰的面積

B　空白值 (Blank)

a_i　第 i 個波峰加入的濃度

v_i　第 i 個波峰所代表之分析物的體積

S　靈敏度 (Sensitivity)

C　分析物的濃度除以總體積

由於，式(1)爲一非線性函數 (Nonlinear equation)，故可利用最小平方根法 (Least-square method) 去求S和C的解。利用此法的好處是：有許多現成的套裝軟體 (Package) 可利用，如 SPSS[6b], BMDP[7]。但缺點是：根據皮爾 (Beer's law) 定律，只有在線性條件下，所得的C值才可靠。

因此，將式(1)改爲以下線性關係：

$$A_i = B + Sa_i + Dv_i \qquad (2)$$

其中：$i = 1, 2, \ldots N$　有N個波峰

A_i　第 i 個波峰的面積

B　空白值 (Blank)

a_i　第 i 個波峰加入的濃度

v_i　第 i 個波峰所代表之分析物的體積

S　靈敏度 (Sensitivity)

D=SC　S和C的乘積

雖然將式(1)改爲式(2)之線性關係，但依統計理論而言，利用最小平方法來求得B、S、D的值，並不是一個很好的方法，因爲C爲D和S的比值，所以它的平均值 (Mean) 和標準差 (Standard Deviation) 是毫無意義[8-9]。

所以在此採用幾何表示 (Geometric Expression) 建立以 v_i 爲橫軸，a_i 爲縱軸，A_i 爲高度的感應面 (Response Plane) 來處理。在此一感應面中，無法直接獲得分析物濃度資料。若將此一平面延伸交於 v_i 和 a_i 所構成的底面時，可得一直線，則此一直線的斜率即爲分析物的濃度。此線的斜率並不受到空白值的影響，因爲只要任一平行於底面的平面和感應面相交皆可決定出分析物的濃度（感應面的斜率）。

實 驗

儀 器：

1. 16位元電腦：CPU 8088, 640KB RAM

步 驟：

1. 波峰的模擬：當分析物經一理想的管柱（Column）時，應當呈現出高斯（Gaussian）分佈，可由式(3)表之：

$$Y(Z)=h_g * \exp(-Z^2/2) \qquad (3)$$

其中：$Z=(t-t_g)/\sigma_g$

t	溶洗時間
t_g	呈現高斯峰時，最高點的時間
σ_g	標準差（S.D.）
h^g	波峰的高度

但在實際的狀況下，分析物經常受到注入（Injector）或偵測器(Detector)的延遲（Delay）影響[10]，出現前伸（Fronting）或拖尾（Tailing）的波峰，所以有時間常數（Time Constant）的產生，用以修正高斯峰，因此可將式(3)改爲以 E(Z) 當作輸入函數（Input Function）的微分方程式（Differential Equation）：

$$Y(Z)+(\tau/\sigma_g)(dY(Z)/dZ)=E(Z) \qquad (4)$$

其中：τ 時間常數（Time Constant）

式(4)的微分方程可用一積分因子（Integrating Factor）解之[11]

2. 利用 Rland Delley 所提出的方法產生波峰[12]。假設在液相層析實驗時，有一干擾波峰存在（圖1），且在不同體積且未知濃度的分析物中（9, 15, 21, 27毫升）加入已知濃度的分析物，假設未知濃度的分析物爲 1M，經波峰模擬後可得（表1）和（圖1至圖13）的結果。

表 1. 不同體積的分析物加入已知濃度分析物所得的面積

分析物	面積	分析物	面積	分析物	面積
9 毫升	1.1277	加 0.100 M	1.3783	加 0.150 M	1.5036
15 毫升	1.6289	加 0.125 M	1.9421	加 0.175 M	2.0674
21 毫升	2.1300	加 0.150 M	2.5059	加 0.205 M	2.6437
27 毫升	6.6312	加 0.200 M	3.1323	加 0.225 M	3.1950

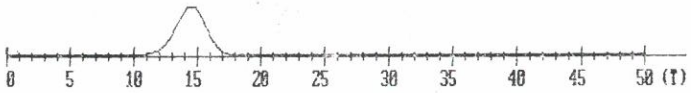

圖 1. 假設有干擾波峰存在

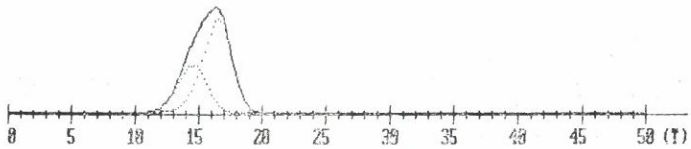

圖 2. 9毫升的分析物＋干擾存在

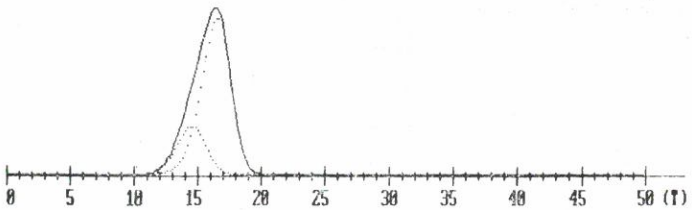

圖 3. 15毫升的分析物＋干擾存在

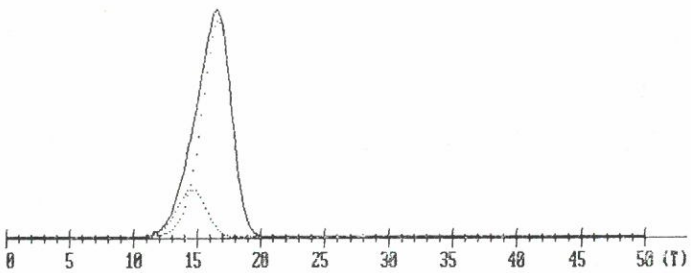

圖 4. 21毫升的分析物＋干擾存在

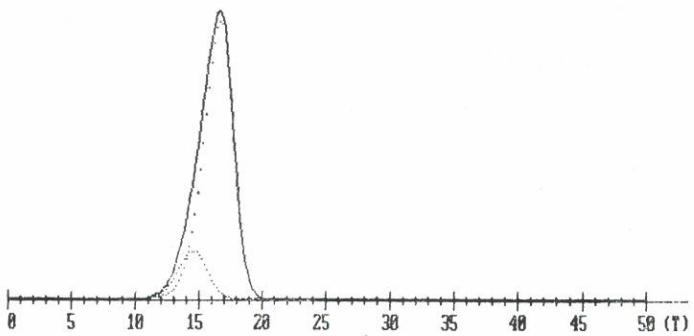

圖 5. 27毫升的分析物＋干擾存在

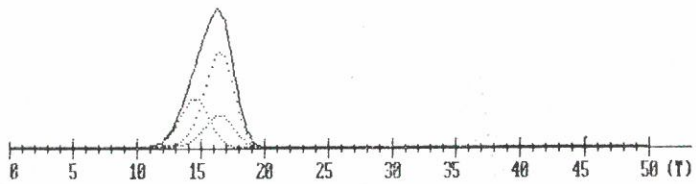

圖 6. 9毫升的分析物+0.1M的分析物+干擾存在

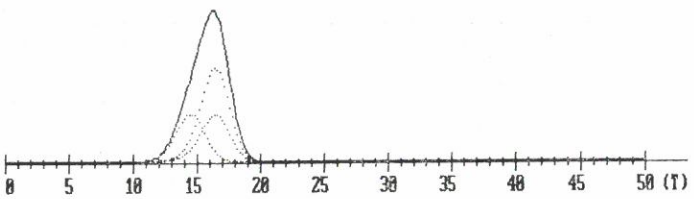

圖 7. 9毫升的分析物+0.150M的分析物+干擾存在

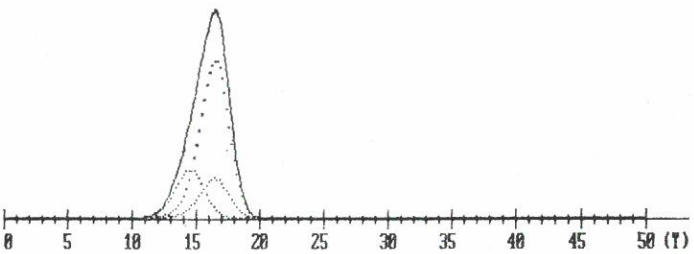

圖 8. 15毫升的分析物+0.125M的分析物+干擾存在

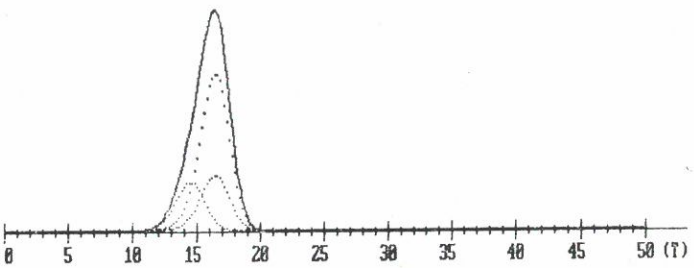

圖 9. 15毫升的分析物+0.175M的分析物+干擾存在

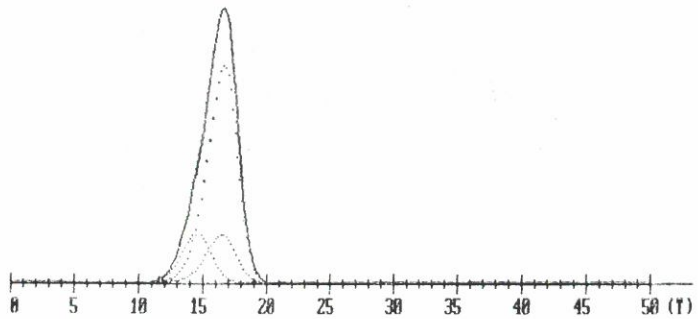

圖 10. 21毫升的分析物＋0.150M的分析物＋干擾存在

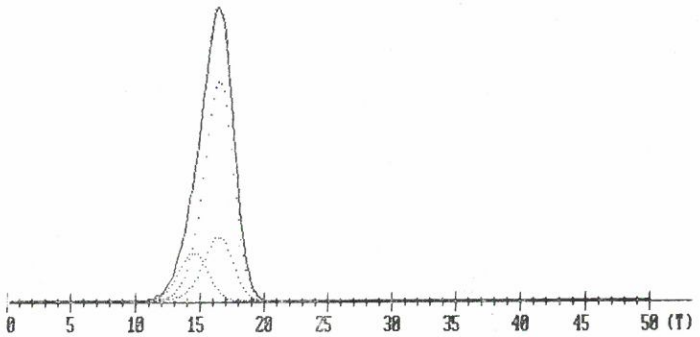

圖 11. 21毫升的分析物＋0.205M的分析物＋干擾存在

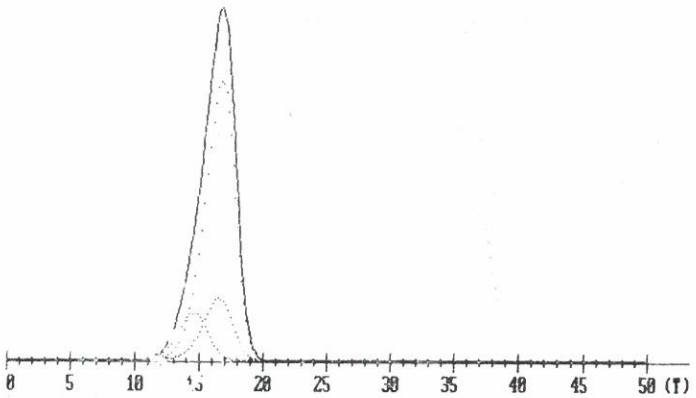

圖 12. 27毫升的分析物＋0.200M的分析物＋干擾存在

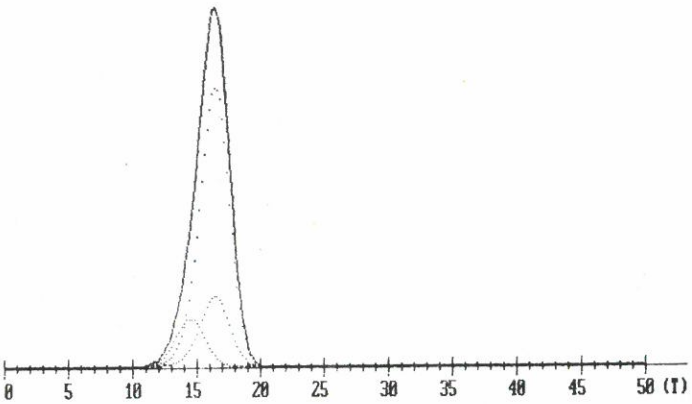

圖 13. 27毫升的分析物＋0.225M的分析物＋干擾存在

3. 將表1所得的資料輸入 GSAM 程式之後，可得表2和圖14的結果，分析物的濃度爲 1.00010 M，和先前假設分析物爲 1M 的值，完全符合。

表 2. 經 GSAM 程式後，可知分析物的濃度爲 1.00100 M

Point	Sample	Addition	Response	Point	Sample	Addition	Response
1	9.0000	0.0000	1.1277	11	21.0000	0.2050	2.6437
2	15.0000	0.0000	1.6289	12	27.0000	0.2250	3.1950
3	21.0000	0.0000	2.1300				
4	27.0000	0.0000	2.6312				
5	9.0000	0.1000	1.3783				
6	15.0000	0.1250	1.9421				
7	21.0000	0.1500	2.5059				
8	27.0000	0.2000	3.1323				
9	9.0000	0.1500	1.5036				
10	15.0000	0.1750	2.0674				

Sample: (0.00⊖30.00) Sample: Slope＝0.084 Intercept＝0.376 R＝ 1.0000
Add. : (0.00⊖ 0.30) Add. : Slope＝2.506 Intercept＝0.000 R＝ 1.0000
Rsp. : (0.00⊖ 5.00) Concentration ＝1.00010 Blank＝0.376 Sensitivity＝2.506

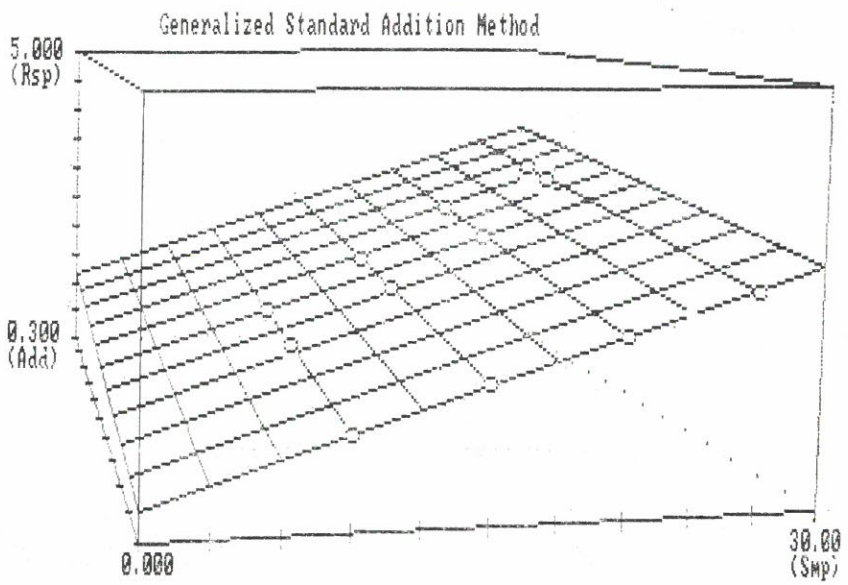

圖 14.　經 GSAM 程式後所得的感應平面

結 果 討 論

1. 式(1)中所用的單位及關係式如下：

A_t	無單位
B	無單位
$S=\varepsilon b$	(1/M)
$a_t=(V_x*C_x)/V_t$	(M)
$C=C_s/V_t$	(M/L)
$v_t=V_s$	(L)

其中 V_t=30 毫升

C_s：分析物的未知濃度

V_s：分析物的體積

C_x：加入已知濃度分析物的濃度

V_x：加入已知濃度分析物的體積

2. 因爲一切資料皆由電腦模擬產生，減少許多的干擾因素，所以從表 2 可以看出相關因子（Correlation Factor）皆爲 1，可知表 1 輸入的資料是線性

(Linear)，故可得到十分滿意的結果。換言之，在眞實的實驗過程中，若能降低實驗的誤差，必可得到十分可靠的結果。

3. 由於本法中需要的資料非常多而且需要高精確度，若以傳統人爲的方式來獲取可靠的資料實爲困難，因此自動取樣就非常的需要，在以後的工作上會將機器人使用在自動取樣及自動線上濃縮上，以減少人爲取樣的誤差並可得到可靠的結果。

結　　語

以往分析化學難以處理的空白值（Background）問題，利用本法就可以解決，同時本法稍經修改亦可應用於原子吸收光譜（AA），紅外光譜（IR），紫外光譜（UV）等分析方法。因爲本實驗之目的只是爲了消除層峰法的干擾峰並求出分析物的濃度，所以利用波峰的面積當做輸入資料，節省分析的時間。若是爲了分離重疊的波峰（Overlapping peaks）可將波峰的高度當做輸入資料來處理。在 AA, IR, UV 的分析方法，亦是用波峰的高度當做輸入資料，以消除空白值的問題。

參 考 文 獻

(1) B.E.H. Saxberg and B.R. Kowalski, *Anal. Chem.* 51, 1031 (1979).
(2) B. Vandeginste, J. Klaessens and G. Kateman, *Anal. Chim. Acta.* 150, 71 (1983).
(3) R.W. Gerlach and B.R. Kowalski, *Anal. Chim. Acta.* 134, 119 (1982).
(4) D.W. Osten and B.R. Kowalski, *Anal. Chem.* 57, 908 (1985).
(5) S. Piepponen, T. Alanko and P. Minkkinen, *Anal. Chim. Acta.* 191, 495 (1986).
(6) SPSS (Statistical Package for Social Sciences), North-western University, Evanston, IL.
(7) BMDP (1983) Biomedical Computer Programs, BMDP Statistical Software, LosAngeles, CA.
(8) M.G. Moran and B.R. Kowalski, *Anal. Chem.* 56, 562 (1984).
(9) J.H. Kalivas and B.R. Kowalski, *Anal. Chem.* 55, 532 (1983).
(10) Roland Delley, *Anal. Chem.* 57, 388 (1985).
(11) McWilliam, I.G.; Bolton, H.C. *Anal. Chem.* 41, 1755 (1969).
(12) Roland Delley, *Anal. Chem.* 58, 2344 (1986).

The Application of A Simplified GSAM Method to the Problem Solving of HPLC Background Correction

TAIN-DOW CHEN and SHOW-CHUEN CHEN

Department of Chemistry

ABSTRACT

A simple and general standard-addition method for a single-component determination has been adapted to solve the problem of HPLC background correction. The details of the method and examples by computer-simulated HPLC problems are discussed.

評估一新型銅離子電極對強干擾銀離子之抗拒性

化學系

饒忠儒　陳壽椿

摘　要

本文是評估一首次在文獻上出現的一種離子選擇電極，可以無懼强干擾離子的存在而能繼續操作。並探討銅離子電極在强干擾之銀離子存在下，其斜率、E° 值以及使用壽命之變化。

I. 引　　言

自 1960 年代起人們對離子選擇電極 (Ion-Selective Electrode) 開始發生興趣，迄至於今日，已二十餘年。其間所發表之論文數以萬計。而其之所以受到重視，則在於操作簡便且靈敏度高之原故。然而，它亦有其自身之缺陷，亦即在某些强干擾離子存在下，電極會受到不可逆之損害，使其線性消失而無法使用或甚至毫無訊號。此亦即是困擾 ISE 的使用者及研究者長達二十餘年，而至今仍舊無法解決之癥結所在。本文，即對此作一探討。

一般而言，ISE 的製備方法可由文獻[1,2] 得到詳盡的資料，而其感應 (Response) 的原理探討，則可參閱文獻[4-9]，但是關於研究干擾離子之文獻，就不易獲得，我們只能以早期的英美化學家之研究論文[10-17]，來做爲本實驗之基礎。但可以確定的一點是，至今所有市場上的電極都會在說明書上警告避免使用含有强干擾離子的樣品；可見這問題存在的一般性。

在沒有干擾離子存在之情況下，ISE 測定之原理，可由能斯特方程式(Nernst Equation) 表示：

$$E = E^\circ - RT/nF * \text{Log } a_i \qquad (1)$$

其中，a_i 爲初級離子 (Primary Ion) 之活性 (Activity)，n 爲離子之電荷，而在常溫常壓下，RT/nF 又可以簡化成 $0.0591/n$，因此，(1)式變爲：

$$E = E^\circ - 0.0591/n * \text{Log } a_i \qquad (2)$$

然而，在干擾離子 (Interference Ion) 的存在下，ISE 的電位與活性的關係，就必需做適度的修正了，一般是以尼可羅斯基方程式(Nicolsky Equation) 方程式來表示：

$$E=E^{\circ}-RT/n_i F * Log(a_i+k_{ij} a_j^{n_i/n_j}) \quad (3)$$

其中 a_i 爲初級離子的活性

a_j 爲干擾離子的活性

n_i 爲初級離子的價數

n_j 爲干擾離子的價數

k_{ij} 爲 j 對 i 之選擇係數 (Selectivity Coefficient)

在 $n_i=n_j$ 之情形下，理論上 MJ 對 MI 之選擇係數 k_{ij} 可表爲二者 k_{ij} 的商，即：

$$k_{ij}=\text{ksp (MI)}/\text{ksp (MJ)} \quad (4)$$

此種表示法可見於文獻[10-16]，而對於 $n_i \neq n_j$ 之情況，k_{ij} 可表爲：

$$k_{ij}=\text{ksp (MI)}/\text{ksp (MJ}_z)^{1/z} \quad (5)$$

此二式詳細之推導過程，可參考文獻[15]。

而我們在此次實驗中，關於干擾離子之部份，則是參照 Srinivasan and Rechnitz[17] 之方法而來。

II, 實　　驗

一、試劑及器材

碳　棒 (聯勤電池廠 3 號電池用碳棒)
氯化鉀 (E. Merck G.R. 級)
硫酸銅 (E. Merck G.R. 級)
濃鹽酸 (E. Merck G.R. 級)
硝酸銀 (E. Merck G.R. 級)
氯化銅 (E. Merck G.R. 級)
硫化鈉 (R.D.H., West Germany, G.R. 級)
PVC 管
二液型環氧樹脂 (市售 AB 膠)
去離子水 (12 MΩ)
單心銅線
BNC 接頭 (3C)

二、儀器

PH Meter (JENCO 6209)
參考電極 (BROADLEY JAMES CORPORATION)

三、步驟

電極之製備：

製備方式可參照文獻[1-3]之方法改良，分爲A、B、C三組。A組電極先浸入濃鹽酸中，以超音波振盪5分鐘，取出碳棒，倒掉鹽酸，再振盪清洗，重覆此步驟，至棄置之鹽酸廢液澄清爲止。此時，再將碳棒浸入濃鹽酸中，封口，置於通風櫥中，隔夜。次日取出隔夜之碳棒，以去離子水沖洗，並以超音波振盪，至PH值約略爲七，再浸於1M之硫化鈉溶液中，浸隔夜。次日再取出浸泡硫化鈉隔夜之碳棒，不經去離子水沖洗，直接浸入1M之硫酸銅溶液中，至少4小時。此時，碳棒表面即已塗佈上一層硫化銅。取出塗佈完成之碳棒，陰乾，再以拭鏡紙輕輕磨光碳棒表面。此時，表面再經一道特殊之處理方式[18]，然後以二液型環氧樹脂爲接着劑，以PVC管封口，乾燥約6小時。接着灌入飽和氯化鉀溶液作內導液，至半滿爲止，置入導線，以鋁箔封口，即完成電極之製作。需要特別注意的是，不要使導線之金屬和鋁箔接觸，以免干擾產生。B組電極的製法和A組完全相同，只是在用鹽酸清洗之前，將碳棒的一端磨成圓錐形。C組電極，製法和A組同，只是省略掉最後一步之表面處理步驟。電極完成後，即可開始測試。

電極之測試：

將製成之電極，浸入 10^{-7}～10^{-1} M的硫酸銅標準溶液中，測各濃度之E值（電位值），作校正曲線，求出其截距，線性範圍（Linear Range），斜率，及γ值（相關係數）。再依前法，將電極浸入配製完成的 10^{-5} M $Ag^+/10^{-4}$ M $CuSO_4$－10^{-1} M $Ag^+/10^{-4}$ M $CuSO_4$ 溶液中，再作一次校正曲線，然後取出電極，浸入0.1 M $CuCl_2$ 溶液中，24小時後取出，再浸入 10^{-7}－10^{-1} M 的 $CuSO_4$ 溶液中，再作一次校正曲線。

III. 結果與討論

一銀離子對銅離子之干擾係數

在可考的參考文獻中，均未出現該係數之具體數據，而一般僅在文獻[7]中以"干擾極强"（Interferes Strongly）一語帶過，而這也是我們所能得到的唯一資料。在本實驗中，我們依文獻[16,17]，以及直接解尼可羅斯基方程式之聯立方程式等三種方法，欲求出該係數，然而三種方法所求出之值，差異極大，而莫一是衷。但是，由方程式(3)：

$$E = E^\circ - RT/n_iF * \mathrm{Log}\ (a_i + k_{ij}\, a_j^{n_i/n_j})$$

可知，在 k_{ij} 項極大，而 a_i 爲一定值之情況下，a_i 可忽略不計，而電位E對Log a_i 作圖，可以得一直線。而在 k_{ij} 極小，趨近於零，而 a_i 固定之情形下，所得之E值，幾乎爲一定值，亦即所得之電位與 a_i 無關。而我們由實驗所得之結果，圖1和圖2觀之，均一斜率爲負之直線。圖1是A電極於5分鐘取值所

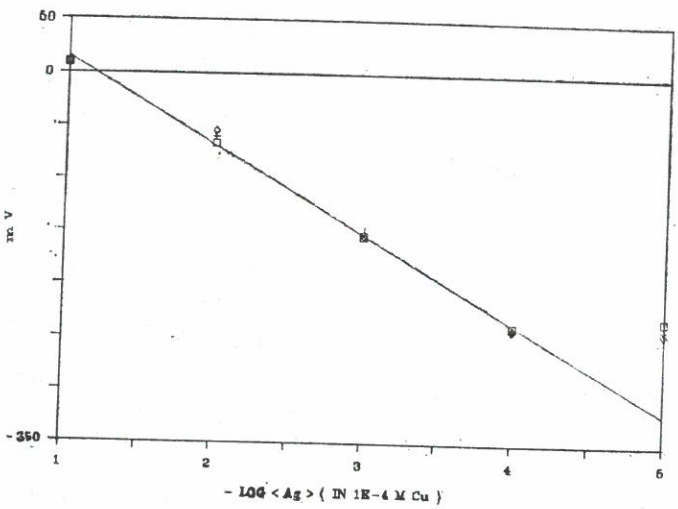

圖1. A電極，在 10^{-4} M 硫酸銅溶液作背景溶液時，其對銀離子之校正曲線。斜率−83.600，r 值0.9983，線性範圍10^{-1} 到 10^{-4}。

作對銀離子的校正曲線。B電極之校正曲線，亦類似於圖1所示。圖2爲C電極之校正曲線。此二圖均是固定銅離子在 10^{-4} M，而改變銀離子的濃度，由 10^{-4} M−10^{-5} M 所作之曲線。由於每條曲線之斜率均爲很大的負值，因此，我們可以斷定，其干擾係數非常之大，但是，大到什麼程度，有待進一步測定。

二、浸泡 $CuCl_2$ 溶液以去除干擾效應

在 ISE 的使用中，最大的限制即是在電極本身，如果遇到强干擾離子，則干擾離子便會與電極上的初級離子產生離子交換作用，而使電極遭到不可逆的損害，而使電極對初級離子的感應狀況，不再呈線性的關係。在一般的固態電極 (Solid State Electrode)，其干擾的程度，與干擾離子和初級離子對塗佈於電極上的陰離子之 ksp 的比值有關[10-15]。針對於此，我們發現，在電極接觸過强干擾離子後，可以藉着泡在 0.1 M 的 $CuCl_2$ 水溶液中 24 小時，而使電極再生。但值得注意的是，這種處理方式，僅對經過表面處理過之電極有效。而且干擾離子本身必須是能和 Cl^- 形成錯化物 (Complex) 之物種才有效，這也是使用上的限制。我們可以由圖3和圖4的結果，證實此種處理方式的功效。圖3爲電極 A 在測試銀離子前，由 10^{-1} M−10^{-7} M 的硫酸銅溶液，在5分鐘取值之校正曲線。而圖4，則是在測試過銀離子後，以 0.1 M $CuCl_2$ 浸泡24小時，然後作校正曲線之結果。B電極之測試結果，亦與A電極雷同。由以上圖形，可以得知，$CuCl_2$ 的確可以使受過强干擾離子之電極，恢復其對初級離子之線性關係。相對於圖5，圖5是A電極在受到銀離子干擾後，未用 $CuCl_2$ 處理，而僅泡在

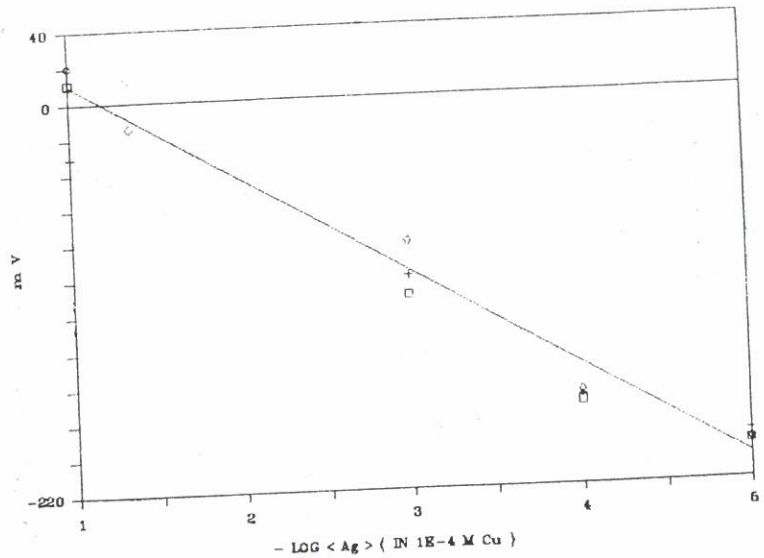

圖2. C電極，在 10^{-4} M 硫酸銅溶液作背景溶液時，其對銀離子之校正曲線。斜率－54.0566，r 值 0.9697，線性範圍 10^{-1} 到 10^{-5}。

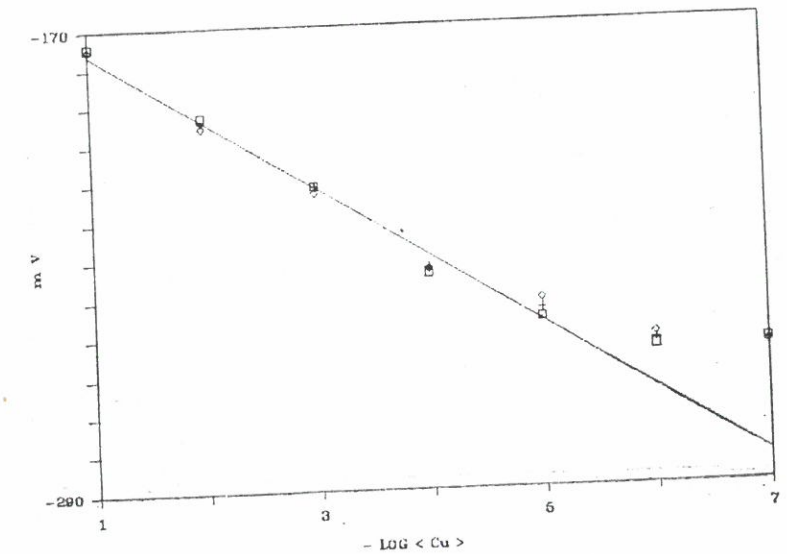

圖3. A電極，在未受銀離子干擾前，其對銅離子之校正曲線。斜率－17.7333，r 值 0.9955，線性範圍 10^{-1} 到 10^{-5}。

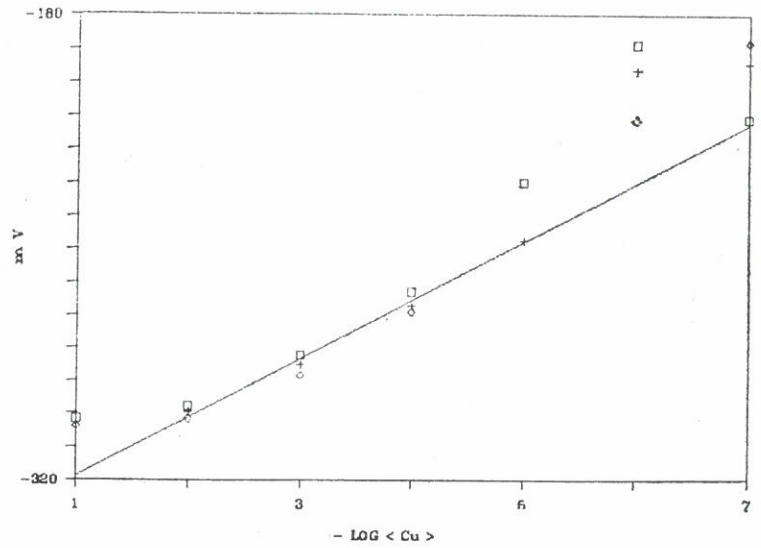

圖4. A電極，在受到銀離子干擾之後，其對銅離子之校正曲線。斜率－17.6067，r 值 0.9973，線性範圍 10^{-2} 到 10^{-5}。

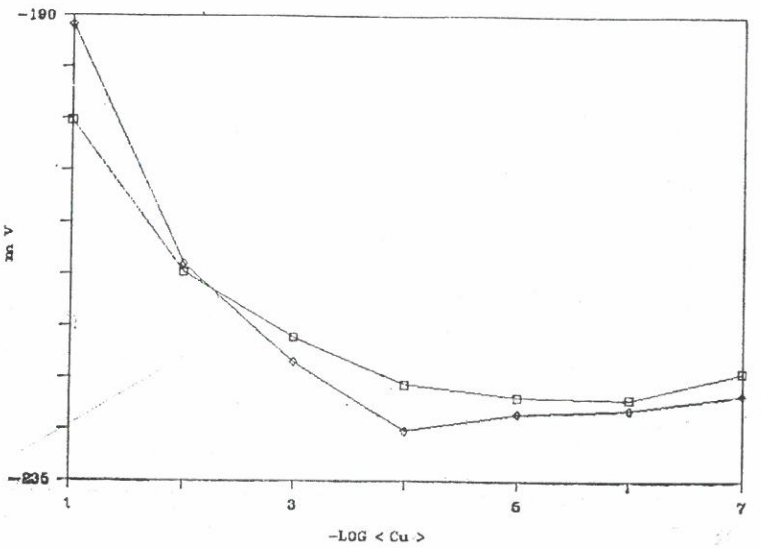

圖5. A電極，在受銀離子干擾後，未用 $CuCl_2$ 處理，而僅泡在水中 2 小時，電極對銅離子之校正曲線。

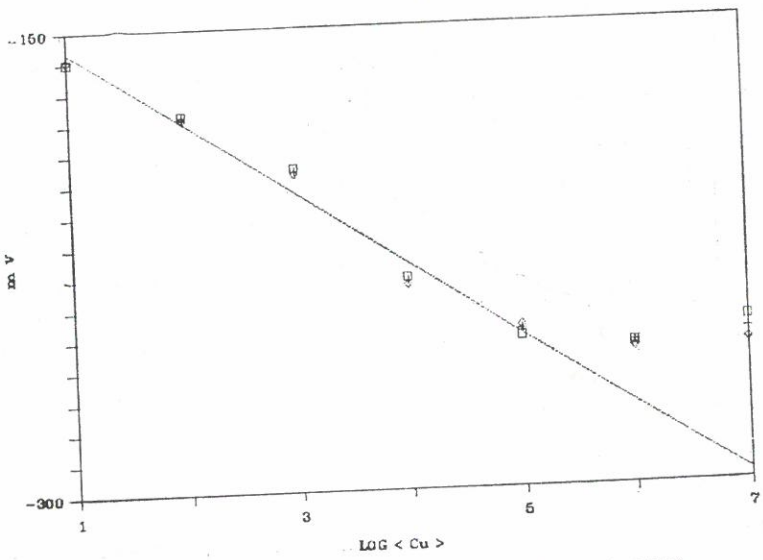

圖6. C電極，在未受到銀離子干擾之前，其對銅離子之校正曲線。斜率−23.4633，r 值 0.9827，線性範圍 10^{-1} 到 10^{-5}。

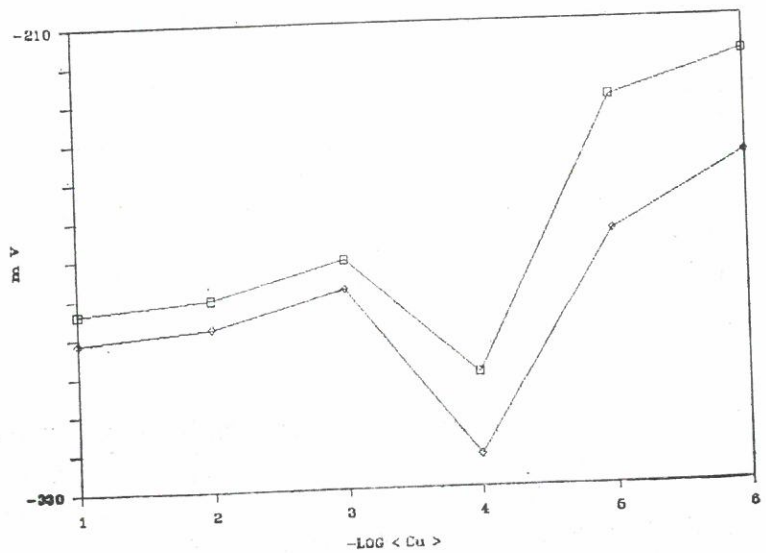

圖7. C電極，在受到銀離子干擾之後，其對於銅離子之校正曲線。

水中 2 小時之校正曲線，我們可以明顯的見到，其對於銅離子濃度改變所受之感應，幾乎沒有線性可言， $CuCl_2$ 的功效，由此可見。但這種處理方式，其效用也僅限於表面上經特殊處理過的電極而已。

三、電極表面之特殊處理

前文以提及 $CuCl_2$ 的功效，只可見於表面有特殊處理過之A組和B組電極。而對未經表面處理的C組電極，$CuCl_2$ 就無法發揮其功效了。我們可以由圖 6 和圖 7 的結果看出，C組電極在經過測試銀離子的步驟以後（圖 7 ），雖然也經過 $CuCl_2$ 相同的處理過程，然而其原先所擁有對銅離子的線性關係（圖 6 ）已經完全消失。由此可見，在電極製作過程中，多加最後的一步處理工作是非常的重要——能够有效的解決干擾離子的問題。這不但是離子選擇電極最迫切的需要，也是進一步能够將 ISE 之技術應用於化學程序分析儀 (Process Analyzer)的關鍵，這個表面處理的技術將另文發表。

四、電極之缺陷

雖然，由前文所述可知，以往困擾 ISE 研究者和使用者的不可逆之强離子干擾現象，我們已有能力予以克服。傳統的 ISE， 一旦經强干擾離子的干擾後，就完全失去其效用，而依我們的製程製作的電極，即使受到强干擾離子的干擾後，依然可以使用。但是電極本身仍有其使用上之缺陷。譬如，在經過特殊處理過的電極， $CuCl_2$ 的處理方式，雖然可以恢復其線性，但其使用範圍會減小一個乘方（一個 order），且其斜率明顯的由負變爲正，但此可以在電極製成後，立即先以强干擾的銀離子溶液浸泡，則其斜率即可維持不變，此時電極即使再受到强干擾離子干擾，也不會有由負變正的現象出現，而且此種電極在銀離子濃度低於 10^{-2} M 時，銀離子對電極幾乎沒有干擾，而一般水溶液中，銀離子幾乎不可能達到如此高的濃度，因此，在使用上是毫無問題的。這些結果，我們整理在表 1 中，以供參考。然而，導致這些變化的原因，目前仍不明瞭。而且，由於表面處理的方法，仍未臻完善，使得電極僅能使用於 PH 值 4～7 的水溶液中。這些均是我們日後繼續研究改進之重要課題。

IV. 結　　論

大致而言，自傳統的離子選擇電極發展至今，干擾離子之不可逆損害一直困擾着科學家，這也是離子選擇電極一直未能扮演它應有的角色的原因。近年來，將離子選擇電極應用於化學程序線上分析之趨勢甚囂塵上，唯基本上的問題，如本文所述之不可逆的干擾破壞，倘未能解決，則其應用亦甚爲有限，充其量僅能使用於簡單製程的工廠內，做線上檢測監視之用，因爲干擾離子並不存在於該系統中。本文所述之方法，雖未臻完善，但由初步的實驗已可驗證其可行性，以後

表 1.

		電極 A			電極 B			電極 C		
		斜率	線性範圍	r 値	斜率	線性範圍	r 値	斜率	線性範圍	r 値
20 秒 取値	未測 Ag^+ 以前	−18.5866	10^{-1}—10^{-5}	0.9974	−13.8900	10^{-1}—10^{-5}	0.9798	−23.7133	10^{-1}—10^{-5}	0.9801
	測 Ag^+ 時	−81.4166	10^{-1}—10^{-4}	0.9960	−62.7566	10^{-1}—10^{-4}	0.9867	−54.5800	10^{-1}—10^{-5}	0.9665
	測過 Ag^+ 以後	20.2300	10^{-2}—10^{-5}	0.9791	29.1367	10^{-1}—10^{-4}	0.9844	—	—	—
5分鐘 取値	未測 Ag^+ 以前	−17.7333	10^{-1}—10^{-5}	0.9955	−14.6500	10^{-1}—10^{-5}	0.9791	−23.4633	10^{-1}—10^{-5}	0.9827
	測 Ag^+ 時	−83.8600	10^{-1}—10^{-4}	0.9983	−66.8900	10^{-1}—10^{-4}	0.9938	−54.0566	10^{-1}—10^{-5}	0.9697
	測過 Ag^+ 以後	17.6067	10^{-2}—10^{-5}	0.9973	27.8667	10^{-1}—10^{-4}	0.9771	—	—	—

的工作當是針對：

一、如使使干擾離子的影響減至1%以下。

二、如何改進表面處理技術，俾能使用於中性溶液以外的條件下。

等幾項主題，繼續做更深入之研究探討，我們將另文發表。

參考文獻

(1) A. Palanivel and P. Riyazuddin, *J. Chem. Educ.* **61**, 920 (1984).
(2) Jane-Yu Liu, Jia-Jen Chen and Show-Chuen Chen, *Fu Jen Studies* **19**, 83 (1985).
(3) Jong-Ru Rau, Rong-Jong Lii and Show-Chuen Chen, *Fu Jen Studies* **20**, 43 (1986).
(4) R.P. Buck, *Anal. Chem.* **40**, 1432 (1968).
(5) J. Sandblom, G. Eisenman and J.L. Walker, Jr. *J. Phys. Chem.* **71**, 3862 (1967).
(6) W.E. Morf, *The Principles of Ion-Selective Electrodes and Membrane Transport* (Elsevier Scientific Publishing Co., Amsterdam, 1981), Chap. 14.
(7) Arthur K. Covington, *Ion-Selective Electrode Methodology*, **Vol. I,** (CRC Press Inc., Roca Ration, Florida, 3rd. Printing, 1984), Chap. 9.
(8) Ernö Lindner, Klara Tōth and Ernö Pungor, *Anal. Chem.* 48, 1071 (1976).
(9) W.J. Baedel and D.E. Dinwiddie, *Anal. Chem.* **46**, 873 (1974).
(10) W.E. Morf, *The Principles of Ion-Selective Electrodes and Membrane Transport* (Elsevier Scientific Publishing Co., Amsterdam, 1981), Chap. 10.
(11) A.K. Covington, *Ion-Selective Electrode Methodology*, **Vol. I,** (CRC Press Inc., Roca Ration, Florida, 3rd. Printing, 1984), Chap. 1.
(12) A.K. Covington, *Ion-Selective Electrode Methodology*, **Vol. II,** (CRC Press Inc., Roca Ration, Florida, 3rd, Printing, 1984), Chap. 4.
(13) G.J. Moody, *IUPAC Ion-Selective Electrode* (Page Bros (Norwich) Ltd., Norwich, England, 1973), p. 421.
(14) D.S. Papastathopoulos and M.I. Karayannis, *J. Chem. Educ.* **57**, 904 (1980).
(15) Werner E. Morf, Günter Kahr and Wilhelm Simon, *Anal. Chem.* **46**, 1538 (1974).
(16) Charles R. Martin and Henry Frelser, *J. Chem. Educ.* **57**, 512 (1980).
(17) K. Srinivasan and G.A. Rechnitz, *Anal. Chem.* **41**, 1203 (1969).
(18) S.C. Chen and J.R. Rau, details will be published elsewhere.

The Evaluation of The Immunizability of a Novel Cu Ion Selective Electrode Against Stronglv Interferent Silver Ion

JONG-RU RAU and SHOW-CHUEN CHEN

Department of Chemistry

The evaluation of a first-time reported ion selective electrode with immunity from interferent ions is presented. The variation of the Cu electrode slope, E° values and its life under the influence of interferent silver ion are studied.

葡萄果汁脫二氧化硫方法之研究

輔仁大學食品營養研究所

陳　雪　娥

摘　　要

二氧化硫廣泛地作爲化學防腐劑使用，可以防止微生物之生長，抑制酵素性及非酵素性褐變的產生等，本實驗以酸性偏亞硫酸鉀作爲葡萄果汁中間貯藏之防腐劑，同時研究脫二氧化硫條件及脫二氧化硫過程中對果汁品質的影響。結果顯示 hydroxymethylfurfural 在脫二氧化硫過程中會少量形成，而 methyl anthranilate 會有相當量減少；SO_4 的含量會增加可能是由於 SO_2 氧化形成；至於其他成分則變化很少。

引　　言

二氧化硫的使用歷史悠久[14]，自古以來，人類即已知道使用二氧化硫來保存食物。在釀酒業方面，早期的埃及人和羅馬人使用燃燒硫所產生的氣體，來烘燻殺菌；一直到今天，葡萄酒釀造過程中，如：酒桶殺菌，控制微生物汚染，貯存期間防止葡萄酒過度氧化等，依然採用二氧化硫。在肉製品保存方面，1813年已有英國人使用二氧化硫來保存肉類和水產品。在製糖工業方面，1858年，也有人使用二氧化硫來防止褐變作用。至於蔬果保存方面，19世紀後葉，美國加州廣泛使用二氧化硫來抑制各種酵素性反應；在第二次世界大戰期間，英國和北美洲，使用二氧化硫來製造乾燥蔬果[5]。近年來，二氧化硫也可充當氧化劑，可逆性破壞 Cystine 的雙硫鍵，使蛋白質分子鍵固定結合成網狀組織，增加麵糰氣體的保留，有利於餅乾的製造[14]。1975 年，歐洲共同市場通過使用二氧化硫來保存葡萄汁[12]。

目前，臺灣地區葡萄年產量鉅增，由於加工葡萄之採收期很短，無法在短期內加工成成品；故此，需要一個中間貯藏法來調節大批生產的葡萄汁。二氧化硫貯藏法，無疑是一廉價又能達到保存效果的貯藏法，在石油價格高漲，能源危機的今天，冷凍和冷藏貯藏法所消耗的成本龐大，而二氧化硫保存果汁，不需事先經過殺菌，加熱等前處理，只要添加足量的二氧化硫，保持在一密閉的貯存容器（如：不銹鋼槽），放置於室內陰涼處；即能發揮保存的效果。此外，葡萄汁 pH 約 3.0～3.4，在此酸性條件下，二氧化硫的抑菌效果良好；同時，在去二氧化硫過程中，SO_2 氣體亦容易去除，不妨礙果汁之成品加工[8,9,12,13]。

本實驗的目的即在了解二氧化硫貯藏法在臺灣的氣候條件下對於葡萄果汁保

存及防腐的有效性，並探討去除二氧化硫的過程對果汁品質的影響。

材料與方法

材　　料

康歌葡萄（*Vitis labrusca* cv. Concord）採自臺灣土地銀行南澳分場，以流水洗滌，去梗，選別，瀝乾，置於冷凍室（−20°C）貯藏備用。

果汁的製造

冷凍葡萄在室溫下解凍，把果實破碎，放入雙重釜，加熱至 50°C 拌攪，加入 0.3% 果膠分解酶（Pectinol，西德 Röhm 公司），作用約 1 小時後，再以油壓機榨取果汁，所得之果汁裝於不銹鋼桶，冷却至室溫，然後置 −20°C 冷凍貯藏備用。

二氧化硫的添加法

冷凍果汁在室溫完全解凍後，添加 SO_2，添加方法是以粉狀酸性偏亞硫酸鉀（Potassium metabisulphite）$K_2S_2O_5$ 加入果汁中（以 50% 有效 SO_2 濃度計算），把盛裝容器密閉，再加以適當搖混，以求 $K_2S_2O_5$ 能充分溶解。

將添加二氧化硫的果汁置於室溫下貯藏，觀察其發酵情形。

二氧化硫去除法[12,17]

二氧化硫去除法（Desulphiting process）之裝置如圖 1，主要是由 pre-

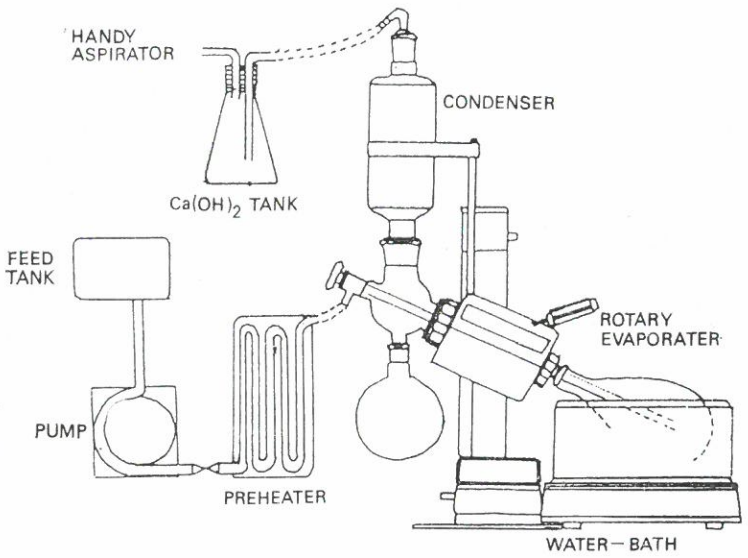

Fig. 1. Schematic drawing of the desulphiting process.

heater 及 heat evaporator (Yamato: Model RE-51B-6) 組成。果汁樣品由貯存桶經馬達抽取到 preheater (水浴微管間接加熱裝置)，將果汁加熱到相當溫度後，再送到 rotary evaporator。載滿香氣和 SO_2 的蒸氣，經過冷凝管以後，香氣得以回收，而 SO_2 氣體會被 handy aspirator 抽取到 $Ca(OH)_2$ 中和槽，進行中和作用，然後排出廢氣。

脫硫 (Desulphitation) 條件爲：

溫度	: 90°C
時間	: 15 min
rotary evaporator 的轉速	: 25-30 rpm
載氣體 (carrier gas)	: N_2 (pure)

二氧化硫測定法[4]

SO_2 之測定分 Free-SO_2 測定法及 Bound-SO_2 測定法，其裝置如圖 2。

(a) Free-SO_2 測定法

取 50 ml 果汁置圓底燒瓶A中，在梨形瓶B內加入 25 ml 之 0.3% H_2O_2，50 ml 蒸餾水及 5～6 滴混合指示劑 (混合指示劑由下列成份組成：methyl red 100 mg, methylene blue 50 mg, 50% alcohol 至 100 ml)。A, B 二瓶接裝完妥後，由C加入85% H_3PO_4 15 ml，通入 N_2 氣，氣泡徐徐在A, B兩瓶產生；D瓶可加足量 H_2O_2 及混合指示劑，作用是收集過多的 SO_2；待酸和果汁作用20分鐘後，取下B瓶，以 0.01 N NaOH 滴定，得 X_1 值。

Free-SO_2 量 (ppm) $= 6.4\ X_1$

(b) Bound-SO_2 測定法

樣品取量及測定法與 Free-SO_2 者相同，唯在 A 瓶處，設電熱包加熱，作用20分鐘後，同樣以 0.01N NaOH 滴定，所得 X_2 值爲 total-SO_2

Bound-SO_2 量 (ppm) $= 6.4\ (X_2\text{-}X_1)$

果汁品質測定：

(a) pH 值測定：

果汁以 digital pH meter (Suntex, Model Sp-7) 直接測定。

(b) Brix 測定：

以 Hand Refractometer (ATAGO N_1) 直接測定。

(c) 可滴定酸的測定[6]：

取 25 ml 果汁至玻璃燒杯，加熱去除空氣，加 50 ml 蒸餾水，冷却至室溫，用 1/3 N NaOH 滴定到 pH 7.0。

(d) 還原糖測定法[6]：

採用 Luff'-Schooyl 方法測定。

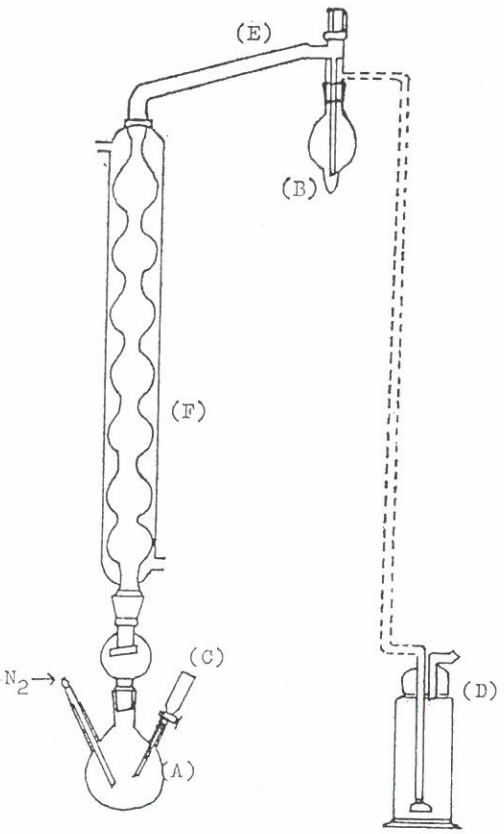

Fig. 2. Semimicro apparatus for SO_2 determination.

A: Round-bottom flask, B: Pear shaped flask,
C: Adapter, D: Collecting vessel,
E: Connecting adapter, F: Condenser.

(e) 顏色的測定：

以 color and color difference meter (Model 100 DA, Nippon Denshoku Kogyo, Co. Ltd) 直接測定 L, *a*, *b* 值。(標準白板 L=97.3, *a*=0.2, *b*=0.3)

(f) Anthocyanin 的定量[2]：

採用酸鹼度差額法 (pH differential method) 測定，A, B兩管中，各加入 1 ml 果汁及 1 ml 含有 0.1% HCl 之95%酒精，A管再添加 10 ml 2% HCl; B 管則添加 10 ml pH 3.5 buffer (由 0.2 M Na_2HPO_4 303.5 ml，加 0.1 M 檸檬酸 695.5 ml，調 pH 至 3.5)，以分光光度計 (Spectropho-

tometer: Hitachi 220 S)，在 520 nm 下測吸收值。A值與B值之差距，即是果汁之 Anthocyanin 量。另以 Malvidin chloride (Sigma 公司出品) 爲標品，依同法畫標準曲線 (calibration curve)，可從標準曲線求待測果汁之 Anthocyanin 濃度，以 ppm 表示。

(g) methyl anthranilate 的定量[2,8]：

取 10 ml 果汁，加約 50 ml 蒸餾水，用 Kjeldahl Apparatus 蒸餾；備一已裝 10 ml 蒸餾水的三角瓶，收集蒸餾液至約 95 ml；然後加水至 100 ml，以分光光度計在 217nm 測吸光度，所得值爲果汁 methyl anthranilate 含量值之 $\frac{1}{10}$。另配製不同濃度之 methyl anthranilate 標品，直接在 217 nm 測吸光度，製標準曲線，果汁中之 methyl anthranilate 量亦可從標準曲線中求得其濃度，以 ppm 表示。

(h) Hydroxymethylfurfural 的測定[6]：

A, B兩管中各加入 2 ml 果汁及 5 ml *p*-toluidin 試藥 (*p*-toluidin 10 g 加冰醋酸 10 ml，加 isopropanol 至 100 ml)，A管再加 0.5% barbituric acid 1 ml；B管則加等量蒸餾水，爲對照組，在 550 nm 下測吸光度。另以不同濃度之 5-Hydroxymethyl-furfuraldehyde (Sigma 公司出品) 爲標品，依同法製標準曲線，所得值亦以 ppm 表之。

(i) 灰分的測定[6]：

取 50 ml 果汁置於磁碟上，用水浴加熱法濃縮果汁，碳化後，再以 550°C 灰化，至恒重，灰分量以%表之。

(j) $SO_4^=$ 的測定[6]：

50 ml 果汁灰化後，加入 5 ml 25% HCl，加熱溶解，加水至 100ml；取 25 ml sample 置入定量瓶，加 2 ml Mg solution (5.5 g $MgCl_2$+7.0 g NH_4Cl+25 ml 10% NH_4OH→ 稀釋至 100 ml) 及 0.8 ml 10% Ammonium hydroxide，加水至 25 ml，離心。把上層液倒入備有 1 ml NaCl solution, 3 ml $BaCrO_4$ solution 之三角瓶，不停震盪 2～3 小時；加入 2 ml 10% Ammonium hydroxide，再次離心。取上層液於 430 nm 測吸光度。空白試驗是採用 5 ml 25% HCl 加水至 100 ml，再取其中 20 ml 依同法測定。

配置不同濃度 Na_2SO_4 (aq) (295.7 mg Na_2SO_4 相當於 400 ppm $SO_4^=$)，取 20 ml 加水已備有試劑之定量瓶，依同法操作；空白試驗是以 20 ml 蒸餾水取代 Na_2SO_4 溶液，而製成標準曲線。果汁中 $SO_4^=$ 量可從標準曲線中求取，以 ppm 表示之。

結果與討論

二氧化硫的添加及保存效果

二氧化硫能抑制微生物的生長，致使果汁達到保存的效果。在實驗中，以 600, 800, 1,000, 1,200, 1,400, 1,600 及 2,000 ppm SO_2，在室溫下保存果汁，觀察其變化；發現對照組在三天內即有發酵作用，而添加了二氧化硫的果汁，即具備抑制微生物生長的效能，其中以添加 1,000 ppm SO_2 以上之果汁可以保存 4 個月而沒有發酵的現象產生。

二氧化硫的添加量，視果汁種類，pH 及微生物污染程度而決定。本實驗是以粉末狀 $K_2S_2O_5$ 直接添加到果汁中，然後充分攪拌混合。此法雖然簡單方便，但是，也要考慮粉末狀 $K_2S_2O_5$ 的溶解度及擴散情形[1]，同時 HSO_3^- 會和果汁中糖類結合，形成複合物 Hydroxysulphonates。SO_2 氣體也會和空氣作用或揮發，而致使添加到果汁中的 $K_2S_2O_5$ 有效量減少。葡萄汁中的細菌易受 SO_2 抑制，而黴菌和酵母對 SO_2 抗力較强[5,10,14]；本實驗爲了達到充分的抑菌和防腐效果，所以採用 1,200 ppm SO_2 保存葡萄汁。而 $K_2S_2O_5$ 有效量是以 50%計算；因此，每公升果汁添加 2.4 g 粉末狀 $K_2S_2O_5$。

對於添加了二氧化硫果汁，HSO_3^- 會和 Anthocyanin 結合，形成無色 polymer，不過，此褪色作用爲熱逆反應，對果汁的色澤影響不大。

二氧化硫之脫除

針對去除果汁中的二氧化硫，本實驗是採用加熱使 SO_2 氣體釋出的原理，設計了如圖 1 的實驗室型的裝置。以二氧化硫貯存的果汁，經馬達抽取到管式間接加熱裝置，進行瞬間加熱到 80°C，再送到 Rotary Evaporator，以高溫短時，把二氧化硫去除。N_2 爲 carrier gas，在 Handy Aspirator 的協助下，把 SO_2 氣體抽到中和槽。SO_2 和 $Ca(OH)_2$ 作用，生成 Calcium Sulfite[17]，至於果汁中的香氣，經冷凝後得以回收。

說到去除二氧化硫的條件，已知在低 pH，高溫下，有利於二氧化硫的去除，Lluch 等人[9]亦證實此論點，在 pH 2.5, 3.0, 3.5 和 4.0 的果汁進行去二氧化硫實驗，SO_2 去除率分別是 63%，59%，50%，和 41%。本實驗在求取二氧化硫去除條件中，亦作了類似探討，在 pH 2, 3, 4 以不同時間溫度去除二氧化硫。實驗結果如表 1，發現在低 pH，高溫時，二氧化硫去除效果最佳。

另一方面，加熱時間愈短，則果汁品質受破壞愈小。表 2 及表 3 說明，在 90°C 加熱，去二氧化硫過程所耗時間與去二氧化硫效果的關係。本實驗是考慮到加熱時間，果汁品質與去二氧化硫效果三個因素，來決定去二氧化硫條件。從表 2 及表 3 得知，20分鐘與30分鐘的去二氧化硫效果無顯著差異；而10分鐘與15分鐘者，則去二氧化硫率有顯著差異。爲了保持果汁品質不因長時間加熱而破壞

Table 1. Effect of time and temperature on the desulphiting process of Concord grape juice with pH 2, pH 3 and pH 4

Conditions			Free-SO_2		Bound-SO_2		Total-SO_2	
pH	temperature	time (minutes)	ppm	%	ppm	%	ppm	%
pH 2	Original		516.0	32.0	1095.0	67.9	1611.0	100.0
	RT	60′	158.0	9.8	214.0	13.3	372.0	23.0
		120′	86.0	5.3	116.0	7.1	202.0	12.5
	50°C	60′	50.0	3.1	168.0	10.4	217.0	13.5
		120′	29.0	1.8	81.0	5.0	110.0	6.8
	90°C	60′	9.6	0.6	6.4	0.4	16.0	1.0
		120′	10.0	0.6	5.7	0.3	16.0	0.9
pH 3	Original		541.0	45.4	650.0	54.5	1191.0	100.0
	RT	60′	538.0	45.1	551.0	46.3	1089.3	91.0
		120′	542.0	45.5	485.0	40.7	1027.3	86.0
	50°C	60′	451.0	37.9	542.0	45.4	992.0	83.3
		120′	263.0	22.1	462.0	39.0	708.0	61.1
	90°C	60′	4.2	0.4	24.6	2.1	28.8	2.5
		120′	1.6	0.1	11.2	0.9	12.8	1.0
pH 4	Original		745.0	61.1	475.0	38.9	1220.0	100.0
	RT	60′	720.0	59.0	458.0	37.5	1178.0	96.5
		120′	687.7	56.3	452.0	37.0	1139.0	93.4
	50°C	60′	348.0	28.5	751.0	61.5	1099.0	90.0
		120′	293.0	24.0	754.0	61.8	1047.0	85.8
	90°C	60′	172.0	14.1	203.0	16.6	375.0	30.7
		120′	105.6	8.7	223.0	18.3	328.0	27.0

，故採用 90°C 15 min 爲最適合本實驗的去硫條件。

此外，在去硫過程中，部分 Methyl anthranilate 會隨 N_2 及 SO_2 氣體揮發。本實驗也做了此方面的探討。表4說明添加了 10 ppm Methyl anthranilate 的果汁，在 90°C 15 min 去二氧化硫過程後的變化情形。結果發現 Methyl anthranilate 在脫二氧化硫過程中會大量地損失，依本試驗條件其保存率只有45%。

Table 2. Effect of time and temperature on the desulphiting process of pH 3 Concord grape juice, sample 1

Conditions		Free-SO_2		Bound-SO_2		Total-SO_2	
temperature	time (minutes)	ppm	%	ppm	%	ppm	%
Original		416.00	39.3	641.30	60.6	1057.30	100.0
90°C	10′	160.00	15.1	68.40	6.5	229.12	21.6
90°C	20′	7.04	0.6	20.48	1.9	27.52	2.6
90°C	30′	4.16	0.4	21.76	2.1	25.92	2.5

Table 3. Effect of time and temperature on the desulphiting process of pH 3 Concord grape juice, sample 2

Conditions		Free-SO_2		Bound-SO_2		Total-SO_2	
temperature	time minutes	ppm	%	ppm	%	ppm	%
Original		588.00	58.9	410.00	41.1	998.00	100.0
90°C	5′	224.00	22.4	160.00	16.0	384.00	38.4
90°C	10′	53.00	5.3	73.00	7.3	126.00	12.6
90°C	15′	9.60	1.0	42.00	4.2	51.80	5.2

Table 4. Effect of desulphiting process on methyl anthranilate (MA)*

Conditions		SO_2 (ppm)			MA retention	
temperature	time (minutes)	Free	Bound	Total	ppm	%
Original		373.3	361.0	734.0	17.6	100
90°C	15′	12.6	9.8	22.4	8.0	45

* The sample juice was fortified with 10 ppm MA.

二氧化硫去除對葡萄汁品質的影響

果汁添加二氧化硫固然有保存的效果，但是，果汁中二氧化硫的含量亦有一定的限制。一般而言，Free-SO_2 含量爲 15 ppm 以下[19]。對於果汁中過多的 SO_2，經加熱去二氧化硫過程，可部分去除，去硫溫度愈高時間愈長，則去二氧化硫效果愈完全；但是，亦往往影響果汁的品質，表 5 爲 Concord 葡萄原汁與經 90°C 15 min 去二氧化硫過程後之果汁的成份比較。

Table 5. Changes in chemical composition of Concord grape juice resulting from desulphiting process

Composition	Original	After desulphiting
pH	3.39	3.43
°Brix	14.8	15.2
Titratable acid, g tartaric acid/L	11.6	10.55
Reducing sugar, g/L	126.6	130.9
Anthocyanins, ppm	240	270
Color		
L	18.3	24.6
a	33.7	35.1
b	11.1	12.9
Methyl anthranilate, ppm	6	3
Hydroxymethylfurfural, ppm	5	7
Ash, %	0.23	0.39
$SO_4^=$, ppm	180	520
SO_2, ppm		
Bound-SO_2	1.6	43.3
Free-SO_2	3.2	14.2
Total-SO_2	4.8	57.5

二氧化硫的添加與去除對果汁 pH 和固形物含量沒有很明顯的改變。葡萄中的主要糖分是葡萄糖和果糖，在酸性條件下加熱去二氧化硫，可能促使果汁中多醣物的分解，造成還原糖量稍增加。至於非揮發性酸類而言，葡萄中主要成份是 tartaric acid 和 malic acid，其餘尙有少量 galacturonic acid, glucoronic acid, citric acid 和 phosphoric acid[2]。本實驗是以 tartaric acid 爲指標，在加熱過程中，酸度小幅度下降；Mantgomery 等人[11] 在探討加熱對 Concord 葡萄汁的影響之實驗中，亦得相同結果。可能是在加熱過程中，酸類遭破壞所致。

Concord 葡萄計有 14 種 anthocyanim，其中 peonidin 和 Malvidin 最穩定，而 delphinidin 是最不穩定的色素。在加熱去二氧化硫後，發現 L.a.b 值稍增加，同時，Anthocyanin 量亦增加，這可能是果汁中尙存約 60 ppm SO_2 所致。Sistrunk 及 Gascoigne[16] 針對 concord 果汁添加不同藥劑作研究，亦發現添加了 80 ppm SO_2 者，其 L.a.b 值及 Anthocyanin 較對照組高。此外，Leucoanthocyanin 構造和 anthocyanin 類似，在酸性條件下加

熱，則有可能轉變爲 anthocyanin；而且，在加熱過程中，一些 polymer 也可能會聚合，這些都有可能造成測定值的增加。

至於葡萄的香氣，是由各種 esters, alcohols, aldehydes 及 lactones 組成。對於 Concord 葡萄，其最主要香味物質是 methyl anthranilate[2]；屬於 *o*-aminobenzoic acid 之 methyl ester。Schreier 及 Paroschy[15] 以 GC 鑑定 concord 果實中揮發成份，亦再次證實，Methyl anthranilate 量較其他酯類多。在 1 大氣壓下，methyl anthranilate 的沸點是 266.5°C，於果汁中易保存；通常是以蒸氣蒸餾法收集此香味物，再加以定量。本實驗是將Casimir 等人[3]的方法略加以修正，以 Kjeldahl 蒸餾器來收集香味物，再以比色計測定濃度。Liu 及 Callander[7] 在測定 concord 的 methyl anthranilate 所採用的方法，亦和此類似。Methyl anthranilate 的 UV 吸收曲線在 217 nm 有一最大吸光度；這個結果和 Williams 與 Slavin[18] 的實驗相同。

從實驗結果可知，約50% methyl anthranilate 會在去二氧化硫過程中損失，這可能是部分 methyl anthranilate 隨蒸氣或 SO_2 揮發。在去二氧化硫裝置中，冷凝設備的效能與香味物的回收，有直接關係。目前，工業上利用的去二氧化硫裝置，除了有良好的廻流冷凝系統及 Stripping column 外，經石灰中和後的蒸氣或 carried gas，還是會在裝置中循廻[13]，所以香味的損失不是一大問題。此外，CNS 標準中亦沒有規定果汁不能添加香味物，所以，還是可以採用去二氧化硫後再添加 methyl anthranilate，來彌補損失的部份。

在高溫下，pentose 與 hexose 脫水，生成中間產物 Hydroxy methyl furfural (HMF) 及類似 furfural，具揮發性的羰基化合物，在酸性條件下，果汁加熱後 HMF 及 furfural 量特別多[6]。從表 5 可知，HMF 增加。這說明果汁在去二氧化硫過程中，可能加熱過度而造成 HMF 的產生。同時 furfural 和 HMF 有促進 Anthoyanin 分解的可能，在酸性條件下加高溫，則此二物會形成棕色聚合物，在色澤上也可能使果汁的顏色變得深紅。不過，目前商業上運用的去二氧化硫方法，已能在數秒鐘內完成去二氧化硫作業，因此，不致於對果汁的品質造成威脅[19]。

另一方面，果汁經過二氧化硫貯藏可發現，灰分和 $SO_2^=$ 量增加。這可能是二氧化硫在貯藏期間，因氧化作用而生成 $SO_4^=$ 離子，致使 SO_4 的含量增加。

參考文獻

(1) 王光輝, 製酒科技專論彙編 **6**, 110 (1984).
(2) M. A. Amerine and C. S. Ough, *Methods for Analysis of Musts and Wines* (A Wiley-Interscience Pub., 1980).
(3) D. J. Casimir, J. C. Moyer and L. D. Mattick, *J. Assoc. Off. Anal. Chem.*

59, 269 (1976).
(4) K. Hennig und Ludwig Jakob, *Untersuchungsmethoden für Wein und ähnliche Getränke* (Verlag Eugen Ulmer, Stuttgart, 1973).
(5) M.A. Joslyn and J.B.S. Braverman, *Advance in Food Research* 5, 97 (1954).
(6) Eckhard Krüger and Hans Joachim Bielig, *Betriebs- und qualitätskontrolle in Brauerei und alkoholfreier Getränkeindustrie.* (Verlag Paul Parey, Berlin und Hamburg, 1976).
(7) J.W.R. Liu and J.F. Callander, *J. Food Sci.* 50, 280 (1985).
(8) M.A. Lluch, F. Gasque, A. Fors and B. Laufoote, *Revista de Agroquimica Y Technologia de Alimentos* 17, 87 (1977).
(9) M.A. Lluch, F. Gasque, A. Fors and B. Laufoote, *Revista de Agroquimica Y Technologia de Alimentos* 17, 334 (1977).
(10) L.R. Mattick and D.F. Splittstoesser, *Am. J. Enol. Vitic.* 32, 171 (1981).
(11) M.W. Montgomery, F.G.R. Reyes, C. Cornwell and D.V. Beavers, *J. Food Sci.* 47, 1833 (1982).
(12) H. Müller-Späth, *Weinwirtschaft* 114, 1211 (1978).
(13) R. Potter, *Food Technology in Australia* 31, 113 (1979).
(14) A.C. Roberts and D.J. McWeeny, *J. Food Technol.* 7, 221 (1972).
(15) P. Schreier and J.H. Paroschy, *Can. Inst. Food Technol. J.* 14, 112 (1981).
(16) W.A. Sistruck and H.L. Gascoign, *J. Food Sci.* 48, 430 (1983).
(17) A.V. Slack, *Sulfur dioxide removal from waste gases.* (Nages Data Corporation, U.S.A., 1971) p. 42.
(18) A.T.R. Williams and W. Slavin, *J. Agric. Food Chem.* 25, 756 (1977).
(19) K. Wucherpfennig, *Flüssiges Obst* 42, 451 (1975).

Desulphiting Process of Grape Juice Stored with Potassium Metabisulphite

HSUEH-ERR CHEN

Graduate Institute of Nutrition and Food Science

ABSTRACT

Sulfur dioxide is used as a chemical preservative to reduce or prevent spoilage by microorganisms and as an inhibitor of enzyme-catalyzed oxidation and of non-enzymic browning during storage of many food products. Potassium metabisulphite was used as a preservative for bulk storage of Concord grape juice in this study. Conditions of desulphiting and chemical changes of grape juice resulting from the desulphiting process are studied. Hydroxymethylfurfural was formed in trace amounts during the desulphiting process, and methyl anthranilate decreased in quantity. The content of sulphate also increased as a result of oxidation during the sulphurization period. There were no significant changes in other compositions of grape juice.

SEX DIFFERENCE IN THE DEVELOPMENT OF THE CONCEPT OF EVENT SEQUENCES IN PRE-SCHOOL CHILDREN

SISTER VICTORIA ANNE HUANG

Department of Home Economics

ABSTRACT

The present study is an attempt to measure noticeable sex differences in pre-school children ages $4\frac{1}{2}$-$6\frac{1}{2}$ with regard to the development of the concept of event sequences. The testing for this study was carried out over a period of 4 months and the subjects were chosen randomly from 4 pre-school education institutions in the Taipei suburbs. Out of the original 280 children, 93 (47 boys and 46 girls) actually completed the experiment. Three treatments were used in the instructions of procedure: no stimulating factor; achievement motivation factor and competition factor. The testing materials consisted of nine sets of colored pictures with each set containing 7 pictures. The sets were graded in difficulty from easy to hard. Regardless of the testing treatment used, every child was required to put each set in sequential order. The time used for each set was recorded from the moment the child began turning over the pictures until the completion. The results showed that: 1. there was no sex difference in the development of the concept of event sequences in pre-school children; 2. the experimentor's instructions did not influence the time used to complete the experiment; 3. those sets of increased difficulty (more challenging) were completed faster by male subjects.

INTRODUCTION

It is not unusual in reading the older literature to come arcoss developmental studies of "the time concept." The implied unity is appealing but illusory. One author's time concept is clock and calendar time, another's is relative duration, and a third is historical sequence.

Temporal order, one of the significant portion of time concept, is an important feature of many event sequences, whether the events are observable or presented in narrative form. The ordering of event sequences with causal or other meaningful connections depends upon

both understanding the connections and coordinating them to from a temporal series. Similarly, drawing causal inferences from an observed sequence often requires attending to the temporal order of the events (Friedman, 1982).

Preschool children can understand what time sequences is. Fivush and Mandler, 1985, three experiments were used to test 4-, 5-, and 6-year olds' ability to sequence events. The hypothesis proposed that children initially construct temporal sequences by relying on the organization of their world knowledge instead of inferring logical relations among actions. In the first experiment, children were asked to order pictures of familiar and unfamiliar events in forward and backward order without having previously seen the set in its correct sequence. In the second experiment, children reconstructed previously seen sequences, and in the third experiment, children were shown forward and backward sequencns and reconstructed them in the opposite direction. In all three experiments the same pattern was noted; familiar events in forward order were the easiest to sequence; unfamiliar events in backward order were the most difficult. In an experiment carried out in 1985 by Barbara O'Connell and Anthony Gerard, the development of sequential understanding was tested in children ages 2-3. The study examined the extent to which knowing *that* certain things go together and knowing *how* they do are in dependent aspects of the developing cognitive system. The study showed that subjects as young as 20 months could distinguish familiar, ordered sequences from series of unrelated actions before they could reproduce the order of any type of sequence suggesting that temporal organization is imposed upon primitive representations of familiar events.

Linking object states through transformations is one aspect of the kind of general knowledge that would allow one to use causal principles to reason about and explain events. The ability to make causal inferences or to explain events relies in part on general knowledge about transformations and possible outcomes with respect to object states. This idea is a central component of those theories that describe the structure of representation, be it in terms ot

schemata (e.g., Piaget, 1974; Premack, 1976), scripts (e.g., Schrank & Abelson, 1977) or schematic organization (Mandler, 1978).

The young child's understanding of the relationships that hold between components of an event, object states, and the transformations that link them, has not received much direct investigation. A study by Gelman, Bullock, and Meck (1980) indicates that young preschoolers are also capable of relating object states through appropriate transformations. Gelman *et al* (1980) investigated children's understandings of transformations and object states by asking 3- and 4-year olds to fill in missing elements in three-item picture stories. Each completed sequence consisted of an object, an instrument, and the same object in another state. Some sequences depicted everyday events, others "bizarre" events, such as sewing a cut banana together or drawing on fruit. The latter type of sequences were included to control the possibility that when children had to fill in a missing slot, they did it simply on the basis of everyday memories. If a child was allowed to respond in his or her preferred direction, 80% and 90% of the 3- and 4-year olds' initial choices were correct.

Children's abilities to order a series of elements has typically been studied using problems of relative size (e.g., Elkind, 1964) or of the temporal order of a brief series of observable events or the events in a story (e.g., Brown, 1976; Piaget, 1969).

Crisafi *et al* (1986), conducted five studies in which the learning and transfer abilities of 2-4-year-old children were examined on a task in which they were required to combine two separately learned solutions to reach a goal. The three main findings were: (1) very early competence on the task if it is situated in familiar settings, (2) a developmental trend in the ability to notice the similarity across analogous versions of the problem that differ in surface format but share the same underlying logic, and (3) the success of two forms of assistance in promoting transfer. Their research showed that given a hospitable environment, children as young as 2-3 years of age can combine information and apply a reasoning rule quite broadly.

While it is generally agreed that even young children use temporal information specifically temporal contiguity (e.g., Kuhn & Phelps, 1976; Shultz & Mendelson, 1975; Siegler & Liebert, 1974; Wilde & Coker, 1978), there is disagreement over whether children are limited to the use of *only* temporal contiguity. For example, both Shultz and Mendelson (1975) and Kuhn and Phelps (1976) presented evidence suggesting that initially children were as likely to pick subsequent events as antecedent events when asked for the cause of a particular occurrence. Kun (1978), however, has shown that preschoolers *will* use order information when judging picture sequences of activities.

From the above, we know that preschool children have already the concept of temporal order. The preschoolers can see the sequential relationship between events. Only a few research are on this regard, and in which, nothing was mentioned about the difference of the ability between boys and girls. If a series of interesting related research can be done in this country, it could be applied onto the teaching method of the preschool education and the teaching efficiency of teachers might in turn be raised. In this research, we emphasize the study of the difference between preschool boys and girls in the development of the concept of event sequences.

METHODOLOGY

Subjects

The subjects (n=280) were pre-school children 4½-6½-years old. All children were from four pre-school education institutions in the greater Taipei area and were chosen at random from the list of names presented by the teachers.

Choice of Materials

In preparing the research, 10 different sets were prepared. Each set contained seven (7) colored pictures (25 cm×20 cm). The number of pictures was limited to seven in order to assure that the development of action could be easily determined. In this research it is assumed that more than seven pictures would go beyond the

physical reach of children this age and thus it would be influencing their desire to participate in the research. Also looking at so many pictures at once goes beyond their capacity forcing them to strain their head and eyes in the survey of the pictures required for completion of the project.

The topic of the pictures was taken from things that usually fill their days or occupy their attention. For example, putting on shoes, eating, taking a bath, getting dressed, opening the door, etc. Since children also relate well to cartoon figures and animals assuming the role of human beings, the majority of the sets used a cartoon drawing with animals taking human roles to introduce and develop the topic of the experimental set (Cann & Newbern, 1984).

To determine the degree of difficulty, ten adults were selected at random to participate in the experiment. A demonstration set (Fig. 1), one of the ten sets, showing the progressive stages of a flower from its budding to full-bloom and final withering was shown to the participants. After five seconds (0′ 5″ 0‴) the pictures were collected. Next, a set showing the stages of building a house were placed face down on the table. The subjects were asked to put this group into its proper order. As they began turning the pictures over they were timed. When they finished arranging the sequence the time was recorded and the pictures gathered together. This same method was repeated for the next eight groups. The ten adults had identical introductions to the experiment and identical sets of pictures. Each adult was tested alone. The results of the ten adults show that the pictures can be grouped into two categories: easy and difficult. (See Table 1; Figs. 1, 2 and 3)

Procedure

The procedure used by the experimentor for each of the 280 children was identical. First, the experimentor greeted the child by saying: "Today I'm going to play a game with you and let you see some pretty pictures." Then the child was taken to a quiet, empty room with a large table. Second, the demonstration set (Fig. 1) was presented with the accompanying description: "One

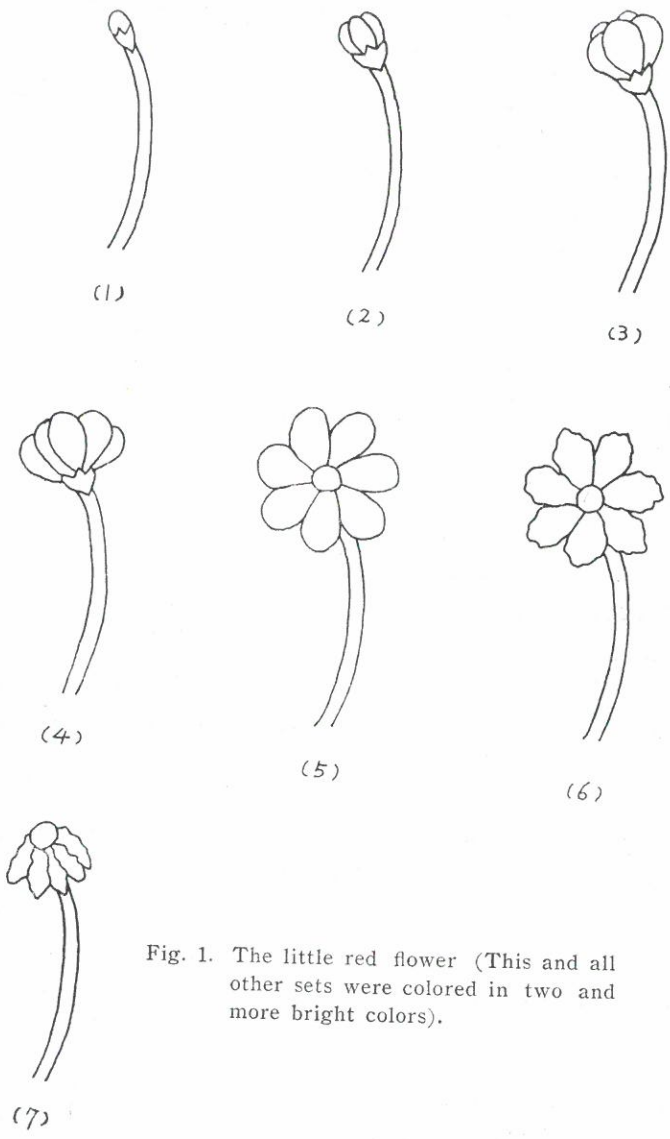

Fig. 1. The little red flower (This and all other sets were colored in two and more bright colors).

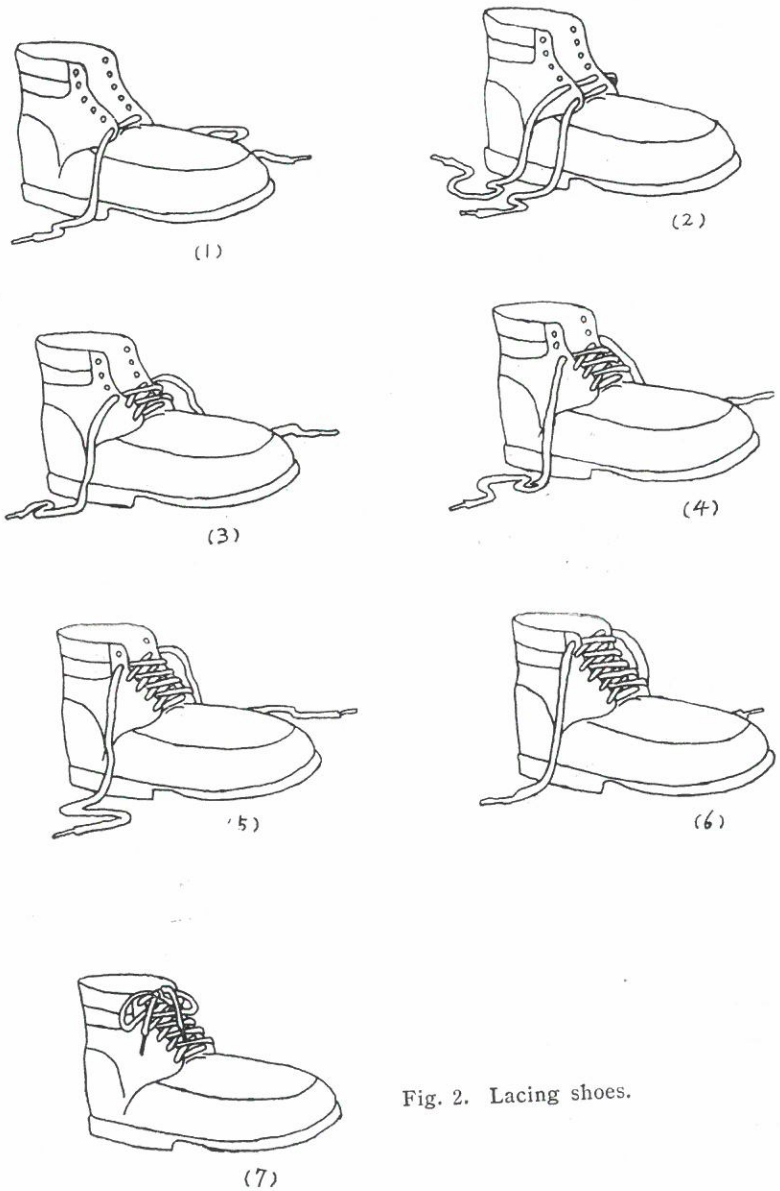

Fig. 2. Lacing shoes.

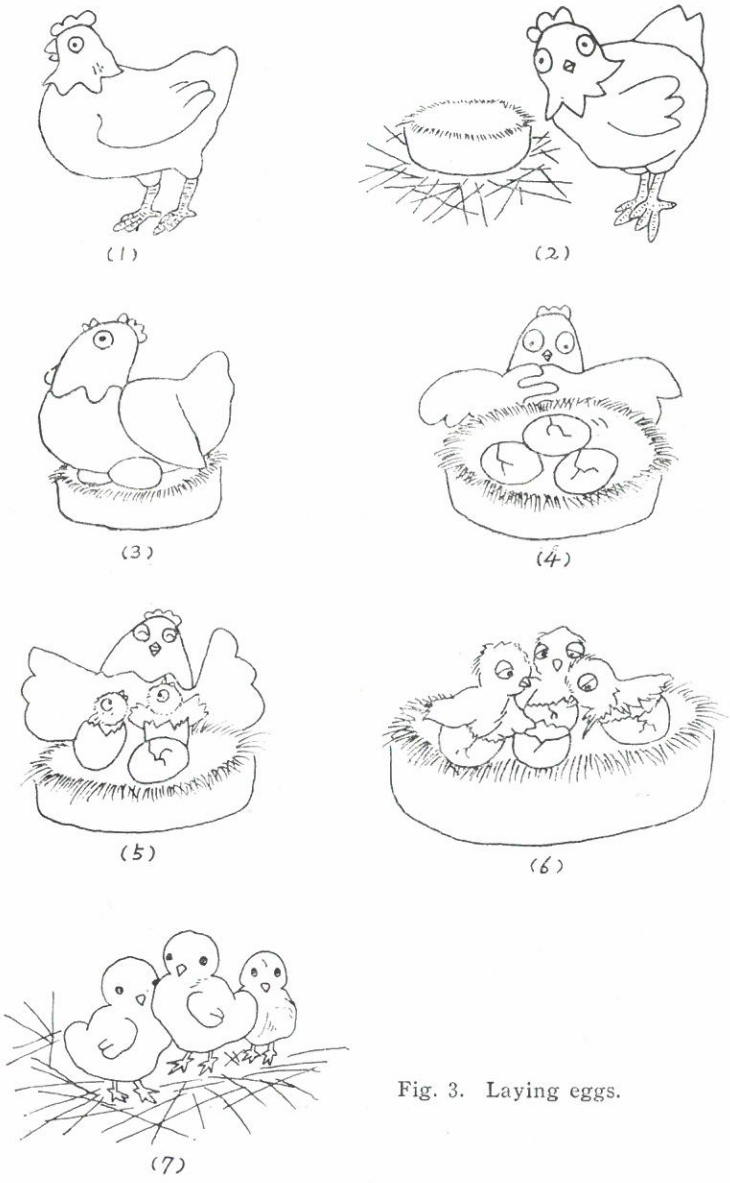

Fig. 3. Laying eggs.

Table 1. Categorized picture sets

Difficulty	Picture set	Topic of the picture set	Reference score $\bar{X}\pm SD$ (N)
Easy	P1	Clown make-up	18.67±3.63 (10)
	P2	Lacing shoes	18.97±3.62 (10)
	P3	House building	18.29±3.34 (10)
	P4	Laying eggs	23.33±9.76 (10)
	P5	Getting dressed	24.15±6.21 (10)
Difficult	P6	Shopping/cooking	38.65±20.36(10)
	P7	Eating dinner	50.85±23.97(10)
	P8	Bathing	68.82±28.79(10)
	P9	Going home	40.16± 9.35(10)

day a small, red flower sprouted. It grew bigger and bigger each day until it finally bloomed completely. After a few days it started to wither until one day it died."

The children were allowed to look at the pictures again and five seconds later they were collected.

Next, the set showing a clown putting on make-up was placed face down on the table. The experimentor began by saying: "Now I'll take out the clown putting on his make-up. Wait until I say 'start', then turn over the pictures and put them in order." When the child began turning over the pictures the timer was started and was stopped only when the child said s/he was finished. The time was then recorded.

After each set the child was invited to give the reasons for the subsequent ordering of the pictures.

The amount of time used by the 280 participants for the clown group ranged from 0′41″1‴ to 5′ up. This number also includes 67 children who were unable to do the set.

Following the completion of testing using this set, 118 children (61 boys and 57 girls) who were able to complete the experiment in three minutes or less and who could offer simple explanations for their sequences were selected to complete the remainder of the experiment using the remaining eight sets.

For the further test, 118 children were divided into three groups. (See Table 2) Each child accepted only one instruction treatment but should finish the other eight sets of pictures (P2~P9 in Table 1). The unselected 162 children all aged between 4½-5. Among the selected 118 children, only four aged from 5-5½ while the others were 5½-6½.

No Stimulating Factor

After greeting to the subject, s/he was taken into a quiet and empty room with a large, rectangular table and on which a set of face-down pictures was laid. The experimentor said: "These are (the lacing shoes) pictures. After I say 'start', you just turn the pictures over and put them in order." The timer was started when the child began to turn the pictures over and it was stopped only after the child had said that the work was completed. The time was then recorded.

The instruction given for the other seven tests was exactly the same. The topic of the pictures was given, without any other stimulation.

Achievement Motivation Factor

After greeting to the subject, the child was taken into a quiet and empty room with a large, rectangular table and on which a

Table 2. Grouping of the 118 children

Instruction treatment	Sex	School 1	School 2	School 3	School 4	Subtotal
No stimulating factor	M	7	5	3	5	20
	F	6	5	4	4	19
Achievement motivation factor	M	5	5	5	6	21
	F	5	4	4	5	18
Competition factor,	M	6	4	4	6	20
	F	6	4	4	6	20
Total						118

set of face-down pictures was laid. The experimentor said: "These are (the lacing shoes) pictures, and after I say 'start', you just turn the pictures over and put them in order. If you do it *faster than last time*, that means you are *improving*. And now I like to see if you are *faster* than last time." The timer was started when the child began to turn the pictures over and it was stopped only after the child had said that the work was completed. The time was then recorded.

The instruction given for the other seven tests was exactly the same. The experimentor announced the topic of the pictures and added, "If you do it *faster than last time*, that means you are *improving*. And now I like to see if you are *faster* than last time."

Competition Factor

The third instruction treatment included the element of peer competitions.

The experimentor greeted to two subjects of the same sex, and then took them into a quiet, empty room with a large, rectangular table. They were seated at the large table with two identical sets of face-down pictures laid. The two children sat opposite to one another with the experimentor at the head of the table to form a triangular seating arrangement. The experimentor said, "Each one of you has a set of (lacing shoes) pictures. After I say 'start', you just turn the pictures over and put them in order. The two of you will *compete with one another* in speed and I would like to see *who is faster*. Upon completion of the work, you have to say 'finished'. I will help you keep the time (The experimentor showed them the two stop-watches) and see who is faster." The timers were started when the children began to turn over the pictures and were stopped only after the children had said 'finished'. The time was then recorded separately.

The instruction given for the other seven tests was exactly the same. The experimentor announced the topic of the pictures and surely added, "You will *compete with one another* in speeed and I would like to see *who is faster*. ..... and see who is faster."

After each test, regardless of which treatment was used, the subjects were asked to give a brief explanation as the reason of why they arranged the pictures in such order. The time spent for explanations was not recorded.

The testing took a total of four months with each child being tested once every two weeks; at each testing session two sets of pictures were completed. Absences or changes in schedules sometimes caused delays in the testing, however 93 children successfully completed the experiment. The remaining 25 either transferred to another school during the course of the experiment and/or voiced objection to further participation. Among the remaining 25 children, only two aged from 5-5½. The results of the three different treatments is expressed in the following ANOVA TABLE.

Anova Table. No stimulating treatment

Source of variation	SS	*df*	MS	*f*
Between of subjects	300799.4	33		
Sex (B)	3403.4	1	3403.4	0.366 (no sig.)
Subjects within groups	297396	32	9293.63	
Within subjects	309081.2	272		
Instruction treatment (A)	113138.8	8	14142.35	19.462*
A×B	9917.1	8	1239.64	1.705938 (no sig.)
A×subjects within groups	186025.3	256	726.66	

Anova Table. Achievement motivation treatment

Source of variation	SS	*df*	MS	*f*
Between of subjects	87073.3	30		
Sex (B)	11.5	1	11.5	0.0038 (no sig.)
Subjects within groups	87061.8	29	3002.13	
Within subjects	431309	248		
Instruction treatment (A)	71846.2	8	8980.73	5.962*
A×B	10007.2	8	1250.9	0.83 (no sig.)
A×subjects within groups	349455.6	232	1506.27	

Anova Table. Competition treatment

Source of variation	SS	*df*	MS	*f*
Between of subjects	41237.5	27		
Sex (B)	5043.8	1	5043.8	3.623 (no sig.)
Subjects within groups	36193.7	26	1392.06	
Within subjects	221350	224		
Instruction treatment (A)	64943.8	8	8117.96	11.28*
A×B	6748.9	8	843.61	1.1724 (no sig.)
A×subjects within groups	149667.3	208	719.55	

Anova Table. Three factors

Source of variation	SS	*df*	MS	*f*
Between of subjects	454165.8	93		
Instruction treatment (A)	25055.7	2	12527.85	2.62
Sex (B)	91.2	1	91.2	0.019
A×B	8367.4	2	4183.7	0.875
Subjects within groups	420651.5	88	4780.13	
Within subjects	961750.2	743		
Pictures (C)	229651.1	8	28706.39	29.119*
A×C	20277.7	16	1267.35	1.286
B×C	15713.7	8	1964.2	1.992*
A×B×C	10959.5	16	684.97	0.695
C×subjects within groups	685148.2	695	985.82	

* The significance level $\alpha=0.05$.

RESULTS AND DISCUSSION

Result 1: No sex difference arising from instruction factors

Regardless of which of the three instruction factors used, no sex difference could be ascertained. $F(1,88)=0.019$, $P>0.05$. (F: F-value; P: P-value) That is to say, 5-6½-year old children, if they have developed the concept of event sequences, are able to apply it to any situation, therefore the development of the concept of event

sequences, that is, the formation of this ability is not determined by sex. Rather, one must look at the development of cognitive abilities.

Result 2: No sex difference arising from the experimentor's influence

The use of three separate treatments of instruction in giving the experiment also resulted in no measurable difference based on sex. $F(1,32)=0.366$, $P>0.05$; $F(1,29)=0.0038$, $P>0.05$; $F(1,26)=3.623$, $P>0.05$. That is, the experimentor and her instructions had no measurable effect on the child's performance. Using competition factor in the instruction had no measurable effect, therefore, it might not be necessary for the teachers to stimulate the children in their learning by the competitive instruction. Sometimes, the children would feel much frustrated after the competition, they might even lose their confidence and were then afraid to learn.

Result 3: Difference between easier and harder sets based on degree of difficulty and not sex

There are significant differences between the easy sets and the difficult sets. $F(8,256)=19.462^*$, $P<0.05$; $F(8,232)=5.962^*$, $P<0.05$; $F(8,208)=11.28^*$, $P<0.05$; $F(8,695)=29.119^*$, $P<0.05$. Four sets: lacing shoes, building a house, laying eggs, putting on clothes are drawn very simply. The remaining four sets are more complicated. Looking at the statistical results, the adults and children scored about the same. Those sets which the adults found difficult, the children also found harder; and vice versa, those the adults found easy, the children also found easier.

Result 4: No interaction effect between instruction treatments and sex of subject

The three instruction treatments and the sex of the subject showed no interaction effect. $F(2,88)=0.875$, $P>0.05$. It is sometimes proposed that the addition of a competition factor often encourages better performance on the part of male subjects, however, this was not the case in the present study. Therefore, no

interaction effect can be maintained.

Result 5: No interaction effect between instruction treatments and different sets of pictures

There was no interaction effect between the instruction treatments and the different sets of pictures. $F(16,695)=1.286$, $P>0.05$. Regardless of the instruction formula used with each of the eight sets the effect was almost identical.

Result 6: Interaction effect between pictures and sex

There was an interaction effect of pictures and sex. $F(8,695)=1.992^*$, $P<0.05$. The female subjects did the easier pictures faster and the male subjects did the more difficult sets faster. This seems to indicate that with the addition of the challenging factor a sex different is apparent. That is, in cases where the challenge is greater male subjects tend to perform better.

CONCLUSION

From the above six results it seems safe to propose that there is no significant difference based on sex in the development of the concept of event sequences among 4½-6½-year olds. Only with the addition of the challenging factor does any measurable difference become apparent. Further studies can, perhaps, examine in more detail the extent and nature of the environmental stimuli necessary to effect measurable differences in subjects of both sexes in the area of cognitive development.

From the non-selected children, it is clearly seen that those who aged between 4-5 almost did not have the concept of event sequences. Only a few children between 5-5½ have developed this concept. The discovery is quite different from that of Barbara O'Connell and Anthony Gerard (1985). In their research, they discovered that even 20-month old infants could distinguish familiar, ordered sequence from series of unrelated actions. This is also something worthwhile to be done in the future.

Other possible considerations to be included in further studies are:

— the nature of environmental stimuli that produce the different response to challenging tasks in pre-school children;
— the influence of the educational, economic and/or social levels of the parents on the development of the cognitive processes;
— the possibility of differences with regard to urban and rural settings;
— the influence of various teaching methods, e.g., Montessori; Piaget, on the performance of children in a similar experiment.

The present study could also engage in a long-term study of the same children to see if there would be any differences with age. Does the fact of performing the set very fast or very slow now have any impact three years from now in doing the same experiment?

ACKNOWLEDGEMENTS

I would like to extend my gratitude to my four students who acted as my research assistants, Huang Shu Fen, Lee Tzung Wen, Lwo Ching Wen and Tsao Se Yi. They gave tirelessly of their time and talents by drawing the picture sets and conducting the individual experiments. The four were of great help and support in this research project. Besides, I also would like to send special gratitude to Mr. Venne-Shiang Huang of Mathematics Department who did all the statistical analysis in this research. Finally, I like to thank Sr. Lynn Marie Morrison for helping in polishing my English.

REFERENCES

(1) A.L. Brown, The construction of temporal succession by preoperational children. In A.D. Pick (Ed.), *Minnesota Symposia on Child Psychology*, 1976, Vol. 10. Minneapolis: University of Minnesota Press.
(2) A. Cann & S.R. Newbern, Sex stereotype effects in children's picture recognition. *Child Development* 55, 1085-1090 (1984).
(3) M.A. Crisafi & A.L. Brown, Analogical transfer in very young children: combining two separately learned solutions to reach a goal. *Child Development* 57, 953-968 (1986).
(4) D. Elkind, Discrimination, seriation and numeration of size and dimensional differences in young children: Piaget replication study VI. *Journal of Genetic Psychology* 104, 275-296 (1964).

Anova Table. Competition treatment

Source of variation	SS	*df*	MS	*f*
Between of subjects	41237.5	27		
Sex (B)	5043.8	1	5043.8	3.623 (no sig.)
Subjects within groups	36193.7	26	1392.06	
Within subjects	221360	224		
Instruction treatment (A)	64943.8	8	8117.96	11.28*
A×B	6748.9	8	843.61	1.1724 (no sig.)
A×subjects within groups	149667.3	208	719.55	

Anova Table. Three factors

Source of variation	SS	*df*	MS	*f*
Between of subjects	454165.8	93		
Instruction treatment (A)	25055.7	2	12527.85	2.62
Sex (B)	91.2	1	91.2	0.019
A×B	8367.4	2	4183.7	0.875
Subjects within groups	420651.5	88	4780.13	
Within subjects	961750.2	743		
Pictures (C)	229651.1	8	28706.39	29.119*
A×C	20277.7	16	1267.35	1.286
B×C	15713.7	8	1964.2	1.992*
A×B×C	10959.5	16	684.97	0.695
C×subjects within groups	685148.2	695	985.82	

* The significance level $\alpha=0.05$.

RESULTS AND DISCUSSION

Result 1: No sex difference arising from instruction factors

Regardless of which of the three instruction factors used, no sex difference could be ascertained. $F(1,88)=0.019$, $P>0.05$. (F: F-value; P: P-value) That is to say, 5-6½-year old children, if they have developed the concept of event sequences, are able to apply it to any situation, therefore the development of the concept of event

sequences, that is, the formation of this ability is not determined by sex. Rather, one must look at the development of cognitive abilities.

Result 2: No sex difference arising from the experimentor's influence

The use of three separate treatments of instruction in giving the experiment also resulted in no measurable difference based on sex. $F(1,32)=0.366$, $P>0.05$; $F(1,29)=0.0038$, $P>0.05$; $F(1,26)=3.623$, $P>0.05$. That is, the experimentor and her instructions had no measurable effect on the child's performance. Using competition factor in the instruction had no measurable effect, therefore, it might not be necessary for the teachers to stimulate the children in their learning by the competitive instruction. Sometimes, the children would feel much frustrated after the competition, they might even lose their confidence and were then afraid to learn.

Result 3: Difference between easier and harder sets based on degree of difficulty and not sex

There are significant differences between the easy sets and the difficult sets. $F(8,256)=19.462^*$, $P<0.05$; $F(8,232)=5.962^*$, $P<0.05$; $F(8,208)=11.28^*$, $P<0.05$; $F(8,695)=29.119^*$, $P<0.05$. Four sets: lacing shoes, building a house, laying eggs, putting on clothes are drawn very simply. The remaining four sets are more complicated. Looking at the statistical results, the adults and children scored about the same. Those sets which the adults found difficult, the children also found harder; and vice versa, those the adults found easy, the children also found easier.

Result 4: No interaction effect between instruction treatments and sex of subject

The three instruction treatments and the sex of the subject showed no interaction effect. $F(2,88)=0.875$, $P>0.05$. It is sometimes proposed that the addition of a competition factor often encourages better performance on the part of male subjects, however, this was not the case in the present study. Therefore, no

interaction effect can be maintained.

Result 5: No interaction effect between instruction treatments and different sets of pictures

There was no interaction effect between the instruction treatments and the different sets of pictures. $F(16,695)=1.286$, $P>0.05$. Regardless of the instruction formula used with each of the eight sets the effect was almost identical.

Result 6: Interaction effect between pictures and sex

There was an interaction effect of pictures and sex. $F(8,695)=1.992^*$, $P<0.05$. The female subjects did the easier pictures faster and the male subjects did the more difficult sets faster. This seems to indicate that with the addition of the challenging factor a sex different is apparent. That is, in cases where the challenge is greater male subjects tend to perform better.

CONCLUSION

From the above six results it seems safe to propose that there is no significant difference based on sex in the development of the concept of event sequences among $4\frac{1}{2}$-$6\frac{1}{2}$-year olds. Only with the addition of the challenging factor does any measurable difference become apparent. Further studies can, perhaps, examine in more detail the extent and nature of the environmental stimuli necessary to effect measurable differences in subjects of both sexes in the area of cognitive development.

From the non-selected children, it is clearly seen that those who aged between 4-5 almost did not have the concept of event sequences. Only a few children between 5-$5\frac{1}{2}$ have developed this concept. The discovery is quite different from that of Barbara O'Connell and Anthony Gerard (1985). In their research, they discovered that even 20-month old infants could distinguish familiar, ordered sequence from series of unrelated actions. This is also something worthwhile to be done in the future.

Other possible considerations to be included in further studies are:

— the nature of environmental stimuli that produce the different response to challenging tasks in pre-school children;
— the influence of the educational, economic and/or social levels of the parents on the development of the cognitive processes;
— the possibility of differences with regard to urban and rural settings;
— the influence of various teaching methods, e.g., Montessori; Piaget, on the performance of children in a similar experiment.

The present study could also engage in a long-term study of the same children to see if there would be any differences with age. Does the fact of performing the set very fast or very slow now have any impact three years from now in doing the same experiment?

ACKNOWLEDGEMENTS

I would like to extend my gratitude to my four students who acted as my research assistants, Huang Shu Fen, Lee Tzung Wen, Lwo Ching Wen and Tsao Se Yi. They gave tirelessly of their time and talents by drawing the picture sets and conducting the individual experiments. The four were of great help and support in this research project. Besides, I also would like to send special gratitude to Mr. Venne-Shiang Huang of Mathematics Department who did all the statistical analysis in this research. Finally, I like to thank Sr. Lynn Marie Morrison for helping in polishing my English.

REFERENCES

(1) A.L. Brown, The construction of temporal succession by preoperational children. In A.D. Pick (Ed.), *Minnesota Symposia on Child Psychology*, 1976, Vol. 10. Minneapolis: University of Minnesota Press.
(2) A. Cann & S.R. Newbern, Sex stereotype effects in children's picture recognition. *Child Development* 55, 1085-1090 (1984).
(3) M.A. Crisafi & A.L. Brown, Analogical transfer in very young children: combining two separately learned solutions to reach a goal. *Child Development* 57, 953-968 (1986).
(4) D. Elkind, Discrimination, seriation and numeration of size and dimensional differences in young children: Piaget replication study VI. *Journal of Genetic Psychology* 104, 275-296 (1964).

(5) R. Fivush & J.M. Mandler, Developmental changes in the understanding of temporal sequence. *Child Development* 56, 1437-1446 (1985).
(6) W.J. Friedman, *The Developmental Psychology of Time*. New York: Academic Press, 1982.
(7) R. Gelman, M. Bullock & E. Meck, Preschoolers' understanding of simple object transformations. *Child Development* 51, 691-699 (1980).
(8) D. Kuhn & H. Phelps, The development of children's comprehension of causal direction. *Child Development* 47, 248-251 (1976).
(9) A. Kun, Evidence for preschooler's understanding of causal direction in extended causal sequences. *Child Development* 49, 218-222 (1978).
(10) J. Mandler, Categorical and schematic organization in memory. In C.R. Puff (Ed.), *Memory, organization and structure*. New York: Academic Press, (1978).
(11) B.G. O'Connell & A.B. Gerard, Scripts and scraps: The development of sequential understanding. *Child Development* 56, 671-681 (1985).
(12) J. Piaget, *The child's conception of time*. London: Routledge-Kegan Paul, (1969).
(13) J. Piaget, *Understanding causality*. New York: Norton, (1974).
(14) D. Premack, *Intelligence in age and man*. New York: Wiley, (1976).
(15) R.A. Schrank & R. Abelson, *Scripts, plans, goals and understanding*. Hillsdale, N.J.: Erlbaum, (1977).
(16) T. Shultz & R. Mendelson, The use of covariation as a principle of causal analysis. *Child Development* 46, 394-399 (1975).
(17) R. Siegler & R. Liebert, Effects of contiguity, regularity and age on children's causal inferences. *Developmental Psychology* 10, 574-579 (1974).
(18) J. Wilde & P. Coker, Probability, spatial contact and temporal contiguity as principles of causal inference. Unpublished manuscript, Claremont Graduate School, (1978).

學齡前幼兒"事件發生的順序"概念發展上的性別差異

家 政 系

黃 淑 媛

摘 要

本研究旨在探討四歲半至六歲半幼兒"事件發生的順序"此概念的發展是否有顯著的差別差異。以抽樣方式抽取臺北近郊四所幼教機構的 280 名幼兒。其中93名幼兒（男47，女46）完成全部項目。測驗方式按測驗者指導語的不同分三組：①無刺激因素，②激發成就動機，③含有同輩之競爭。測驗項目爲從易至難的九套彩色連續性圖片，每套含有七張圖片。不論那種測驗方式，每一名幼兒須把每套圖片按事件發生的先後順序排列出來。測驗者記錄下幼兒自翻取圖片至完成排列所需之時間。研究結果顯示：①"事件發生的順序"此概念的發展無性別的差異，②測驗者的語言刺激（指導語）並不影響幼兒的完成時間，③難度大、挑戰性大的項目男性表現較女性佳。

ABSTRACTS OF PAPERS BY FACULTY MEMBERS OF THE COLLEGE OF SCIENCE AND ENGINEERING THAT APPEARED IN OTHER JOURNALS DURING THE 1986 ACADEMIC YEAR

Stability of Stable Periodic Orbits

CHING-HER LIN

Bulletin of the Institute of Mathematics, Academia Sinica,
Vol. 14, No. 4, December 1986

Let I be a closed and bounded interval in R and $f: I \to I$ be a continuous function. If f has a stable periodic point with minimal period n, and g is a continuous function close to f, then g has a periodic point of same minimal period n.

Lunping Scintillations and Manila Total Electron Content

JOHN R. KOSTER

Proc. Natl. Sci. Counc. ROC(A), Vol. 11, No. 1, 1987, pp. 50-58

Large plasma depletions, usually called bubbles, form in the post-sunset equatorial ionosphere. These can rise to heights of over 1,000 km and produce severe fading effects of radio signals over a band of latitudes centered on the dip equator. An attempt is made to develop a method of identifying bubble formation in TEC data from a station relatively close to the dip equator (Manila) by determining the value of a variable called BYT. This variable yields highly significant correlations (in the statistical sense) with severe fading (scintillations) of the radio signal from a synchronous satellite received at a station in Taiwan (Lunping), 1,160 km to the north of Manila. There is evidence that BYT actually detects equatorial bubbles. If this is true, it can provide a valuable research

tool, since bubble-associated scintillations affect radio communications as well as all applications in which radio waves are sent through the ionosphere at low latitudes.

太 陽 磁 場 活 動 之 隨 機 性

呂 秀 鏞

國立中央大學地球物理學刊 第27、28期 第199-213頁 七十六年六月

吾人分析太陽黑子資料得知太陽黑子具有隨機特徵，並以隨機磁浮力之發電機模式模擬太陽磁場活動之性質，得知週期與振幅取決於發電機數目（Dynamo Number）與磁浮力效應的大小，週期與振幅之變化則與磁浮力效應及 α 效應之隨機性密切相關。

Comment on H+NO Translation-to-Vibration/Rotation Energy Transfer: A Classical Trajectory Study

FRANK BUDENHOLZER, S.C. HU,
L.M. HWANG and MARK SONG

Journal of Chemical Physics, 86, 3756 (1987)

Classical trajectories were calculated for H+NO vibrationally, rotationally inelastic scattering at a relative translational energy of 2.3 eV over the $^1A'$ surface. The results complement an earlier trajectory study by M. Colton and G. Schatz (J. Chem. Phys. 83, 3413 (1985)). The role of "nearly direct hits" and complex formation are discussed.

Determination of Potassium Ion-Small-Molecule Potentials from Total Cross Section Measurements

FRANK E. BUDENHOLZER, ERIC A. GISLASON*
and ANDREW D. JORGENSEN*

Chemical Physics, 110 (1986), 171-186.

Total cross sections have been measured for K^+ ions scattered N_2, CO, CO_2, CH_4, C_2H_4, C_2H_6, CF_4 and SF_6 in the range $E\theta_R = 5\text{-}100$ eV deg. Here E is the laboratory energy of the K^+ beam, and θ_R is the resolution angle of the apparatus. A procedure has been developed to determine the spherically symmetric part of the intermolecular potential from the cross sections, and the procedure has been tested against realistic trial data. Estimates of the potentials in the region of the potential well are obtained and compared with other theoretical and experimental work on these systems.

* Department of Chemistry, University of Illinois at Chicago, Chicago, IL 60680, USA.

Reactions of Methylphenylvinylsulfonium Tetrafluoroborate With Ketone Enolates

Shang-Shing P. Chou and Jyanwei H. Liu

J. Chin. Chem. Soc., 34, 49-55 (1987)

The reactions of methylphenylvinylsulfonium tetrafluoroborate (1) with the lithium enolates of 1,3-dicarbonyl compounds, acyclic ketones and cyclic ketones have been studied. Cyclopropanes and cyclic ethers are obtained. The reaction mechanisms are also discussed.

Factors Affecting Linear Polyester Formation at Oil —Water Interface

J.W. Hwang, C.P. Chang and D.Y. Chao*

J. of Chin. Coll. Interface Chemistry, 10, 2 (1987)

The preparation of linear aromatic polyester at various reaction temperatures in the presence of surfactant as a phase trasfer catalyst at oil-water interfaces. It has been found that in the presence of small amount of nonionic surfactant, nonyl phenyl polyoxyethylene ether (NP6; NP6 concentration $\ll$ critical micelle

concentration=CMC), the variations of reaction temperatures are seen to be less or no effect on the intrinsic viscosity (=0.42 dl/g) of polyester products in ochlorophenol. As the concentration of NP6 employed in stirred interfacial polycondensation at various reaction temperatures is equivalent to or greater than the CMC, the intrinsic viscosity of polyester products obtained at reaction temperature 40°C is seen to increase dramatically and then decrease rapidly when the reaction temperature is further increased.

Experimental results clearly show that as the stirring rate in interfacial polycondensation is controlled within the range of 4,052,342 rpm at 40°C, the intrinsic viscosity values of polyester products obtained appear to be independent of the rate. But when the stirring rate is elevated to around 2,671 rpm, the intrinsic viscosity of the polyester product is seen to be substantially increased (0.7 dl/g). This may be due to the increased collisions between BPA and diacid chloride molecules at oil-water interface as a result of increased surface areas of BPA and diacid chloride molecules resulting from the high shearing force.

Our intrinsic viscosity data also indicate that in interfacial polycondensation alkyl sulfonate sodium with short carbon chain length C_{10} is superior in catalytic effect to alkylsulfonate sodium with carbon Chain length greater than C_{10}.

* Department of Chemistry, Chinese Culture University.

Halogen-Mediated Electron Transfer between Metallocenes of Ruthenium and Osmium in the Oxidation States 4+ and 2+

T.P. Smith,* D.J. Iverson,* M.W. Droege,*
K.S. Kwan and H. Taube*

Inorg. Chem., 26, 2882 (1987)

The rates of self-exchange for several systems of the class MCp_2X^+/Cp_2 where M is Ru or Os and X is Cl, Br or I, have been

measured by the NMR line broadening method. For each metal, the rates increase along the halogen series as given above, and are more rapid for M=Ru than for the osmium analogs. In considering these data, the possibility is raised that these $2e^-$ self-exchange reactions and those of other metal ions, take place by $1e^-$ steps.

* Department of Chemistry, Stanford University.

Cure Kinetics of an Epoxide/Anhydride/Amine Resin System: A Fractional-Life Method Approach

Sung-Nung Lee and Wu-Bin Yuo

Polymer Engineering and Science, September, 1987, Vol. 27, p. 1317

A fractional-life method coupled with dynamic differential scanning calorimetry (DSC) scan was employed to study the kinetics of the isothermal polymerization of the DGEBA (diglycidyl ether bisphenol A)/HHPA (hexahydrophthalic anhydride)/BDMA (benzyl dimethyl amine) resin system. This method avoids the problem of uncertainty in the total heat evolution in the isothermal DSC scan. The reaction orders obtained for this epoxy resin vary from 1.05 to 1.44 in the temperature range 118-135°C and are believed to be more accurate than those determined in previous studies.

Phosphonate Ylide Complexes of Palladium(II) and Platinum(II): Oxidative Addition and Reductive Elimination, the Crystal and Molecular Structures of *cis*- and *trans*-[$Pt(PPh_3)_2(I)(CH_2P(O)(OCH_3)_2)$]

Ivan J.B. Lin, Luke T.C. Kao, Feng J. Wu,
G.H. Lee* and Y. Wang*

Journal of Organometallic Chemistry, 309 (1986), 225-239

Phosphonate complexes $M(PPh_3)_2(I)(CH_2P(O)(OR)_2)$ (M = Pd and Pt, R = Me and Et) have been prepared by the oxidative addition of $ICH_2P(O)(OR)_2$ to $M(PPh_3)_4$. While the platinum product

isomerized slowly from the *cis*- to the *trans*-isomer, the palladium compound decomposed in solution. Several compounds have been identified from the decomposition reaction: $ICH_2P(O)(OCH_3)_2$, $CH_3P(O)(OCH_3)_2$, $[Pd(PPh_3)_2(CH_2P(O)(OCH_3)_2]I$, $OPPh_3$ and $[Pd(PPh_3)(I)(CH_2P(O)(OCH_3)_2)]_2$. In air, $ICH_2P(O)(OCH_3)_2$ was the major product observed; however, in the absence of air, $CH_3P(O)(OCH_3)_2$ was the major product. A study of the reaction pathway showed that the reductive elimination proceeded via phosphine dissociation. The structures of the *trans*- and *cis*-platinum compounds were determined by X-ray diffraction, and were refined to $R_w = 0.036$ (5,382 observed reflections) and 0.027 (5,274 observed reflections), respectively. The bond lengths of Pt-P, Pt-C and Pt-I *trans* to various ligands clearly demonstrate the order of the *trans* influence: phosphonate > phosphine > I.

* Chemistry Department, National Taiwan University, Taipei 107, Taiwan (R.O.C.)

A Study of the *cis-trans* Isomerization of A Square Planar Pt Ylide Complex

Ivan J.B. Lin and C.P. Chang

J. Chin. Chem. Soc., 33, 273-277 (1986)

The isomerization of *cis*-$Pt(PPh_3)_2(I)(CH_2P(O)(OCH_3)_2)$, 1, was studied by an NMR technique. An Arrhenius plot for the isomerization gives an activation energy of 99.2 KJ/mol, $\Delta H^{\ddagger} = 97$ KJ/mol and $\Delta S^{\ddagger} = -8.3$ J/mol-K. Under a CO atmosphere the *cis* isomer catalytically isomerized to its *trans* form. Free PPh_3 did not catalyze the *cis-trans* isomerization. In the proposed isomerization mechanism the reaction goes through an intramolecular assisted phosphine dissociation, followed by dimer formation. The addition of phosphine to the dimer then completes the isomerization of the original monomer from *cis* to *trans*.

Sulfur Ylide Complexes of Palladium, Preparation of Organometallic Compounds by the Phase Transfer Catalysis Technique

Ivan J.B. Lin, Hanse Y.C. Lai,
Shu C. Wu and Luchen Hwan

Journal of Organometallic Chemistry, 304 (1986), C24-C26

Reactions of $[S(O)(CH_3)_3]I$ in NaOH solutions of various concentrations with $Pd(PPh_3)_2Cl_2$ in $CHCl_3$ in the presence of n-Bu_4NI produced $[Pd(PPh_3)_2\{(CH_2)_2S(O)(CH_3)\}]I \cdot \frac{1}{2}CHCl_3$, (1), and $Pd(PPh_3)(I)[(CH_2)_2S(O)(CH_3)] \cdot \frac{1}{2}CHCl_3$ (2) with good yields. Without the phase transfer catalyst, no ylide complexes were formed. Compounds 1, 2, and the ionic compounds *cis*-$[Pd(PPh_3)_2\{(CH_2)S(O)(CH_3)_2\}_2]I_2$ (3) were also prepared with low yields by the reaction of the ylide $(CH_2)S(O)(CH_3)_2$ with $Pd(PPh_3)_2Cl_2$ in dry THF under an inert atmosphere. The advantages of phase transfer technique are discussed.

Synthesis and Reactions of Some Sulfur Ylide Complexes of Palladium

M.C. Cheng,* S.M. Peng,* I.J.B. Lin,
B.H.H. Meng and C.H. Liu

J. Organomet. Chem., 327 (1987), 275-283

The iodo-bridged sulfur ylide complex $[Pd(\mu\text{-}I)((CH_2)_2(SO)(CH_3))]_2$ 1, was reacted with dithiolates, acetylacetone and various Lewis bases to give $[Pd((CH_2)_2(SO)(CH_3))(S\sim S)]$ ($S\sim S = S_2CN(C_2H_5)_2$, $S_2COC_2H_5$ and $S_2P(OC_2H_5)_2$), $[Pd((CH_2)_2(SO)(CH_3))(acac)]$ (acac=acetylacetonate) and $[PdI((CH_2)_2(SO)(CH_3))(base)]$ (base=PPh_3, $P(OMe)_3$, $P(OPh)_3$ and C_5H_5N). In the presence of a phase transfer catalyst, the reaction rates and yields were greatly increased. Reactions of several related sulfur ylide complexes with I_2, HI and aquous NaOH gave 1. The X-ray single crystal structure

cells: two primary pigment cells and six secondary pigment cells. In both of them, the cytoplasm is rich in rER, glycogen, mitochondria and microtubules at the early stages. The commashaped primary pigment cells and the spindle-shaped secondary pigment cells contain many morphologically mature pigments at P4 stage. The structure of secondary pigment cell is obviously different from those of primary pigment cells at the early stage.

* Institute of Zoology, Academia Sinica, Nankang, Taipei, Taiwan, Republic of China.

The Study of Female Sex-Pheromone Glands of Tea Tortrix, *Homona coffearia* Nietner and Small Tea Tortrix, *Adoxophyes* sp.

Chung-Hsiung Wang and Der-Fe Wu

N. S. C. Sexpheromone Monograph, 185-196 (1986, 9)

The sex-pheromone glands of the female tea tortrix, *Homona coffearis* N., and the female small tea tortrix, *Adoxophyes* sp., as in other species of Tortricidae, are derived from the intersegments between the 8th and 9th abdominal segments. The former is a Y-shape dorsal sac but the later is a typical nonbranched dorsal sac.

The sex-pheromone gland of the tea tortix can be divided into 3 parts. The anterial part of gland, about one-third the length of the gland, is separated into 2 coma-like pouchs. These pouchs invaginate deeply into the lateral sides of the 7th abdominal segment. The middle part of the gland belongs to closed type gland and the posterial part, about half the length of the gland, is the open-type gland. The modified intersegmental membrane of the posterial part is discontinous at the lateral sides. There are some variations in the size and shape of the gland lumen in different parts of the gland. The individual differences in the morphology of the lumen were also observed. The glandular epithelium consists of tall columnar cells. The cuticle of the gland with many tiny hairs is thinner than the rest of the intersegmental membrane.

The gap between the gland cells is found in the well-developed gland (3-day-old female adult). The nuclei with round or elipsoid shapes are located at the middle part of the cells. The cytoplasm contains many acidophilic secretary granules which are accumulated at the distal part of the cells and form an acidophilic layer beneath the cuticle of glands. The relationship between glands and body weights of pupae was investigated. So far, the results indicate that the 3-day-old sex-pheromone gland of the tea tortrix is the most active time for the releasing of sex pheromone and the development of the sex-pheromone gland depends upon the condition of insect.

The sex-pheromone gland of small tea tortrix can only be divided into 2 parts. The anterial part of the gland, about three-fourths the length of the gland, is a sac-like gland which invaginates deeply into the dorsal side of the 7th abdominal segment. The homogenous cytoplasm contains acidohilic secretary granules. The relationship between glands and body weights of pupae was investigated too, and the result also indicated that the development of the sex-pheromone gland depends upon the condition of the insect.

Techniques of Fuzzy Query Translation for Database Systems

Shyi-Ming Chen, Jyh-Sheng Ke* and Jin-Fu Chang**

Proceedings of International Computer Symposium, 1986, December 17-19, Tainan, Taiwan, R.O.C.

This paper presents an intelligent user interface with fuzzy query translation capability for retrieving information from the relational database system. It places emphasis on user-friendliness and flexibility for the inexperienced users. The query language HQL, which allows for fuzzy queries, is introduced. The concept of semantic graph and λC_i-level fuzzy variable translation technique are also described in details. With the aid of the intelligent user

interface, the existing database system can itself behave more intelligently, and will be more suitable for use by the inexperienced users.

* Dr. Ke is currently associated with Institute for Information Industry, R.O.C.
** Department of Electrical Engineering, National Taiwan University.

百香果採收成熟度之研究 (一)
對果汁一般品質之影響

史宏財* 方祖達* 陳雪娥

中國園藝 33 (1), 51-64, 1987

臺灣栽培雜交種百香果夏果之果汁含量依果實成熟度，以自然落果發生之前後一日者爲最高，卽果汁佔全果重之 42.5%。維生素丙含量則隨果實成熟而遞減。但至完全成熟自然落果前後三天內含量趨於穩定約在 20～22 mg/100 g 果汁。落果後若貯藏於 20°C 達一星期，果皮中紫紅色花青素會滲溶於果腔內，使榨汁時流入果汁中，類胡蘿蔔素含量隨成熟度之增加而增加。採收後百香果隨貯藏期而糖分及有機酸含量亦隨之改變。就官能品評之結果類示果汁香味和果實成熟度及果汁色澤呈高度正相關 ($r=0.94$ 及 $r=0.87$)。綜合結果吾人可確定加工製汁百香果採收成熟度以落果至落果後未超過 3 日以上者品質較佳，可供原料品質參考。

* 國立臺灣大學園藝學研究所研究生及教授

百香果採收成熟度之研究 (二)
對果汁中碳水化合物之影響

史宏財* 方祖達* 陳雪娥

中國園藝 33 (1), 68-81, 1987

由 HPLC 分析得知百香果自授粉至發育 35、42 及 49 天等果汁中蔗糖含量是先增加後減少，而果糖及葡萄糖則繼續隨果實成熟而增加。二者比率近於 1，貯藏後蔗糖與葡萄糖增加的原因可能是因爲澱粉之水解等原因促成。澱粉含量以自然落果時的果汁中含量最低。HPLC 分析出百香果汁中含有18種非揮發性

有機酸，主要爲檸檬酸約佔 90% 以上，蘋果酸、琥珀酸、乳酸、草酸及鳥頭酸依次存在。不同採收成熟度百香果汁中碳水化合物之變化可提供果汁加工及品管檢驗上之參考。

* 國立臺灣大學園藝研究所研究生及教授

葡萄酵素性褐變之研究
I. 金香葡萄聚酚氧化酶之性質探討

金蘭馨　陳雪娥

食品科學　第十三卷　第三、四期　第180-187頁　七十五年

以成熟的金香葡萄果實爲材料，經分離、初步純化後所得之部分純化酵素液，作爲探討聚酚氧化酶性質之對象。實驗結果顯示，金香葡萄之聚酚氧化酶若以兒茶酚當基質，最適反應 pH 在 6.5～7.0 之間，最適反應溫度爲 30°C。其熱不活化作用爲一次動力式，活化能爲 38.84 Kcal/mol。聚酚氧化酶對鄰二羥酚化合物有高度的特異性，且對不同之酚化物各有其最適反應之 pH 值，故其相對活性則隨試驗之 pH 而異。在抑制劑方面，二氧化硫及抗壞血酸的抑制效果優於 EDTA 及硫脲 (thiourea)。

以鷄胸肉鹽溶性蛋白質爲黏合劑製造低鈉鹽重組肉

黃以珪　鄭淑文　蔣見美　蔡啟民

食品科學　第十四卷　第一、二期　第59-65頁　七十六年

本試驗以鷄胸肉中鹽溶性蛋白質爲黏合劑，直接添加於肉粒中，試製低鈉鹽冷凍重組猪排，並與直接加鹽於猪排中之對照組比較其製品品質之差異。在不添加食鹽與三聚合磷酸鈉，含 5% 鹽溶性蛋白質溶液之情況下，其結着力爲 77 g/cm²。添加 0.6M 食鹽及 0.5% 三聚合磷酸鈉之後，其結着力增至 251 g/cm²。以後者 10% 添加量製造重組猪排，其鈉離子含量較直接加鹽抽提製造之對照組，即含有 0.75% 食鹽與 0.125% 三聚合磷酸鈉者爲低，(自 3.52 mg/g 減爲 1.54 mg/g)。其保水率、烹煮損失及結着性均較優，在 −20°C 貯藏期間，其色澤較佳，TBA 值亦較低。經官能品評結果，其外觀、嫩度、咬感、風味及接受性等較對照組均無顯著差異。採用本試驗方法製造之重組肉，含鈉最低，其製品品質與組成均能使人接受，爲一種有開發潛力之保健食品。